LIÈGE université
Gembloux
Agro-Bio Tech

Eosinophils inhibit response to chemotherapy: mechanisms, preclinical and clinical study in mesothelioma

WILLEMS Mégane

Promoteur: Luc WILLEMS

Année civile: 2023

COMMUNAUTÉ FRANÇAISE DE BELGIQUE
UNIVERSITÉ DE LIÈGE – GEMBLOUX AGRO-BIO TECH

Eosinophils inhibit response to chemotherapy: mechanisms, preclinical and clinical study in mesothelioma

Mégane WILLEMS

Dissertation originale présentée (ou essai présenté) en vue de l'obtention du grade de doctorat en sciences agronomiques et ingénierie biologique

Promoteur(s) : Luc WILLEMS
Année civile : 2023

Abstract

Malignant pleural mesothelioma (MPM) is a rare and highly aggressive cancer affecting the pleura and is mainly caused by asbestos exposure. Prognosis for MPM patients remains globally poor notably due to the advanced stage of the disease at presentation and because of its resistance to available treatments. Therapeutic approaches have been disappointing, and treatments used have not proven their ability in significantly prolonging survival in comparison to supportive care. The possibility of curative resection is extremely rare and the impact of chemotherapy on the outcome of patients with MPM is still limited. The biological mechanisms that mediate this partial or lack of response are unknown. However, emerging evidence indicates that the tumor microenvironment (TME) is a key factor. Although only 0.5% to 1.7% of patients with malignant tumors may present eosinophilia, MPM is one of the cancers where excess of eosinophils in the peripheral blood has a strong association with survival.

In the first part of my thesis, a retrospective study of MPM patients' clinical data was conducted. Results show that a cutoff of 220 eosinophils/µL of blood splits the patients' cohort into two groups with significantly different median overall survival after chemotherapy. The corresponding two-year overall survival rates are also significantly different. The response to standard chemotherapy is significantly reduced in the AEC $\geq$ 220/µL subset, based on progression-free survival and disease control rate.

The second part of my work consisted in confirming the observed correlation in patients, by using an in vitro model based on the EOL1 cell line and primary eosinophils isolated from healthy donors' blood. *In vitro* analyses in 2D and spheroids models highlight that eosinophils' supernatant inhibits MPM cells response to chemotherapy. Transcriptomic data reveals that protein binding, response to stimulus and intracellular vesicle are the most significantly enriched gene ontology terms. Experimental evidence further demonstrates that recombinant galectin-10 to the culture medium inhibits the proapoptotic effect of cisplatin and pemetrexed. Conversely, depletion of CLC-P/Gal10 from the medium suppresses the inhibitory effect of eosinophil supernatant. Finally, mice experiments highlight potential management of patients presenting an excess of blood eosinophils prior to chemotherapy administration.

This thesis reveals a potential novel prognosis marker for MPM patients with experimental, preclinical and clinical evidence supporting the role of eosinophils in the pathogenesis and therapy of MPM. This offers new prospect for an oriented and personal care.

Résumé

Le mésothéliome pleural malin (MPM) est un cancer rare et agressif qui affecte la plèvre et qui est principalement provoqué par l'exposition à l'amiante. Le pronostic des patients atteints du MPM est toujours globalement mauvais en raison de l'état avancé de la maladie lorsque les patients se présentent, et à cause de la résistance aux traitements disponibles. Les approches thérapeutiques ont été décevantes, et les traitements utilisés n'ont pas prouvé d'efficacité à prolonger la survie des patients de manière significative par rapport aux soins palliatifs. La possibilité de résection chirurgicale est extrêmement rare et l'impact de la chimiothérapie sur le patient atteint de MPM reste très limité. Les mécanismes biologiques qui médient ce manque de réponse ou cette réponse partielle ne sont pas connus. Cependant, de plus en plus d'évidences indiquent que le microenvironnement tumoral (TME) est un facteur clé.

Même si seulement 0,5% à 1,7% des patients atteints de tumeurs malignes peuvent présenter une éosinophilie, le MPM est l'un des cancers pour lequel un excès d'éosinophiles dans le sang périphérique présente une forte corrélation avec la survie des patients.

Dans la première partie de ma thèse, une analyse rétrospective des données cliniques de patients atteints de MPM a été réalisée. Les résultats montrent qu'un seuil de 220 éosinophiles/µL de sang sépare la cohorte de patient en deux groupes présentant des médianes de survies globales après chimiothérapie significativement différentes. Les taux de survie globale à deux ans sont également significativement différents. La réponse à la chimiothérapie est significativement réduite dans le sous-groupe avec un AEC $\geq$ 220/µL, en se basant sur la survie sans progression de la maladie et le taux de contrôle de la maladie.

La seconde partie de mon travail a consisté à confirmer la corrélation observée chez les patients en utilisant un modèle *in vitro* basé sur la lignée cellulaire EOL1 et des éosinophiles primaires isolés de sang de donneurs sains. Les analyses *in vitro* en modèle 2D et sphéroïdes mettent en évidence que le surnageant d'éosinophiles inhibe la réponse des cellules de MPM à la chimiothérapie. Les analyses transcriptomiques révèlent que la liaison des protéines, la réponse aux stimuli et les vésicules intracellulaires sont les termes de « gene ontology » les plus enrichis. Les évidences expérimentales démontrent par ailleurs que l'addition de galectine-10 recombinante dans le milieu de culture inhibe l'effet pro-apoptotique du cisplatine et du pemetrexed. A l'inverse, la déplétion de CLC-P/Gal10 du surnageant élimine cet effet inhibiteur du surnageant d'éosinophiles. Finalement, les expériences en souris ont mis en évidence un traitement potentiel pour les patients présentant un excès d'éosinophiles sanguins avant chimiothérapie.

Cette thèse révèle un potentiel nouveau marqueur de pronostic pour les patients atteints de MPM, avec des évidences expérimentales, pré-cliniques et cliniques qui supportent un rôle des éosinophiles dans la pathogenèse et la thérapie du MPM. Cela offre de nouvelles perspectives pour un traitement orienté et personnel des patients.

Acknowledgments

J'aimerais d'abord remercier mon promoteur de thèse, Luc Willems, de m'avoir permis d'effectuer ma thèse dans son laboratoire. Merci d'avoir cru en moi dès le départ, et de m'avoir poussée à me lancer. La décision ne fût pas évidente (comme tu le sais) mais je ne le regrette absolument pas. Merci pour les nombreux échanges et tes conseils.

Je tiens également à remercier les membres de mon comité de thèse pour leurs conseils avisés et leur aide au long de cette thèse. Merci tout particulièrement au Pr. Arnaud Scherpereel, ainsi qu'à Eric Wasielewski, pour leur aide quant à l'analyse des données patients. Merci également à Christophe Blanquart pour ses conseils et pour les futures collaborations.

I would also like to thank Jo Raskin for the collaboration on the clinical analysis.

Merci également à Malik Hamaïdia pour m'avoir donné l'opportunité de commencer ce projet lors de mon TFE et pour ton encadrement lors de celui-ci.

Je tiens particulièrement à remercier toute l'équipe d'épigénétique et, plus particulièrement, les doctorants : Hélène, Clotilde, Thomas 1, Alexis, Aurélie, Mélanie, Louise, Xavier, Thomas 2, Roxane et Léa. Merci pour la bonne ambiance et l'entre-aide continue ! Sans vous, ma thèse n'aurait pas été la même. Merci pour tous ces bons moments passés, et tous les fous rires, au labo et en dehors.

Hélène, tu as été ma première rencontre au labo et ma première amie à Liège. Merci d'avoir aidé une bruxelloise à se sentir un peu moins perdue et seule dans cette nouvelle ville. Durant ces quatre années, on aura partagé beaucoup de choses. Au-delà de ton soutien au laboratoire et de l'entre-aide, merci de m'avoir fait un peu découvrir ta région et pour les nombreux moments passés ensemble. Cette thèse n'aurait pas été pareille sans toi.

Clotilde, merci pour les discussions que nous avons eues pour les encouragements. Je regrette de n'avoir pas pu partir en Australie avec Hélène et toi ! Si Nantes en était un aperçu, il ne fait nul doutes que ce voyage aurait été extraordinaire et ponctué de nombreux fous rires.

Thomas 1, on aura commencé cette aventure en même temps et on y sera arrivés ! On se connaissait avant, mais j'ai découvert une belle personne lors de ces quatre années. On se sera serré les coudes, merci de m'avoir (souvent) écoutée. Grâce à toi, j'aurai aussi découvert que les cellules n'apprécient pas le hard rock ni le métal haha. Courage pour la dernière ligne droite, tu y es presque !

Alexis, ton aide pour cette fin de thèse aura vraiment été précieuse ! Je te serai à jamais reconnaissante pour mon article clinique et pour ton aide lors de celui-ci. Je ne pense pas que j'aurais aussi bien géré la situation sans ton aide. Merci également d'être toujours disponible pour échanger des idées et aider.

Aurélie, on n'aura pas beaucoup travaillé ensemble car nos sujets ne s'y prêtent pas. Cependant, on aura quand même bien rigolé. Tu as toujours le petit mot ou la petite phrase bien placée ☺.

Méla, malheureusement on n'aura pas bossé longtemps ensemble mais « ce fût bref mais intense » haha. Évidemment, merci pour ton aide aux souris, mais surtout merci pour ta bonne humeur, ton franc parlé et ton humour. Ton passage au laboratoire ne sera pas passé inaperçu. Tes nouveaux collègues ont de la chance de t'avoir ☺.

Louise, d'abord cokotteuse, puis TFIste et maintenant collègues. Quel chemin parcouru ! A part ton aide évidente dans les manips et au labo, tu as également su me porter une oreille attentive quand j'en avais besoin et je t'en remercie. Bonne chance pour la suite de ta thèse, tu en es plus que capable !

Roxane et Léa, votre arrivée au labo est beaucoup plus récente mais vous faites déjà partie intégrante de l'équipe. Je suis heureuse de vous avoir rencontrées. Vous êtes toute les deux de belles personnes que j'apprécie énormément ! Je vous souhaite beaucoup de courage pour les années à venir, mais nul doute que vous allez vous serrer les coudes avec les autres et que vous allez y arriver. Roxane, tu es souvent là pour aider les autres au besoin. Léa, merci pour ton aide en bioinformatique, j'ai déjà beaucoup appris grâce à toi !

Xavier et Thomas 2, on a un peu moins eu l'occasion de discuter mais vous m'avez déjà bien fait rire. Courage pour la suite !

J'aimerais aussi remercier Jean-Rock tout d'abord pour son aide au labo mais aussi pour l'organisation des évènements (dont on ne se lasse pas). Merci pour les nombreux fou-rire et pour ton soutien sans faille. Finalement, encore merci de m'avoir poussée à demander un TFE à Luc car sans ça, je n'en serais pas là.

Finalement, je tiens à remercier les deux étudiantes que j'ai eu la chance d'encadrer lors de leurs TFE, Hélène H et Louise. Vous encadrer a été une opportunité géniale. Merci pour votre travail. Je vous souhaite beaucoup de réussite pour la suite.

Je tiens également à remercier sincèrement Audrey pour son aide et la gestion de la culture cellulaire mais surtout, pour son écoute. Je pense que tu as eu droit à tous les moments pas faciles, mais tu as toujours su poser une oreille attentive et trouver les mots justes.

Merci également aux membres de la plateforme imagerie : Alex, Gaëtan, Rafaat et Céline. Merci pour votre aide précieuse dans les analyses confocales et cytométrie en flux.

Je tiens ensuite à remercier tout particulièrement mon parrain, Alex, sans qui je n'en saurais sûrement pas là aujourd'hui. Merci pour ton soutien, ton aide durant mon master ainsi que pour tes conseils pertinents et avisés. Merci d'avoir pris le temps d'ouvrir mes cours de Math et « Froid et sec » ! Merci de m'avoir prêté une oreille attentive dans les moments les plus difficiles.

Évidemment, merci également à mes parents et mes beaux-parents. Vous avez souvent entendu parler de cette thèse et bien que vous n'ailliez pas toujours tout

compris, vous m'avez également prodigué de précieux conseils. Merci de m'avoir soutenue et d'avoir toujours cru en moi lors de mon parcours parfois (souvent) semé d'embuches et avez su m'aider à remonter la pente. Merci de m'avoir écoutée lors des moments de doutes.

Merci aussi à mon frère Colin qui, bien que tu n'aies quasi rien compris à ma thèse, m'as toujours écoutée et soutenue. Toi-même tu sais.

Finalement, je ne peux pas ne pas remercier mes ami(e)s ! Ces quatre dernières années loin ne nous auront pas empêché de nous voir même si j'aurai été un peu (beaucoup) moins disponible.

My et Amélie, je crois que vous aurez vécu ma thèse avec moi haha ! Toujours là pour m'écouter, me soutenir et rigoler. J'ai pu tout vous dire et ça m'a beaucoup aidée, merci mille fois les filles !

Jelica et Ced (et My, encore haha), toujours prêts à rigoler. Vous m'avez à de nombreuses fois aidée à me changer les idées et merci pour ça !

Clément, Lucie, Martin et Elaine, nous avons chacun pris des directions différentes mais nous sommes toujours là les uns pour les autres et c'est ça qui compte. Merci pour tout !

Margaux et Marie, les années ont passé depuis la secondaire et vous êtes toujours là ! Vous êtes toujours là pour les moments importants. Merci les copines !

Alex, merci pour ton soutien et ton intérêt constant pour mon travail. Tu es beaucoup plus loin maintenant, mais cela ne t'empêche pas d'être présent à ta manière. Merci pour les nombreux « memes » scientifiques qui m'auront bien fait rire haha.

Caro, à force de vivre en colloc, tu n'auras pas eu le choix que d'être témoin de toutes mes humeurs liées au boulot et à la thèse. Merci pour ton écoute et ton soutien ! Merci aussi pour les nombreuses soirées vins/sushi. Merci aussi à Sylvie pour les nombreuses soirées repas haha.

Table of contents

List of figures

List of tables

List of acronyms

ABC	ATP Binding Cassette
ADCC	Antibody-Dependent Cellular Toxicity
AEC	Absolute Eosinophil Count
AML	Acute Myeloid Leukaemia
Ang1	Angiopoietin 1
APC	Antigen Presenting Cell
APRIL	Activation and Proliferation-Inducing Ligand
ATP7A	P-type ATPase 1
ATP7B	P-type ATPase 2
BP	Biological Process
CCL	Chemokine Ligand
CFSE	Carboxyfluorescein Succinimidyl Ester
CLC	Charcot-Leyden Crystal
CLC-P	Charcot-Leyden Crystal Protein
CMP	Common Myeloid Progenitor
CRC	Colorectal Cancer
CRD	Carbohydrate-Recognition Domain
CT	Computed Tomography
CTLA4	Cytotoxic T-lymphocyte 4
CTR1	Copper Transporter 1
CTR2	Copper Transporter 2
DAMP	Damage-Associated Molecular Pattern
DC	Dendritic cell
DCR	Disease control rate
DDS	Double strand breaks
Dif-EOL1	Differentiated EOL1
DHF	Dihydrofolate
DHFR	Dihydrofolate Reductase
DRESS	Drug Rash with Eosinophilia and Systemic Symptoms

dTMP	Deoxythymidine Monophosphate
dUMP	Deoxyuridine Monophosphate
ECOG	European Cooperative Oncology Group
ECP	Eosinophil Cationic Protein
EDN	Eosinophil-Derived Neurotoxin
EET	Eosinophil Extracellular Trap
EoP	Eosinophil Progenitor
EPE	Eosinophilic Pleural Effusion
EPX	Eosinophil Peroxidase
ER	Endoplasmic Reticulum
EZH2	Enhancer of Zeste Homolog 2
FC	Constant Fragment
FDA	U.S. Food and Drug Administration
FELASA	Federation of Laboratory Animal Science Association
FR-α	Folate Receptor-α
FSC	Forward Scatter
Gal10	Galectin-10
GARFT	Glycinamide Ribonucleotide Formyltransferase
GG-NER	Global Genomic NER
GI tract	Gastro-Intestinal tract
GM-CSF	Granulocyte Macrophage-Colony-Stimulating Factor
GMCSF- Rα	GM-CSF Receptor subunit alpha
GMP	Granulocyte-Macrophage Progenitor
GO	Gene Ontology
GSH	Glutathione
GSTπ	GSH-S-transferase
H3K27	Histone H3 Lysine 27
HE	Hypereosinophilia
HES	Hypereosinophilic Syndrome
HIV	Human Immunodeficiency Virus
HSC	Hematopoietic Stem Cell

IARC	International Agency for Research on Cancer
ICI	Immune Checkpoint Inhibitor
iEos	Inflammatory Eosinophils
Ig	Immunoglobulin
IL-3Rα	IL-3 Receptor subunit alpha
IL-5Rα	IL-5 Receptor subunit alpha
ILC	Innate Lymphoid Cell
INF-α/γ	Interferon alpha/gamma
kDa	Kilodalton
KEGG	Kyoto Encyclopedia for Genes and Genomes
LAG-3	Lymphocyte-Activation Gene 3
LPLase	Lysophospholipase
MBP	Major Basic Protein
MBP	Major Basic Protein
MCP	Monocyte Chemotactic Protein
MDSCs	Myeloid-Derived Suppressor Cells
MF	Molecular Function
MHC	Major Histocompatibility Complex
MIP-1α	Macrophage Inflammatory Protein-1 Alpha
MMP	Matrix Metalloproteinase
MMR	Mismatch Repair
MRP	Multidrug Resistance-associated Protein
MT	Metallothionein
NEA	N-ethylmaleimide
NER	Nucleotide Excision Repair
NET	Neutrophil Extracellular Trap
NF-κB	Nuclear Factor-κB
NOD	Nucleotide-binding Oligomerization Domain protein
OCT2	Organic Cation Transporter 2
ORR	Overall Response Rate
OS	Overall Survival

PAMP	Pathogen-Associated Molecular Pattern
PBE	Peripheral Blood Eosinophilia
PCFT	Proton-Coupled Folate Receptor
PD-1	Programmed Cell Death 1
PET	Positron Emission Tomography
PFA	Paraformaldehyde
PFS	Progression-Free Survival
pI	Isoelectric point
PM	Pleural Mesothelioma
PRG2	Proteoglycan 2
PRR	Pattern Recognition Receptor
RAGE	Receptor for Advanced Glycation End-products
RANTES	Regulated upon Activation, Normal T cell Expressed and Secreted
rEos	Tissue-Resident Eosinophils
RFC	Reduced Folate receptor
RIG-1	Retinoic acid-Inducible Gene I
RNAse	Ribonuclease
RNS	Reactive nitrogen species
ROS	Reactive oxygen species
SA-β-gal	Senescence-Associated β-Galactosidase
SARS-CoV-2	Serve Acute Respiratory Syndrome Coronavirus 2
SASP	Senescence-Associated Secretory Phenotype
scRNAseq	Single-cell RNA sequencing
Siglec-8/F	Sialic acid-binding Immunoglobulin-like Lectin 8/F
SSC	Side Scatter
TAMs	Tumour-Associated Macrophages
TATE	Tumour-Associated Tissue Eosinophilia
TC-NER	Transcription-Coupled NER
TCR	T-cell receptor
TGF-β	transforming growth factor-β
THF	Tetrahydrofolate

TILs	Tumour-Infiltrating Lymphocytes
TIM-3	T-cell immunoglobulin and mucin domain containing-3
TLR	Toll-Like Receptor
TME	Tumour Microenvironment
TMN	Tumour-Node Metastasis
TNF-α	Tumour Necrosis Factor Alpha
Treg	Regulatory T cells
TS	Thymidylate Synthase
UICC	Union for International Cancer Control
VEGF	Vascular Endothelial Growth Factor
WHO	World Health Organization
WT-1	Wilm's-Tumour 1

Chapter 1

Introduction

1. Pleural mesothelioma

Mesothelioma is a rare and aggressive cancer that arises from the mesothelial cells lining serous surfaces such as the pleura, peritoneal and pericardial cavities and, less frequently, the tunica vaginalis. Pleural mesothelioma (MPM) is the most common form of mesothelioma, accounting for 70 – 80% of the cases, followed by peritoneal mesothelioma (10 – 30%) [1–3] (**Figure 1**). MPM is a relatively rare cancer with world-standardized incidence rates per 100,000 persons of 0.7 and 0.3 in United States, and 1.7 and 0.4 in Europe for males and females, respectively [4].

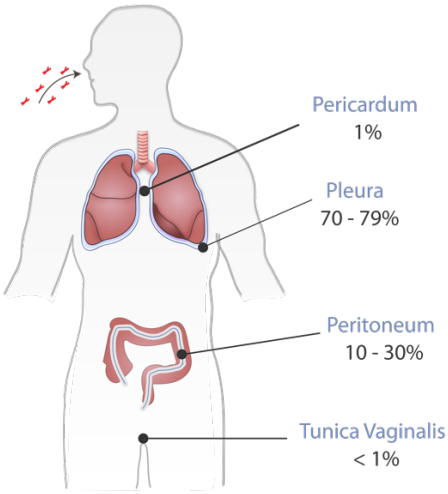

Figure 1 – **Mesothelioma localization.** Pleural mesothelioma (MPM) represents 70 – 80% of mesothelioma cases. Peritoneal, pericardial and testicular mesothelioma are rare.

1.1. Histology

According to histological morphology, three main subtypes are identified: epithelioid (60-80%), sarcomatoid (10%) and biphasic (10-15%) which is a mixture of epithelioid and sarcomatoid features (**Figure 2**) [4,5]. While all MPM subtypes are aggressive tumours with poor prognosis (9-12 months), several studies highlight a link between histological subtype and patient's outcome [6]. With 12–27 months of survival, the epithelioid subtype has the best prognosis. In contrast, survival time in sarcomatoid MPM is only 4–18 months. The biphasic subtype depends on the proportion of sarcomatoid and epithelioid features but has an intermediate prognosis of 5–21 months [2,7]. Histological characterization is thus of importance.

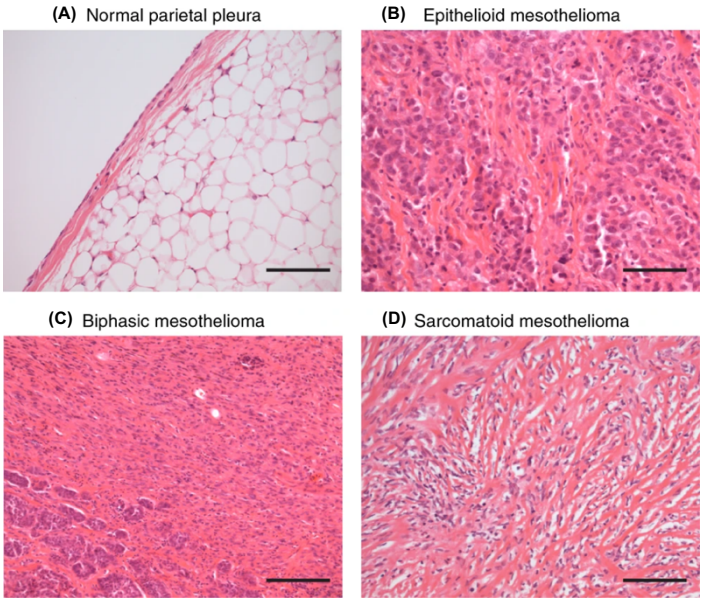

Figure 2 – Mesothelioma histological subtypes compared to normal pleura. Haematoxylin and eosin staining of normal pleura **(A)**, epithelioid **(B)**, sarcomatoid **(C)** and biphasic **(D)** MPM subtypes, revealing flat and cuboidal cells for epithelioid MPM *versus* spindle cells and abundant stroma in sarcomatoid MPM. Scale bar = 200 µM. (Obacz J. *et al*, 2021)

1.2. Aetiology

1.2.1. Asbestos

Asbestos, the commercial name derived from the ancient Greek term "*amiantos*" meaning imperishable, refers to a group of six naturally occurring fibrous crystalline [2,8]. This group is divided in two major subgroups, according to chemical composition and crystalline structure (**Table 1**). The first group, called amphiboles, comprises of crocidolite, actinolite, tremolite, anthophyllite and amosite whereas the second, called serpentine, only contains chrysotile, the most commercially distributed form [9].

For a long time, asbestos has been viewed as a "magic mineral" because of its low price and great physical properties. Indeed, asbestos presents a high heath resistance, flexibility, strength and insulation properties in term of electricity, acoustic and heath.

Table 1 – Different asbestos types, properties and historic use.

Group	Asbestos type	Usual name	Properties	Historic use
Serpentine	Chrysotile	White asbestos	Long, curly fibres that weaves and are composed of calcium, magnesium, and iron oxides	Construction (*e.g.*, cement, asphalt), automotive parts (*e.g.,* brakes, disks), textiles, plastics, roof sealants, boiler rubber door sealing, paper
Amphiboles	Crocidolite	Blue asbestos	Fibres of small size mainly composed of iron and sodium silicate	Cement, insulation, roof tiles and floor tiles
	Tremolite	–	Long, thin, and flexible fibres composed of iron, magnesium and chrome	Plumbing, insulation, sealants, paints, roof tiles and found in talc.
	Amosite	Brown asbestos	Thin, needle-like fibres with high level of heath resistance and composed of iron and magnesium	Cement, insulation (chemical, electrical and acoustic), pipes fittings, ceiling tiles, fireproof products, joints, structural steel
	Anthophyllite	–	Long, needle-like fibres primarily composed of iron and magnesium	Rarely used but occasionally found in cement and isolation
	Actinolite	–	Long, sharp, and flexible fibres composed of iron, magnesium, calcium and silicon.	Rarely used but sometimes used in drywall, cement, insulation, paint and sealant

According to the World Health Organization (WHO) and the International Agency for Research on Cancer (IARC), all types of asbestos are classified as type I carcinogens (*i.e.,* definite carcinogen to humans) [10]. The link between asbestos and MPM development has been demonstrated more than 50 years ago by a direct relationship between national asbestos consumption and deaths due to asbestosis and MPM [8,11].

Occupational asbestos exposure is the principal risk factor for MPM (~80% of cases) [12]. The high-risk categories include plumbers, seamen, mechanics, electricians, smelting workers, welders and painters for men, and woodworkers, glass makers, textile workers and building caretakers [8]. Besides occupational exposure, para-occupational and domestic exposure have been identified as risk factors. Those are mainly associated to living with an asbestos worker or washing clothes of an asbestos worker [10]. Neighbourhood exposure to mines and asbestos-related industries has also been linked with MPM development. Finally, naturally occurring asbestos found in a number of regions such as Greece, Italy and Turkey also accounts for MPM cases [8].

Despite the complete or partial ban of asbestos use since the 1970's in most countries, incidence of MPM is still increasing worldwide [13,14]. This is mainly due to the long latency period of 30 to 60 years between exposure and neoplasm development

[13,15]. Asbestos exposure also persists due to already installed asbestos-containing materials or naturally occurring asbestos [14]. Furthermore, asbestos use is still increasing in some countries, such as India and China, because of its unique physical properties [16,17].

Of note, the exposition to asbestos does not necessarily lead to mesothelioma, as only ~5% of the high-risk workers exposed to asbestos are at risk to develop mesothelioma [18]. Furthermore, half of the asbestos-related workers will die of some asbestos-related condition, other than mesothelioma. Indeed, asbestos exposure as also been linked with lung cancer, ovarian cancer, laryngeal cancer, gastrointestinal (GI) tract cancers (oesophagus, stomach and colorectal). [17]

1.2.2. Non-asbestos causes

Despite asbestos being identified as the main cause of mesothelioma, about 20% of patients have never been exposed to asbestos [19]. Furthermore, rare cases of mesothelioma in children have been reported [12]. As mesothelioma develops after a long latency period following asbestos exposure (~30 to 60 years), those cases also suggest that other factors are involved in mesothelioma.

First, other fibres such as erionite and fluoroendenite have been linked to mesothelioma cases in some clusters [12,19]. Indeed, **erionite** is another naturally occurring silicate mineral that belongs to the zeolite group and that possess similar properties to crocidolite. It composes zeolite stones used to build houses in Cappadocian villages in Turkey and North Dakota where high incidences of mesothelioma cases have been observed [20,21]. Studies in mice have also highlighted that erionite is more carcinogenic than asbestos [19].

In addition, nanotechnologies and, more especially, **carbon nanotubes** are widely used in industrial, medical and environmental applications. However, concerns have been raised about medical and environmental health as carbon nanotubes share physical (shape and diameters) and cytotoxic properties with asbestos fibres [19]. Furthermore, studies in mice have highlighted a link between mesothelioma and carbon nanotubes [22]. This suggests that carbon nanotubes could have the same effects in the lungs as asbestos fibres.

Finally, patients that have undergone **ionizing radiotherapy** for primary tumours in the abdominal-pelvic area have a significant risk to develop mesothelioma. The radioactive contrast product “Thorotrast” has also been reported as a possible cause of mesothelioma. [23]

1.3. Tumorigenesis

How asbestos fibres reach the pleura is still not totally known. Inhaled asbestos fibres pass from the nasal cavity to the trachea and then to the lung parenchyma where they go to the pleural space through the pulmonary alveoli. Asbestos fibres proceed through the pleura towards the visceral pleura under the negative pressure of the pleural cavity [24]. Fibres will finally reach the parietal pleura where most cases of MPM occur [25,26].

Under normal conditions, particles that enter the pleural space are eliminated by the pleural fluid to the nearest lymph node through stomata (**Figure 3**) [25]. However, some asbestos fibres are too long to pass the stomata and thus accumulate in the parietal pleura [27]. As these fibres cannot dissolve or fragment into shorter fibres, they will cause pleural irritation and lead to biological events that will eventually lead to the development of MPM [25,28,29].

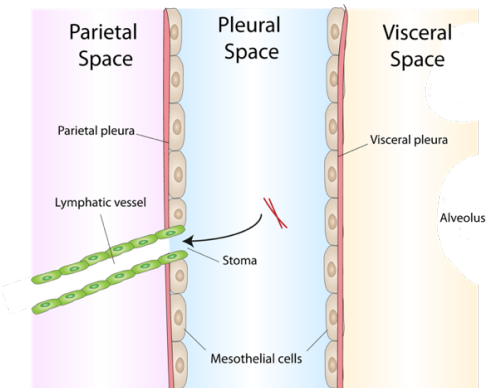

Figure 3 – Schematic representation of fibre clearance. Inhaled fibres pass from the alveoli to the pleural space. Fibres are eliminated by the pleural fluid through a stoma in the parietal pleura into a lymphatic vessel to enter lymph flow.

The precise tumorigenesis of mesothelioma remains unclear but is multifactorial and depends on exposition as well as fibre type, size and shape, biopersistence and surface properties [30,31]. When asbestos fibres accumulate in the pleura, they can directly interact with MPM cells through the iron they are associated with. This interaction will lead to the production of reactive oxygen (ROS) and nitrogen (RNS) species via the Fenton reaction [24]. Furthermore, mesothelial cells in contact with asbestos fibres produce inflammatory cytokines and growth factors such as vascular endothelial growth factor (VEGF) that will attract leukocytes at the site of inflammation [2,25]. Recruited macrophages will attempt to phagocyte the fibres and will undergo "frustrated phagocytosis", which will lead to the production of ROS, inflammatory cytokines and free radicals [25].

The production of cytokines by mesothelial cells and macrophages will persists as fibres aren't cleared. This ongoing inflammatory environment will lead to the malignant development of mesothelial cells and onset of MPM [2] (**Figure 4**).

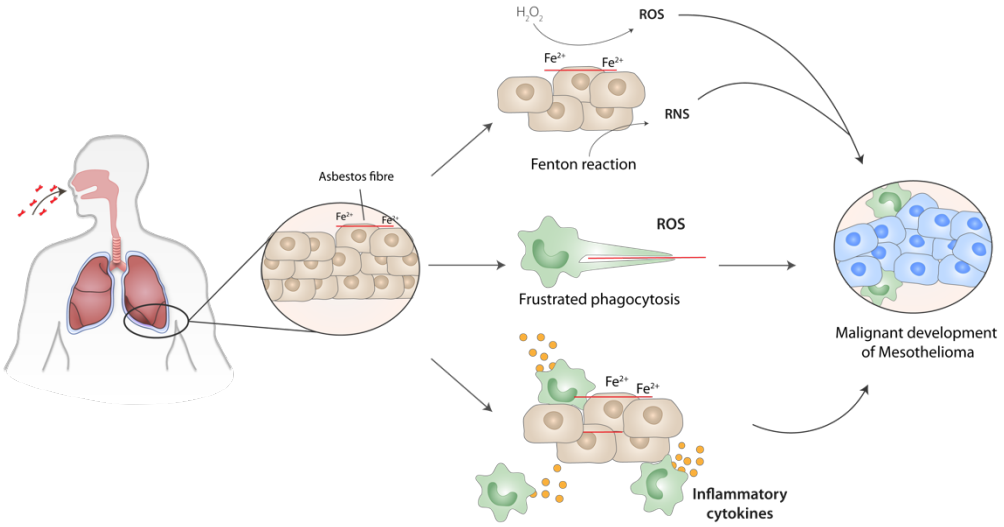

Figure 4 – Pleural mesothelioma tumorigenesis. Mesothelial cells in contact with asbestos fibres produce inflammatory cytokines and growth factors. This will attract pleural macrophages which will attempt to phagocyte the fibres. Unable to phagocyte the fibres, macrophages will undergo the so-called "frustrated phagocytosis" which will lead to the production of ROS, inflammatory cytokines, and free radicals. In addition to the inflammatory cytokines produced by mesothelial cells, this inflammatory environment will eventually lead to pleural mesothelioma development.

1.4. Microenvironment

The tumour microenvironment (TME), as illustrated previously with the infiltration of macrophages, is crucial for MPM pathogenesis, tumour growth, invasion, and outcome. The cellular composition of MPM microenvironment is heterogenous and contains endothelial, stromal and immune cells [2,32]. Besides this intra-tumour heterogeneity, the microenvironment also varies among patients and histological types of MPM [32]. Generally, the infiltrating immune cells include tumour-associated macrophages (TAMs), tumour-infiltrating lymphocytes (TILs), myeloid-derived suppressor cells (MDSCs), granulocytes and NK cells [32–34]. Of those, TAMs and TILs are the most abundant cells found in MPM [32]. As MPM arises from asbestos exposure and chronic inflammation, its microenvironment is unique and mainly immunosuppressive [2,35].

TAMs represent 25% to 42% of immune cells infiltrating MPM [32,36]. They are mainly derived from blood-circulating monocytes differentiation after migration in the tissue. Macrophages are known for their plasticity and, depending on the TME, will be activated in either M1 or M2-TAMs [37]. Of note, this dichotomic activation model is an oversimplification used for laboratory studies, and transcriptomic analysis highlighted that a continuous spectrum exists in-between M1 and M2 [38,39]. M1-like macrophages exert pro-inflammatory and antitumor activity, whereas M2-like macrophages are seen as pro-tumorigenic and participate in immunosuppression.

In MPM, M2-like macrophages have been found in tissues and pleural effusions [40]. Moreover, pleural effusions from MPM patients have been shown to recruit monocytes and polarize them into M2-like macrophages [41]. In this light, proportion of M2-like macrophages has been suggested to be a prognosis factor for MPM [42]. However, this conclusion is controversial and the prognosis role of M2-like macrophages is still debated [36].

After TAMs, $CD3^+$ TILs are the second most abundant immune cells in MPM microenvironment, with infiltration ranging from 20 to 42% of the immune cell infiltrate [33,36,43]. Circulating T-cells are activated in secondary lymphoid organs via their T-cell receptor (TCR) and their major histocompatibility complex (MHC) by antigen presenting cells (APCs) [44]. TILs can be distinguished in two categories: $CD4^+$ T cells (or T helper), which present pro-tumorigenic properties, and $CD8^+$ T-cells (or T cytotoxic), presenting cytotoxic properties. Among those, $CD8^+$ T-cells are the most predominant T-cells in MPM and are linked to a favourable prognosis [32,36]. Of note, $CD4^+$ T helpers enhance the cytotoxic activity of $CD8^+$ T-cells [43].

However, due to chronic stimulation of their TCR with MHCI, and combined with co-stimulatory signalling through anti-cytotoxic T-lymphocyte 4 (CTLA-4), TILs become anergic or "exhausted" [45–48]. CTLA-4 is exclusively expressed by T-cells and regulates the amplitude of their activation [43,49]. CTLA-4 interacts with the co-stimulatory receptors CD80 (B7-1) and CD86 (B7-2) expressed by macrophages, DCs, and B-cells, preventing their binding to CD28 and inhibiting the subsequent T-cell activation and proliferation [50]. These T-cells are then functionally deficient. T-cell exhaustion is molecularly distinct from **T-cell anergy**, which is a state of non-responsiveness following antigen presentation [50]. **Exhaustion** is a dysfunction of antigen-specific T-cells with hierarchical loss of cytokine production, proliferative and cytotoxic capacity [45,50]. Features of this dysfunctional state include overexpression, simultaneously or not, of co-inhibitory receptors such as CTLA-4, programmed cell death 1 (PD-1), lymphocyte-activation gene 3 (LAG-3, CD223), and the T-cell immunoglobulin and mucin domain containing-3 (TIM-3, CD366) [45].

1.5. Diagnosis

Usually, MPM patients are diagnosed at a late stage because of the late onset and non-specific symptoms. Indeed, those symptoms usually include unilateral pain in the chest, fatigue, fever, cough and dyspnoea [51]. Those symptoms cannot be used alone as diagnosis criteria. Indeed, the standard diagnosis includes several workups including anamnesis of occupational history with emphasis on asbestos exposure, several imaging exams, immunohistochemical staining and blood tests [4,52].

Imaging techniques include chest X-ray, computed tomography (CT) scan and positron emission tomography (PET)-CT which can reveal pleural effusion and/or thickening, which are indicative of MPM, but lacks the necessary sensitivity for MPM diagnosis [4]. However, they are used for disease staging through tumour-node metastasis (TMN) classification. If the initial anamnesis and imaging techniques are indicative of MPM, pathological sampling of pleural effusion or a biopsy is recommended. Pleural effusion cytology is controversial and thus the final diagnosis is made by immunohistochemical staining of biopsies (usually thoracoscopic) [52]. Immunohistochemistry is based on several biomarkers and can help make the distinction between adenocarcinoma and MPM, but also allows for histological subtype identification [6,53]. Indeed, the combination of two mesothelioma (*e.g.,* calretinin, Wilm's-Tumour 1 (WT-1), mesothelin) and two adenocarcinoma (*e.g.*, MOC-31, Ber-EP4, thyroid transcription factor 1) markers is recommended for MPM diagnosis [54,55]. This is sufficient for the epithelioid subtype but for sarcomatoid subtype discrimination, cytokeratin 5/6 staining is also recommended [4].

1.5.1. Staging

Staging of the disease is of importance as it can help determine the followings steps for treatment or palliative care. Currently, the 8th revision of the Union for International Cancer Control (UICC) TMN classification of malignant tumours is used for MPM. It is based on the description of the primary tumour size (T), the presence or not of lymph node metastasis (N) and distant metastasis (M) (**Table 2**). Staging of the disease is based on the grouping of the TMN classification (**Table 3**).[4,52,56]

Table 2 – 8th revision of the Union International Cancer Control (UICC) TMN classification of malignant tumours. The classification is based on the description of the primary tumour size (T), presence of lymph node metastasis (N) and distant metastasis (M).

Stage	Category	Description
T	Tx	Primary tumour cannot be assessed
	T0	No evidence of primary tumour
	T1	Tumour involving ipsilateral pleura (previously T1a) or visceral pleura (previously T1b) pleura only
	T2	Tumour involves ipsilateral pleura or visceral pleura with at least one of the following features: - Lung parenchyma invasion - Diaphragm muscle involvement - Confluent visceral pleural tumour (including fissures)
	T3	Tumour involves ipsilateral pleura or visceral pleura with at least one of the following features: - Endothoracic fascia invasion - Extension into the mediastinal fat - Solitary, completely respectable focus invading soft tissues of the chest wall - Non-transmural pericardium invasion
	T4	Tumour involves ipsilateral pleura or visceral pleura with at least one of the following: - Soft tissues of the chest wall diffuse or multifocal invasion - Any rib involvement - Peritoneum invasion through the diaphragm - Any mediastinal organ invasion - Direct extension to the contralateral pleura - Spine or brachial plexus invasion - Pericardium transmural invasion (with or without pericardial effusion) or myocardium invasion
N	Nx	Regional lymph nodes not assessable
	N0	No regional lymph node metastases
	N1	Metastases in the ipsilateral bronchopulmonary, hilar, or mediastinal lymph nodes (including the internal mammary, peridiaphragmatic, pericardial fat pad, or intercostal lymph nodes)
	N2	Metastases in the contralateral bronchopulmonary, hilar, or mediastinal lymph nodes or ipsilateral or contralateral supraclavicular lymph nodes
M	Mx	Presence of distant metastases not assessable
	M1	No evidence of distant metastases
	M2	Evidence of distant metastases

Table 3 – Stage grouping according to TMN classification.

Stage	T	N	M
I			
Ia	T1	N0	M0
Ib	T2,3	N0	M0
II	T1,2	N1	M0
III			
IIIa	T3	N1	M0
IIIb	T1–3	N2	M0
IV	T4	N0–2	M0
	Any T	Any N	M1

1.6. Treatments

To this day, MPM is still an incurable cancer with a poor prognosis, with patients 5-year overall survival (OS) of 5-10% after diagnosis [57–59]. First-line treatments options in MPM include surgery, radiotherapy, systemic therapy, and immunotherapy. Treatment strategy is guided by staging, histological subtype, age, patient's functional status and preference [3,4]. Indeed, historically, age, sex, tumour grade and stage, and histology have been shown to be independent prognostic factors [60]. Surgery and radiotherapy are thus limited to a small subset of patients with early-stage disease [12].

1.6.1. Chemotherapy

Until recently, chemotherapy based on a DNA crosslinking agent, cisplatin or carboplatin, and an antifolate, pemetrexed, has been the only modality to improve OS for patients [61,62]. The phase III clinical trial conducted by Vogelzang *et al.* demonstrated an OS benefit of 12.1 months *vs* 9.3 months for the combination compared to cisplatin monotherapy [63]. Of note, in the MAPS study, the addition of bevacizumab, an anti-VEGF antibody, to this regimen improved median OS up to 18.8 months vs 16.0 months in the control arm [61]. Despite this improvement in OS, bevacizumab has not received approval for MPM treatment by the U.S. Food and Drug Administration (FDA) or European Medicines Agency because it was not designed as a registration trial [51].

Since 2003 and until 2021, the standard-of-care for unresectable MPM has thus remained the chemotherapy based on the combination cisplatin and pemetrexed [63].

Pemetrexed is internalized by the cells through three membrane receptors: the reduced folate receptor (RFC), the folate receptor-α (FR-α), and the proton-coupled folate receptor (PCFT) [64]. Once in the cytoplasm, pemetrexed is polyglutamated by folylpolyglutamate synthetase (FPGS) to its pharmacologically active form: pentaglutamated pemetrexed [65]. Pentaglutamated pemetrexed then inhibits at least three enzymes that are crucial for the folate pathway: thymidylate synthase (TS), dihydrofolate reductase (DHFR) and glycinamide ribonucleotide formyltransferase (GARFT) [65]. TS catalyses the transformation of deoxyuridine monophosphate (dUMP) to deoxythymidine monophosphate (dTMP), whereas DHFR catalyses the reduction of dihydrofolate (DHF) to tetrahydrofolate (THF) [66]. GARFT catalyses THF transformation to methylene-THF. TS and DHFR are enzymes involved in pyrimidine synthesis, whereas GARFT is involved in *de novo* purine biosynthesis. Thereby, pemetrexed inhibits DNA synthesis, cell replication and DNA repair (**Figure 5**)[67,68]. Among the three enzymes, TS is believed to be the main target of pemetrexed [69].

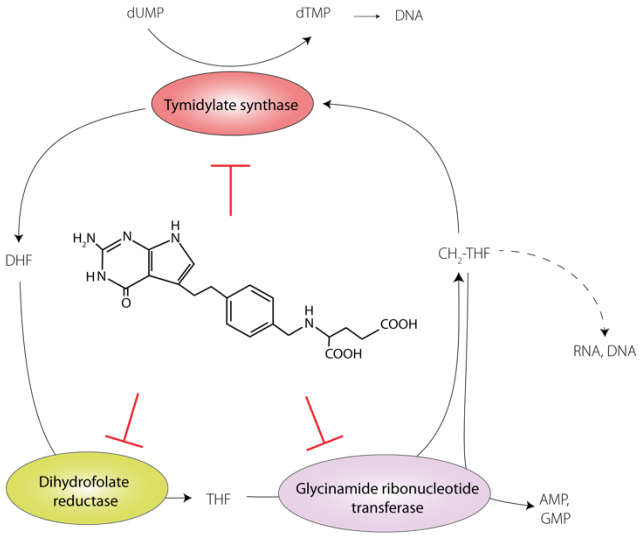

Figure 5 – Pemetrexed mechanism of action. Pemetrexed inhibits the three folate-dependent enzymes: thymidylate synthase, dihydrofolate reductase and glycinamide ribonucleotide transferase. The inhibition of these enzymes leads to DNA synthesis, cell replication and DNA repair impairment.

Cisplatin, on the other hand, is uptaken by cells via the copper transporter 1 (CTR1) or through passive diffusion across the plasma membrane under a chloride gradient [70]. In the cytoplasm, cisplatin is activated by hydrolyzation because of the low concentration of chloride in the cytoplasm (~ 4–20 mM *vs* 100 mM in the bloodstream) [71]. The chloride ligand is then replaced by a single or two molecules of water (*i.e.*, mono- or di-aquation), the mono-aquated form being the most reactive. The formed component is a potent electrophile that can react with a nucleophile such as nitrogen donors on nucleic acids [70,72]. Activated cisplatin forms cisplatin-DNA adducts through covalent bonds to the N7-site purine residue, which induces interstrand and intrastrand crosslinks [68,70]. Those crosslinks interfere with DNA replication, which arrests the cell cycle in S phase in an effort to repair the damage [50,73]. If the damage is not repaired by the DNA damage reparation machinery, the crosslinks lead to DNA double strand breaks (DDS), which will eventually lead to apoptosis (**Figure 6**) [72].

Beyond DNA damage, aquated cisplatin can also react with proteins, which has been linked to cellular damage [68,72]. The oxidative stress created by the production of ROS can induce apoptosis both through intrinsic and extrinsic pathways [70].

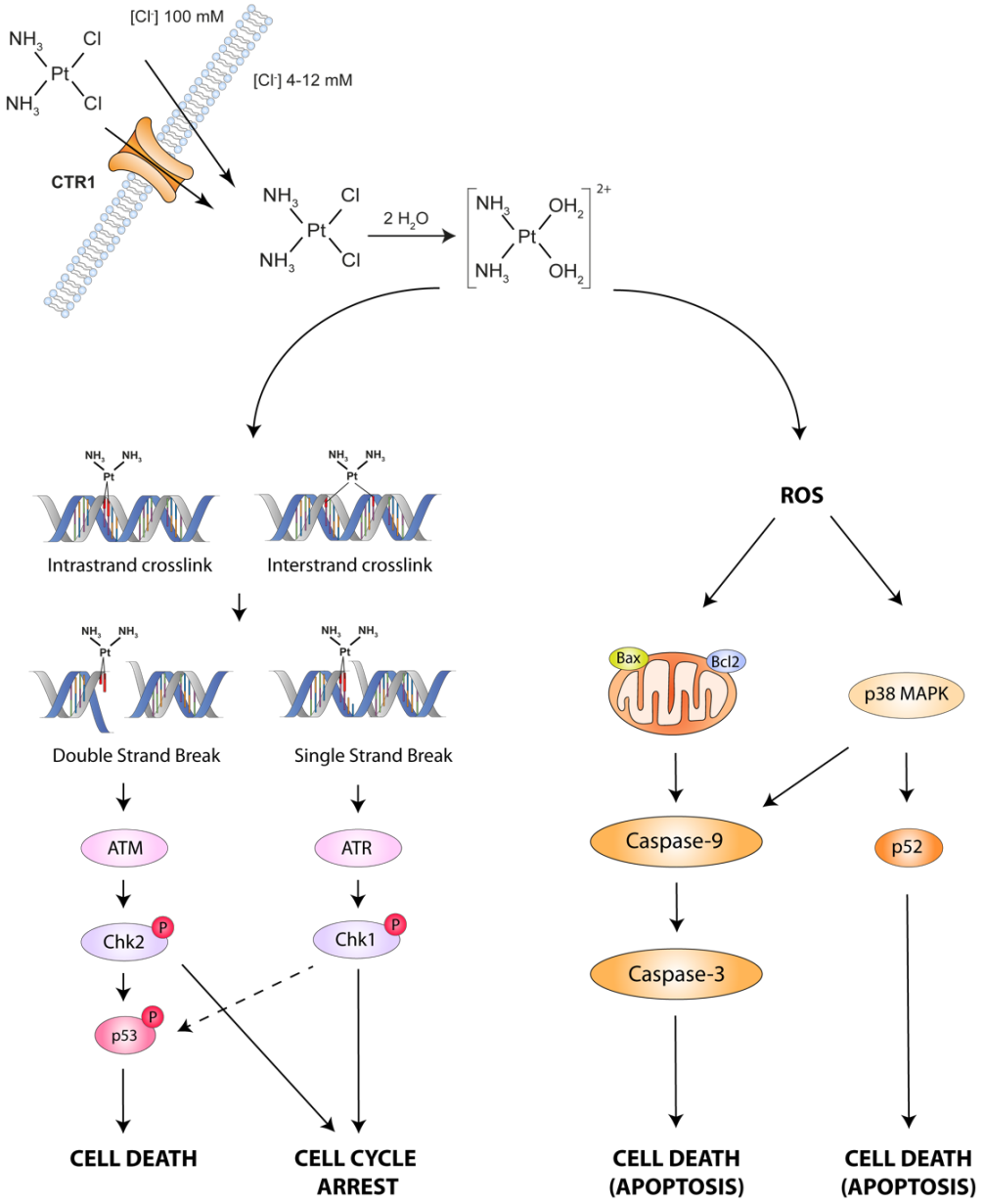

Figure 6 – Cisplatin intrinsic mechanisms of action. Cisplatin forms adducts with DNA, resulting in interstrand or intrastrand links that, unrepaired, lead to DNA strand breaks, apoptosis, and cell cycle arrest. Cisplatin also induces to oxidative stress leading to apoptosis.

1.6.2. Chemoresistance

The major drawback of chemotherapy is that patients relapse quickly and become resistant to the treatment.

Regarding cisplatin, three intracellular adaptative mechanisms have been accepted to be responsible for driving cisplatin resistance: alteration of accumulation, intracellular detoxification and DNA damage repair (**Figure 7**) [70,71,74]. The reduction of cellular accumulation is the most prominent mechanism of cisplatin resistance. It can be the results of two independent mechanisms: intracellular uptake or export. First, as the uptake of cisplatin is mediated by CTR1, its reduced expression is correlated with cisplatin resistance [75]. Indeed, studies in cervical cancer and lung cancer have demonstrated that CTR1 expression inversely correlates with cancer cells resistance to cisplatin [76–78]. This mechanism may thus account for instances of acquired cisplatin resistance observed with clinically relevant doses of cisplatin [79]. Others ions transporters, the copper transporter 2 (CTR2) and the organic cation transporter 2 (OCT2), have also been correlated with cisplatin resistance [80]. However, this has only been demonstrated in certain types of cancers.

Beyond mediating cisplatin influx, the copper transport system is also involved in cisplatin efflux via the copper exporters. The most predominant are the two P-type ATPases 1 and 2 (ATP7A and ATP7B) [80]. Furthermore, members of the ATP binding cassette (ABC), such as the ATPase-like multidrug resistance-associated protein (MRP) family, are responsible for the efflux of a variety of drugs [68]. Among these, only MRP2 is the most accepted transporter to be associated with cisplatin resistance, by exporting of platinum-glutathione (GSH) conjugates via an ATP-dependent mechanism [50,80].

Following aqua-activation in the cell, cisplatin can be inactivated by scavengers such as nucleophilic GSH and cysteine-rich metallothionein (MT) [50,68,79]. Cisplatin interaction with GSH can occur in a nonenzymatic manner due to the high reactivity of aquated cisplatin, or can be catalysed by GSH-S-transferase (GSTπ) [50,68].

Another resistance mechanism is associated with an enhanced ability to repair or tolerate DNA adducts [50,79]. Preclinical and clinical studies highlighted that the majority of adducts are removed via the nucleotide excision repair (NER), either via the global genomic NER (GG-NER) or via the transcription-coupled NER (TC-NER) [79,81,82]. TC-NER specifically removes transcription-impeding damages from the transcribed strand to allow transcription resumption, in a highly efficient manner [82]. By contrast, mismatch repair (MMR) can also detect lesion, but does not process them [50,79]. MMR proteins (*i.e.*, hMSH2 and hMLH1) attempt to repair cisplatin adducts, fail and thus activate proapoptotic signals [68,79]. In this light, a deficiency in the MMR system, although infrequent in MPM, is associated with cisplatin resistance [50,79].

Finally, cisplatin resistance also involves a complex interplay of diverse pathways (*e.g.*, PI3K/Akt, MAPK), p53 in activation and overexpression of anti-apoptotic proteins, in a much lesser extend [50].

Because pemetrexed is mainly used in combination with other drugs, mechanisms driving resistance to it have been less characterized [50]. However, known resistance mechanisms include: impaired cell entry, alteration of polyglutamatation, inactivation, overexpression of the folate enzymes targeted by pemetrexed, and augmented export (**Figure 7**) [64]. The impaired cell entry is mediated by reduced expression of PCFT, RFC and FR-α. Pemetrexed accumulation in the cell is balanced by the competitors FPGS and γ-glutamyl hydrolase (GGH) [64]. GGH hydrolyses the polyglutamate tail of activated pemetrexed in the lysosome, leading to its elimination via members of the ABC transporters (i.e., MRP) [50,64]. More importantly, studies in MPM have showed that downregulation of PCFT and TS correlate with pemetrexed resistance [83,84].

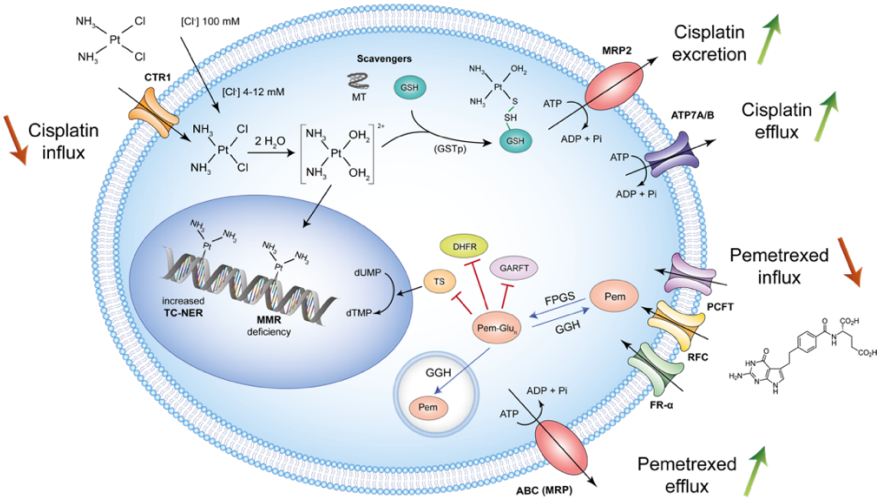

Figure 7 - Main mechanisms of chemoresistance to cisplatin and pemetrexed. Reduced expression of copper transporter 1 (CTR1) leads to a decrease in the cisplatin influx. Aquated cisplatin in the cytoplasm can either generate intrastrand adducts with DNA or be inactivated by metallothionein (MT) or be conjugated with glutathione (GSH) by GSH-S-transferase p (GSTp). In response to DNA-cisplatin adducts, increased transcription-coupled nucleotide excision repair (TC-NER) activity and mismatch repair (MMR) deficiency can lead to cisplatin resistance. Upon inactivation, GSH- cisplatin conjugates will be excreted by the ATP binding cassette (ABC) ATPase-like multidrug resistance-associated (MRP2) transporter exported by the copper-exporting P-type ATPases 1 and 2 (ATP7A/B). Pemetrexed influx is regulated by the proton-coupled folate receptor (PCFT), the reduced folate receptor (RFC), and the folate receptor α (FR-α). In the cytoplasm, pemetrexed is polyglutamated by folylpolyglutamate synthetase (FPGS) and inhibits the enzymes involved in DNA and RNA replication, i.e., thymidylate synthase (TS), dihydrofolate reductase (DHFR), and glycinamide ribonucleotide formyltransferase (GARFT). Overexpression of TS, DHFR, and GARTF leads to chemotherapy resistance. The enzymatic activity of the γ-glutamyl hydrolase (GGH) leads to the hydrolysis of the glutamate tails in the lysosome. The depolyglutamated form is thereafter exported out of the cell by members of the ABC transporters (i.e., MRP) (From Brossel *et al*, 2021).

1.6.3. Immunotherapy

Due to the limitations of chemotherapy (*i.e.*, relapse, resistance, and poor long-term OS), there has been extensive research for other therapies. A hallmark in cancer is an ineffective antitumor response mediated by the immune system, named immune evasion [85]. Indeed, under normal conditions, immune checkpoints are crucial for the maintenance of self-tolerance, thus preventing the development of autoimmunity, and the protection of tissue damage due to the immune response [49,86,87]. The dysregulation of the expression of immune checkpoint proteins in cancers, particularly those involving T cells, is an important immune escape mechanism [49]. Selective blockade of these immune checkpoints, resulting in the amplification of T cells response, thus are the primary targets in clinical testing [49,86]. In this light, blocking the interaction between B7-1 and B7-2 to CTLA-4 restores T cell activation and proliferation and can reverse T cell anergy (**Figure 8A**).

In addition to CTLA-4, PD-1 is also an immune checkpoint that inhibit T cell proliferation and T cell effector functions. As mesothelioma cells express PDL-1, its binding to PD-1 results in immune suppression in the TME. Blocking PD-1/PDL-1 with an anti-PD-1 thus restores T cell functions, proliferation and survival [50] (**Figure 8B**).

In the CheckMate 743 trial, the combination of anti-PD-1 (CD279) and anti-CTLA-4 (CD152) antibodies (Nivolumab and Ipilimumab, respectively), extended mOS from 14.1 months with standard chemotherapy to 18.1 months, and increased the survival rate by 50% [60].

In consequence, the combination of nivolumab and ipilimumab has been accepted both by the FDA and the European Medicines Agency as a first-line treatment for MPM, and has been incorporated in practice guidelines [4].

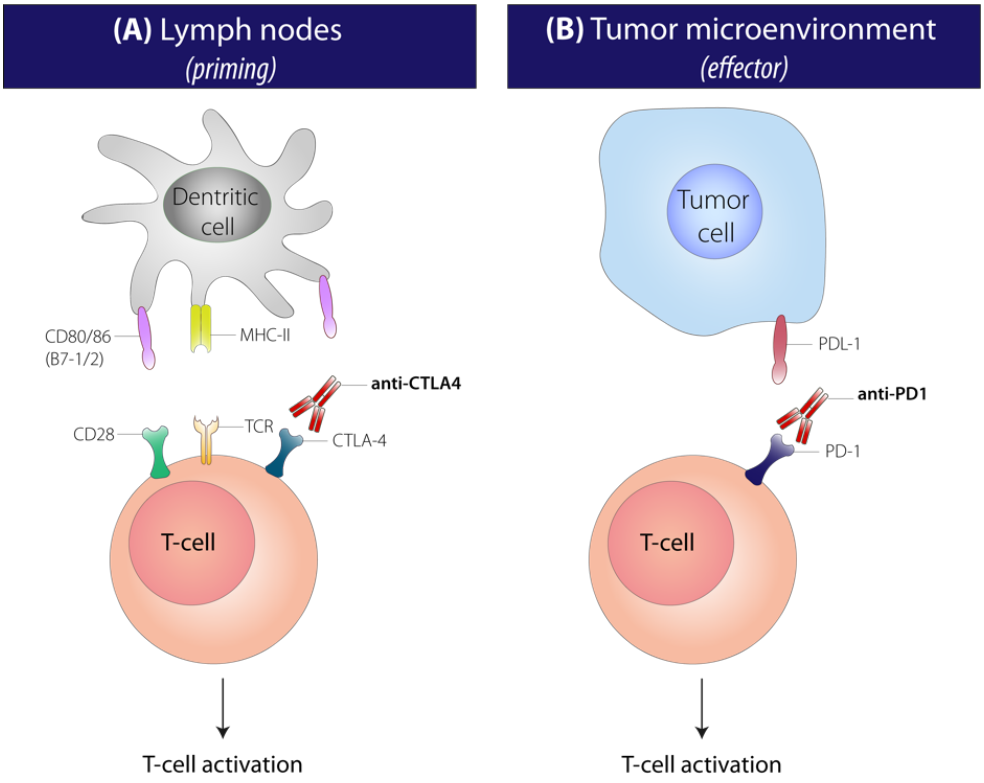

Figure 8 – Amplification of T cell response through anti-PD-1 and anti-CTLA-4. (A) The binding of anti-CTLA4 to CTLA4 provides B7-1/7 binding to CTLA-4 and thus, T cell inhibition by DCs. **(B)** Binding of anti-PD-1 to PD-1 inhibits the binding of PD-L1 from tumour cells, and thus inhibition of T cells in the TME.

2. Eosinophils

Eosinophils were first described, and named, in the 1800s by Paul Elrich on the basis of their staining with the bright-red acidic coal tar dye, eosin [88]. Indeed, eosinophils are characterized by basically charged cytoplasmic granules that present high affinity for the dye, and a bilobed nucleus [89,90].

Eosinophils are granulocytic leukocytes, together with neutrophils and basophils, that are present in all vertebrate species [91–93]. They are multifunctional actors of the innate immunity, which develop in the bone marrow from pluripotent progenitors [94]. They are released in a phenotypically matured state into the peripheral blood, where they represent less than 5% of circulating leukocytes [92,95]. Eosinophils spend only a brief time in the blood (half-life ~18hours) before migrating into the tissues [94,95].

2.1. Eosinophilopoiesis

The common paradigm accepted for eosinophilopoiesis was that eosinophils derive from multipotent hematopoietic stem cells (HSCs), which give rise to a common myeloid progenitor (CMP), which in turn differentiate into a granulocyte-macrophage progenitor (GMP) in mice. However, this paradigm has been revisited after single-cell RNA sequencing (scRNAseq) of myeloid progenitor. Indeed, scRNAseq highlighted that CMP and GMP do not really exist and that HSCs myelopoiesis towards eosinophils rather occurs in a GATA-1-positive pathway [96,97]. The commitment into an eosinophil-specific progenitor (EoP) is regulated by the combination of transcription factors including GATA1 (GATA-binding proteins), c/EBPα and C/EBPε (CCAAT/enhancer binding proteins) and PU.1 (**Figure 9**) [89,94,98]. In most lineages, GATA1 and PU.1 are antagonists. However, in the eosinophil lineage they present a specific synergy that leads to eosinophil granule protein transcription and eosinophil receptor expression [89,99]. Three cytokines further elicit the differentiation of the $GATA1^+$ EoP to eosinophil: granulocyte macrophage-colony-stimulating factor (GM-CSF), IL-5 and IL-3 [100,101]. This eosinophilopoiesis takes about a week and gives rise to a pool of mature eosinophils in the bone marrow [95].

Besides regulating the development of eosinophils in the bone marrow, IL-5 also regulates the expansion of eosinophils and their release in the blood stream. However, even if eosinophils recruitment to the tissue can be IL-5 totally or partially dependent (adipose tissue, GI tract and uterus), in some cases it is IL-5 independent (lungs) [102–105]. Besides IL-5, other cytokines and chemokines, such as eotaxins, are responsible for eosinophils recruitment into the tissues (**Figure 9**) [106–108].

IL-5 is produced by cells from the innate and adaptative immune systems, including type 2 innate lymphoid cells (ILC2s), T-helper cell-2 (Th2) and eosinophils themselves, which regulate eosinophil homeostasis and production [89,95,109].

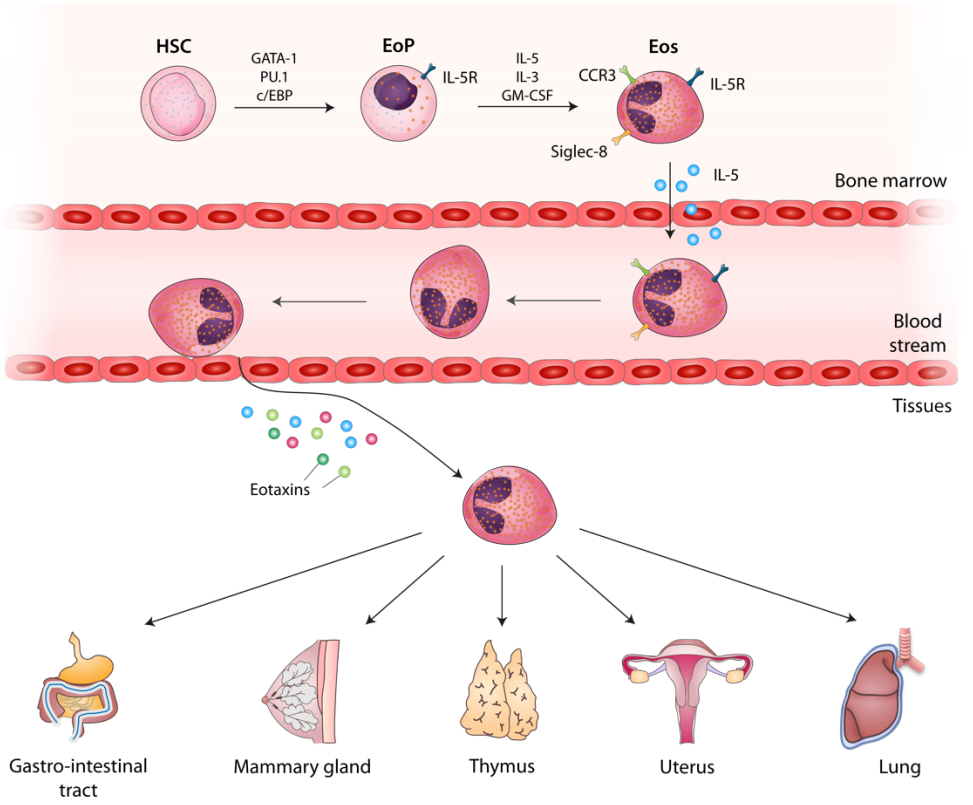

Figure 9 – Eosinophilopoiesis. In the bone marrow, multipotent hematopoietic stem cells (HSCs) give rise to a GATA1^{+} eosinophil progenitor (EoP) on a GATA1 dependent pathway, upon the regulation of three transcription factors: GATA1, PU.1 and c/EBP. The commitment of EoP to an eosinophil is elicited by IL-5, IL-3, and GM-CSF. Release of eosinophils into the bloodstream and in tissues is also mediated by IL-5. Under homeostatic conditions, eosinophils migrate through the vascular endothelium to the gastro-intestinal tract, thymus, mammary gland, uterus, and lung. HSCs: hematopoietic stem cells; EoP: eosinophil progenitor; Eos: eosinophil.

Once in the bloodstream and under homeostatic conditions, eosinophils migrate through the vascular endothelium to the thymus, mammary glands, adipose tissues, uterus and, more importantly, to the gastro-intestinal (GI) tract [89,93]. The recruitment of eosinophil in these tissues is regulated by IL-5 but also by chemokines of the eotaxin family of C-C motif chemokine ligands: CCL11 (eotaxin 1) and CCL24 (eotaxin 2) in human and mice, and CCL26 (eotaxin 3) in humans only [93]. Those eotaxins bind to the eosinophil-specific eotaxin receptor CCR3 (CD193).

2.2. Structure and content

2.2.1. Important receptors for eosinophils' function

Eosinophils express an array of receptors for cytokines, chemokines, adhesion molecules, Fc receptors and pattern recognition receptors (**Figure 10**) [89,90]. They express the receptors for the three cytokines involved in their differentiation, maturation and survival: the alpha subunit of the high affinity receptors for IL-3 (IL-3Rα, CD123), IL-5 (IL-5Rα, CD125) and GM-CSF (GMCSF-Rα, CD116) [90]. Of those, IL-5Rα is the most prominent eosinophil cytokine receptor. Furthermore, eosinophil express receptors for a wide range of other cytokines such as IL-1α, IL-2, IL-4, interferon (IFN)-α, IFN-γ, tumour necrosis factor (TNF)-α [95].

Human and mouse eosinophils express high levels of the G protein-coupled receptor CCR3. Notably, IL-5 primes eosinophils to respond to CCR3 ligands which, together with CCR3 ligands (*i.e.,* eotaxins), account for eosinophils chemotaxis, migration and recruitment in response to multiple ligands [89,90,94]. Besides eotaxins, CCR3 can also bind to the "regulated upon activation, normal T cell expressed and secreted" chemokine (RANTES, CCL5), monocyte chemotactic proteins 2 (MCP-2, CCL8), -3 (MCP-3, CCL7) and -4 (MCP-4, CCL13) [89,95]. Eosinophils also express CCR1 which binds to RANTES, MCP-3 and macrophage inflammatory protein-1α (MIP-1α, CCL3) [94,95].

Another typical marker of eosinophils is the sialic acid-binding immunoglobulin-like lectin 8 (Siglec-8) in human, or its paralog Siglec-F in mouse. Their expression increases with eosinophils maturation and is a late differentiation marker. Siglec-8 or Siglec-F engagement leads to ROS-involved and caspase-mediated eosinophil apoptosis [110].

Moreover, eosinophils express receptors involved in innate and adaptative immunity. Indeed, they express a range of pattern recognition receptors (PRRs), including Toll-like receptors (TLRs). Among the ten TLRs, TLR7 is the only one that has been found to be highly expressed by eosinophils at the mRNA and protein levels, in all studies [94,111]. Expression of other TLRs is varying among studies and is the subject of controversies, except for TLR8 which has never been found [111]. The receptor for advanced glycation end-products (RAGE), retinoic acid-inducible gene I (RIG-1) and nucleotide-binding oligomerization domain protein 1 and 2 (NOD1 and NOD2) are also PRRs expressed by eosinophils [90,94,111]. These PRRs can recognize pathogen associated molecular patterns (PAMPs) and damage-associated molecular patterns (DAMPs), such as the alarmin HMGB1 [90,94].

Regarding the adaptative immunity, eosinophils express multiple immunoglobulin (Ig) constant fragments (FC)-receptors of IgA (FcαRI, CD89), IgE (FcεRI, FcεRII/CD23) , IgG (FcγRII/CD32) [94,95]. Those receptors are involved in the antibody-dependent cellular toxicity (ADCC) and other immune modulatory

functions and pathologic activities in eosinophil-associated diseases [90]. Furthermore, the expression of MHC-II and co-stimulatory molecules for T-cells including CD40, its ligand (CD40L), CD80 (B7-1), CD28 (B7-2) and CD86 can be induced [95,112].

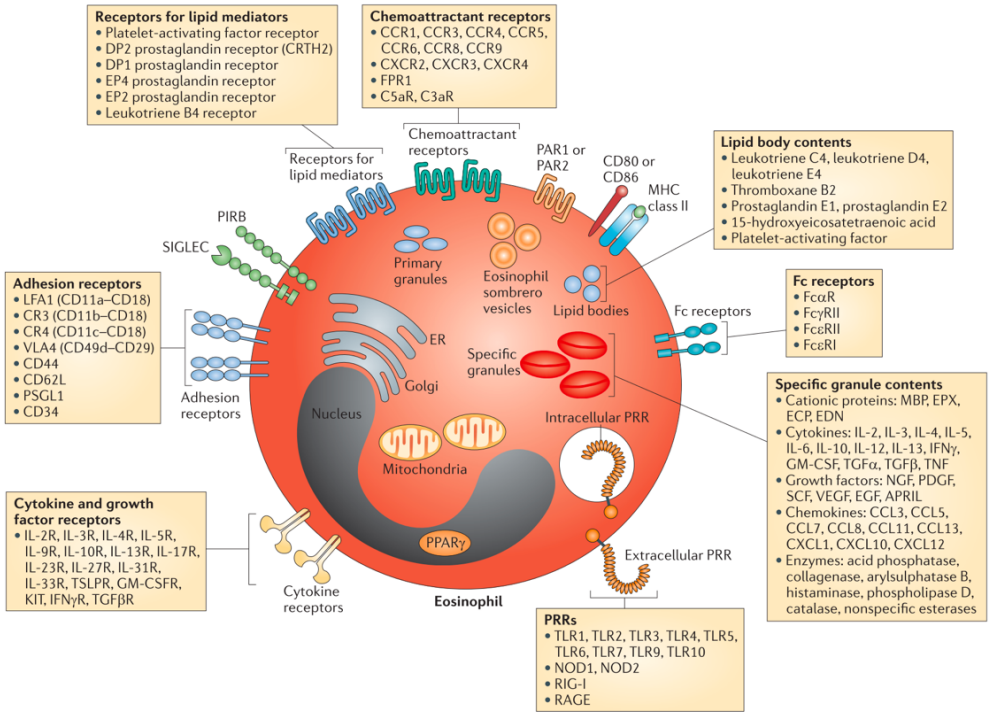

Figure 10 – Eosinophils cellular features. Eosinophils express a broad variety of receptors that modulate adhesion, growth, survival, activation, migration and pattern recognition. (from Rosenberg M. *et al*, 2013) [94].

2.2.2. Specific granules

Eosinophils are distinct from other granulocytes because of their specific and large granules that present an unique crystalloid core [92,95]. Those specific granules, and the cationic proteins that they contain, are essential to eosinophil formation and functions. Specific granules contain the cationic major basic protein (MBP), eosinophil-derived neurotoxin (EDN), eosinophil peroxidase (EPO, or EPX) and eosinophil cationic protein (ECP), as well as an array of cytokines and chemokines [95,113].

The predominant cationic protein in the specific granules is **MBP**, which accounts for ~50% (*i.e.,* 5-10 µg/10^6 eosinophils) of the total protein mass of the granule [89]. MBP is a 13.8 – 14 kDa protein with an isoelectric point (pI) of 11.4 which is encoded by the proteoglycan 2 (PRG2) gene [89,95,114]. MBP is cytotoxic for airways and is partially responsible for tissue damage associated with eosinophil infiltration in

asthma [115]. This cytotoxicity is mediated by an increase in membrane permeability through disturbance of cell surface lipid bilayer charges [115,116].

The second most prominent protein in specific granules, which constitutes ~25% of their total protein mass, is **EPX** [116]. EPX is found in the matrix of specific granules, along with ECP and EDN [95]. It is a two-chain protein with a 50-57 kDa heavy chain and a 11-15 kDa light chain with pI 10.8 [95,116]. EPX is, as its name states, a peroxidase which is distinct from the neutrophil myeloperoxidase despite high sequence homology [95]. Indeed, EPX is specific to eosinophils as it has not been identified in any other cell [117]. Through its peroxidase activity, EPX catalyses halidation reactions that lead to radicals production that take part in defence reaction against microbes [116,117].

The two other cationic proteins, **ECP** and **EDN**, are ribonucleases (RNAses) that share a ~70% homology [117]. ECP is 18 kDa and has a pI of 10.8 whereas EDN is 18-19 kDa with a pI of 8.9 [95,117]. They both exert antiviral activities, and noncytotoxic properties such as maturation of DCs for EDN and inhibition of T cell proliferation, activation of IgG production by B cells and activation of mast cell degranulation by ECP [116].

2.2.3. Galectin-10/Charcot-Leyden Crystal Protein

Besides their specific granules and their basic protein, eosinophils also contain a major hydrophobic protein of the galectin family, galectin-10, also known as Charcot-Leyden Crystal protein (CLC-P/Gal10) [118]. CLC-P/Gal10 is a small (16.5 kDa) slightly acidic (pI ~ 5.1-5.7) protein [118]. Notably, CLC-P/Gal10 is a hallmark of eosinophils as no other cell contains as much of this protein: CLC-P/Gal10 represents 7-10% of the total protein content of eosinophils [118,119]. Its localization in the cell is however still debated as some teams have observed CLC/Gal10 in the cytosol [120,121] and others in *so-called* "primary granules" [122]. Upon its release and under hypoxic conditions or hypotonic eosinophil lysis, CLC-P/Gal10 can form crystals: the Charcot-Leyden crystals (CLC) [123,124]. This crystal formation has been shown to be reversible by antibody treatment [124].

Despite being the fifth most abundant eosinophil protein (after actin, a non-secretory RNAse and histones), a specific ligand for CLC-P/Gal10 has not yet been identified. Early studies have shown a lysophospholipase activity of CLC-P/Gal10 but this role has yet since been the subject of controversy [118,121,125]. However, it has been demonstrated that CLC-P/Gal10 crystals plays a role in type 2 immunity and T cells regulation [119,124].

2.2.4. Degranulation

Degranulation (*i.e.,* the release of granule content in the extracellular space) is a major eosinophil function [94]. Eosinophil granules can be secreted by three main processes: compound exocytosis, cytolysis, and piecemeal degranulation.

During **compound exocytosis (Figure 11A)**, granules membrane fuses with the plasma membrane to form a continuous structure followed by the release of the content of granules [92]. Eosinophil exocytosis has rarely been observed *in vivo*, unlike mast cells and basophils that undergo acute exocytosis [92,95].

Alternatively, during **piecemeal degranulation** (**Figure 11B**), eosinophils use a vesicular transport process [95]. Piecemeal degranulation is a controlled process during which eosinophils release their granule contents piece by piece while remaining intact and viable [92,94]. Proteins and cytokines-derived granules are packaged in small secretory vesicles by selective incorporation [95,126]. The vesicles then migrate in the cytoplasm to the membrane where they release their content to the extracellular space [92].

Another common, but often overlooked degranulation process is eosinophil lysis, or **cytolysis** (**Figure 11C**) [95]. Eosinophil cytolysis is characterized by chromatin decondensation, loss of nuclear and plasma membrane integrity and extracellular expulsion of membrane-bound granules [92,95]. When this process is accompanied by the release of filamentous chromatin structures called eosinophils extracellular traps (EETs), cytolysis is referred as the active cell death **EETosis** [127]. EETosis is also associated with the crystallized form of Gal10, CLC [124,127].

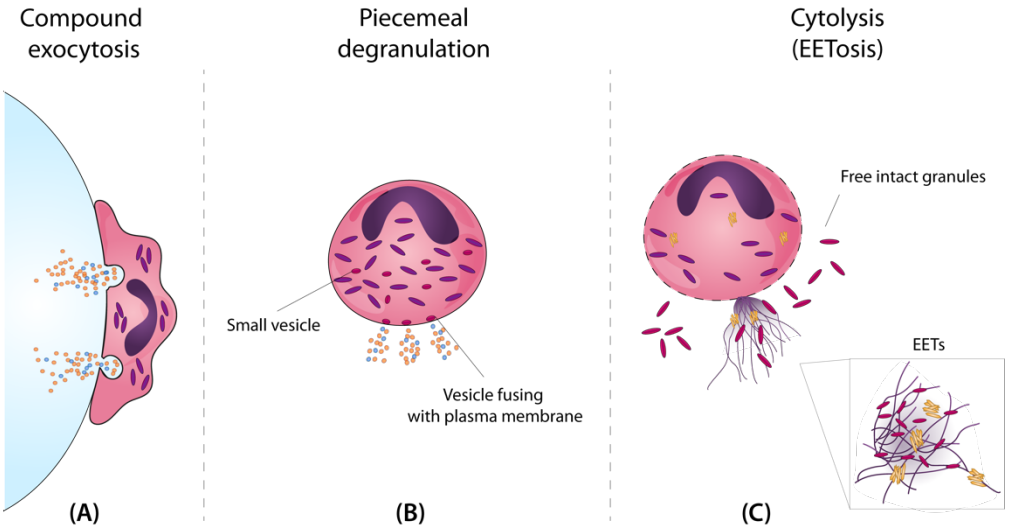

Figure 11 – Eosinophil degranulation. (**A**) Eosinophils can undergo compound exocytosis, wherein granules membranes fuse with plasma membrane to form a continuous structure, and then release the content of their granules. (**B**) Piecemeal degranulation release granule content through small vesicles. (**C**) Eosinophils can also undergo cytolysis, during which chromatin decondensate, they lose their nuclear and plasma membrane integrity and membrane-bound granules are expulsed extracellularly. When this process is accompanied by the release of filamentous chromatin structures (EETs), cytolysis is referred as the active cell death EETosis.

2.3. Functions

2.3.1. Eosinophils pleiotropy and heterogeneity

Emerging evidences indicate that eosinophils are not an homogeneous population of terminally differentiated cells, but rather an heterogeneous population with different tissue-dependent characteristics [93,104,128,129]. Indeed, depending on the tissue they infiltrate, eosinophils can express different receptors such as CD11b (GI tract, thymus, and adipose tissue), F4/80 (mammary glands, lung, and adipose tissue), CD69 (GI tract and thymus), and CD44 (GI tract and thymus) [104,130]. This indicate that eosinophils thus undergo phenotypic changes in response to their microenvironment, including morphological changes, enhanced response to cytokines and various degree of activation [93,128]. Furthermore, recent evidences lead to the functional distinction between tissue-resident eosinophils (rEos) and eosinophils recruited in a pathological context (inflammatory eosinophils, iEos) [103,128,131,132]. However, it is not clear whether rEos and iEos are the same cells with different activation states or if they represent distinct eosinophils subtypes [103].

2.3.2. Tissue-resident eosinophils

Under homeostatic conditions, eosinophils migrate to several tissues (*see 2.1*) where they promote tissue differentiation and development, and contribute to tissue homeostasis (**Figure 12**) [112].

Eosinophils are a major source of the activation and proliferation-inducing ligand (APRIL) and secrete IL-6, which are essential to the survival of bone marrow plasma cells with which they colocalize during maturation [133]. Besides the long-survival regulation of plasma cells, eosinophils are also required for the maintenance of these cells in the lamina propria underlying the gut epithelium [134]. Finally, eosinophils also contribute to the GI tract homeostasis through their involvement in the production and maintenance of IgA-secreting plasma cells. Indeed IgA plays a crucial role in the maintenance of immune homeostasis of the GI tract tissues as well as in the microorganism populations in the gut lumen [134]. Finally, eosinophils are involved in tissue integrity, are required for tissue remodelling, maintain intestinal mucus secretion and promote the development of Peyer's patches [128,131].

In adipose tissues, eosinophils contribute to the metabolism and metabolic health by inducing the polarization of adipose macrophages towards the M2 phenotype through IL-4 production [104,135]. Those macrophages are essential for glucose homeostasis and beige fat development, which in turn improves glucose tolerance and insulin sensitivity, and is known to protect against obesity [104,128].

Eosinophils also infiltrate the uterus following its cycle, with a peak during oestrus and metestrus [92,104,136]. Studies in mice and human have highlighted that eosinophil

recruitment in the uterus concur with the tissue remodelling and repair in the endometrial lining [129,136]. Indeed, eosinophil degranulation coincide with the tissue-degradative process that prepare the cervix for delivery and with the post-partum tissue-regeneration [92,129].

In the thymus, eosinophils take part in tissue regeneration and restore T cell production after damage [137]. They also may play an immune-regulatory role by contributing to the clearance of apoptotic thymocytes and may contribute to central tolerance and negative T cell selection [104,138]. In addition, eosinophils are involved in lung immune homeostasis, especially in the negative regulation of T_H2 cell response [103], wound healing and epithelial remodelling [128,129].

Finally, eosinophils control post-natal mammary gland development, mammary duct branching during puberty and pregnancy [92,104,138]

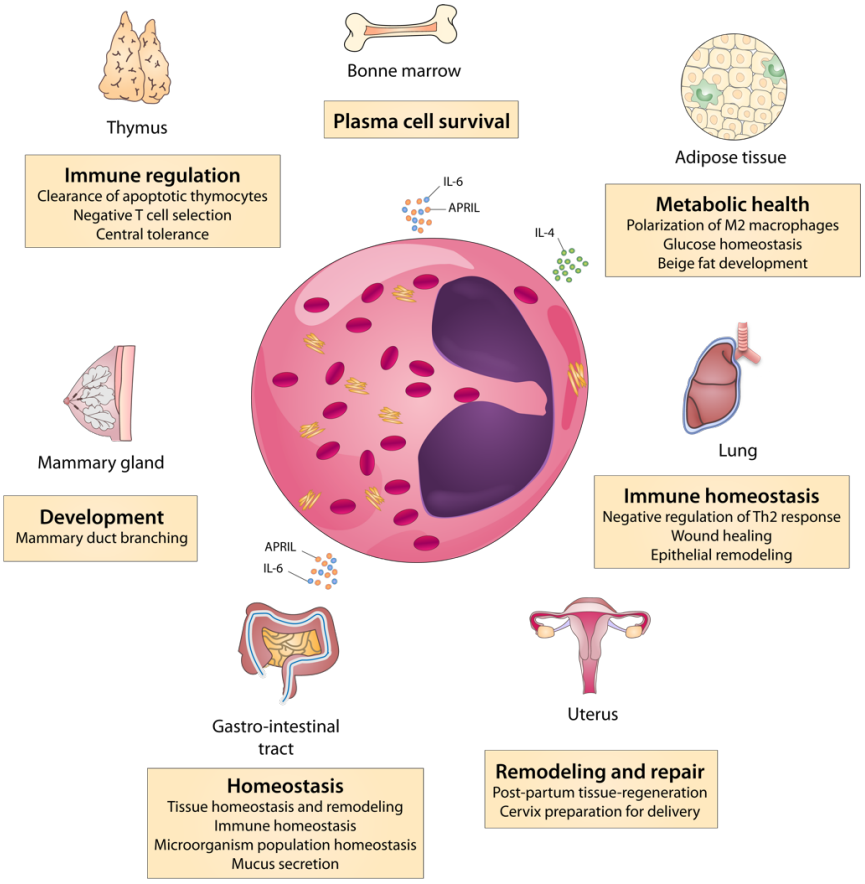

Figure 12 – Homeostatic functions of eosinophils. Eosinophils are responsible for plasma cell survival in the bone marrow, metabolic health of the adipose tissue, immune homeostasis in the lung, remodelling and repair of the uterus, homeostasis of the GI tract and mammary gland development.

2.3.3. Pathogens

Historically, eosinophils have been associated with helminth infection especially since MBP and ECP have been found to exert anti helminthic cytotoxicity *in vitro* [112]. However, the helminthic cytotoxic role of eosinophils are less certain in mice and humans [95]. Moreover, it was demonstrated in mice that in the case of certain parasites (i.e., *Trichinella spiralis, Trichuris muris, Litomosoides sigmodontis*) eosinophils don't have any effect, or are even recruited for their survival [90,139]. Except for schistosomiasis, *in vivo* data supporting a role for human eosinophils are scarce [90,94].

By contrast, MBP and ECP antibacterial properties have been demonstrated both *in vitro* and *in vivo* [94,140]. Indeed, the adoptive transfer of eosinophils to wild-type mice has been found to improve bacterial clearance and to protect against bacterial sceptic shock [141]. Furthermore, it has been demonstrated that ECP has a specific and high affinity for bacterial-wall lipopolysaccharides and peptidoglycans, and can agglutinate to Gram-negative bacteria [142]. Moreover, EETs, constituted of DNA with MBP and ECP, have also been demonstrated to have anti-bacterial properties [94].

Eosinophils may also exert antiviral properties through EDN, as it has been shown *in vitro* and in guinea pigs and mice infected with parainfluenza and influenza A, respectively [140]. Of note, EDN has also been shown to have inhibitory properties against the human immunodeficiency virus (HIV) [143]. Finally, it was demonstrated through *ex vivo* and *in vivo* experiments that both mice and human eosinophils can capture several respiratory viruses and reduce their infectivity [94,144]. More recently, with the COVID-19 pandemic, eosinophils were of particular focus in the serve acute respiratory syndrome coronavirus 2 (SARS-CoV-2). Indeed, several studies have highlighted a protective role of eosinophils against SARS-CoV-2 infection [145–148].

Overall, the interaction mechanisms between eosinophils and pathogens remain to be clarified.

2.3.4. Immune response

In accordance to their antipathogenic functions, eosinophils are part of the ***innate immune response*** through the DAMPs and PAMPs recognition via their PRRs (*see 2.2.1*) [90,94,95]. The recognition of those patterns leads to eosinophil secretion of pro-inflammatory cytokines (IL-1β, IL-6, TNF-α, GM-CSF) and chemokines (IL-8, RANTES) [111]. Furthermore, eosinophils also exert phagocytic capacities although this function is controversial [112,149,150]. Indeed, as explained in the previous section, eosinophils antibacterial function is rather dependent on the rapid release of EETs [150].

Eosinophils are also effectors of the ***adaptative immune response*** through their interaction with effector cells of the adaptive immunity [89,151]. Indeed, eosinophils have the ability to act as "non-professional" APCs as they express MHC-II and co-stimulatory molecules necessary for T cell activation [112,150,152]. Furthermore, eosinophils express cytokines that can either promote T_H2 cell differentiation (IL-4,

IL-5, IL-13) or T_H1 cell (IFN-γ) response upon stimulation [95,112,140]. Of note, there are less evidences that eosinophil can promote a T_H1 phenotype [152].

Besides direct activation of T cells, eosinophils can also crosstalk with DCs *via* their cationic granules [150]. Indeed, DCs can internalize MBP *in vivo*, which results in their DC maturation and activation in the presence of a bacterial PAMP (*i.e.*, CpG-C) [153]. Moreover, EDN has been shown to be a chemotactic factor of DCs which induces maturation and activation, and triggers the production of various proinflammatory cytokines and chemokines [154,155]. Finally, EDN is a specific endogenous ligand of DC's TLR2, which increase the T_H2 cytokine production (IL-5, IL-6, IL-10 and IL-13) by DCs [155]. Collectively, these findings suggest a role of eosinophils cationic proteins as DCs regulators, which also contributes partially to the eosinophil T_H2-promoting role of eosinophils [150,152].

Finally, eosinophils modulate the activity of other leukocytes such as neutrophils, macrophages, mast cells, B cells (see 2.3.2) and bone marrow plasmablasts (**Figure 13**).

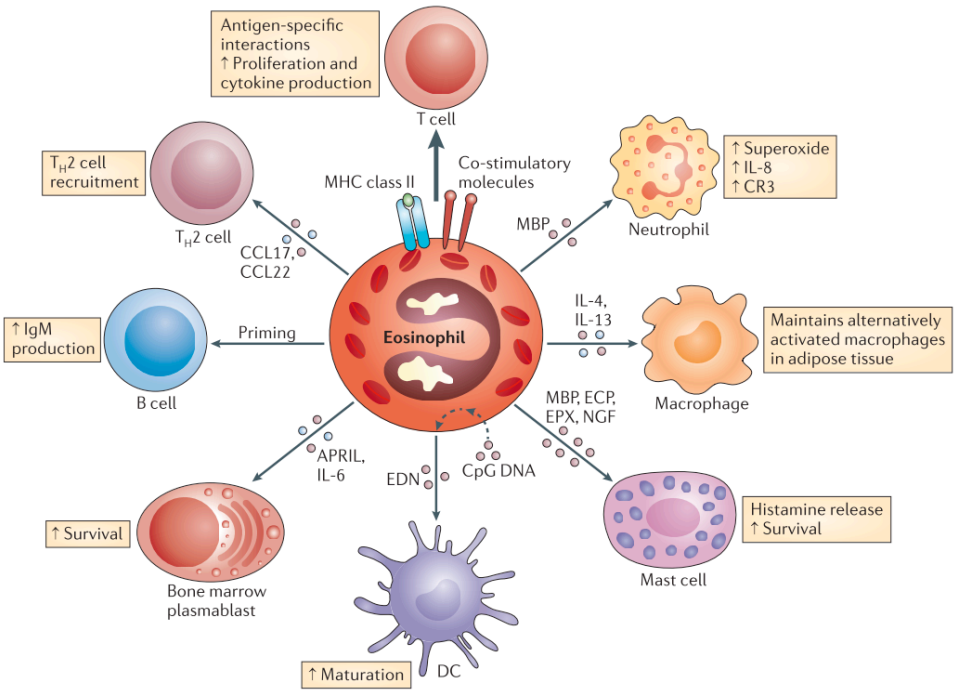

Figure 13 – Eosinophils interaction with other leukocytes. Eosinophils can mediate T cell activation and production, B cell priming, survival of bone marrow cells and mast cells, DCs maturation, activation of alternatively activated macrophages and neutrophil degranulation. (from Rosenberg H. *et al*, 2013).

2.3.5. Asthma and monoclonal antibodies targeting eosinophils

Many disorders are associated with eosinophil accumulation [94]. Among them, asthma is one of the most extensively studied. Eosinophil accumulation in the airways is a common feature of the inflammatory response that occurs in severe asthma [94,95,156,157]. Indeed, eosinophils are recruited to the lung and airway by a cascade of processes directed by activated T_H2 cytokines and by eotaxins [94]. Several studies have highlighted a role for eosinophils in promoting pathogenesis, development of asthma exacerbation and treatment of severe asthma [158,159]. Indeed, eosinophils release their cationic proteins, lipid mediators and reactive oxygen species that cause damage in the airway mucosa and associated nerves [157,160]. Furthermore, EETs release has been shown to enhance type 2 inflammation in severe asthma patients [158]. Finally, a role for eosinophils in tissue remodelling, through transforming growth factor-β (TGF-β) production, has also been highlighted [157,160].

In this light, a focus has been given to therapeutic approaches to regulate eosinophils in asthma. Monoclonal antibodies targeting IL-5 (Mepolizumab and Reslizumab), IL-5Rα (Benralizumab) and IL-4Rα which blocks IL-4 and IL-13 (Dupilumab) have been approved by the FDA for asthma treatment and have proved to be effective in reducing asthma exacerbation and oral corticosteroids use [156]. Among these monoclonal antibodies, Mepolizumab, Reslizumab and Benralizumab target specifically eosinophils. Of note, several monoclonal antibodies targeting cytokines associated with eosinophilia (*e.g.*, IL-5, IL-33) are in clinical trial to treat eosinophilic COPD patients: Mepolizumab (anti-IL-5; NCT04075331), MEDI3506 (anti-IL-33; NCT04570657), REGN3500 (anti-IL-33; NCT04701983 and NCT04751487) and Astegolimab (anti-ST2; NCT03615040).

2.3.6. Eosinophilia

Diverse infectious and allergic diseases are associated with an elevation in blood and/or tissue eosinophils numbers. Peripheral blood eosinophilia (PBE) is defined by an absolute eosinophil count (AEC) exceeding 350 to 550 eosinophils/μL of blood, according to laboratory standards [95,161–163]. Hypereosinophilia (HE) is considered with eosinophilia with AEC superior to 1,500 eosinophils/μL of blood, whereas hypereosinophilic syndrome (HES) is defined as sustained peripheral blood HE (more than 6 months) associated with tissue damage [161,162].

The causes of PBE/HE are broad and can range from being reactive, neoplastic or idiopathic [161,163]. **Reactive PBE**, also called secondary eosinophilia, is generally resulting from an elevation of the cytokines IL-3, IL-5 and GM-CSF that promote eosinophils differentiation and survival, and can be sustained in some disorders [163–165]. Reactive PBE has many causes, such as allergy, atopy, hypersensitivity conditions, drug reactions or eosinophilia-associated diseases (*e.g.*, asthma, eosinophilic esophagitis) [163,164]. Among all reactive PBE cases in the West world, allergic reactions, notably those mediated by IgE-dependent mechanisms, are the most common cause,

with 80% of the cases [165,166]. Some of those allergic reactions, such as the drug rash with eosinophilia and systemic symptoms (DRESS), can potentially be fatal and their symptoms include fever, extensive rash, lymphadenopathy, pneumonia, hepatitis arthritis and renal dysfunction [166]. The second most common cause of reactive PBE is parasitic, comprising 8% of cases in Europe [165]. Of note, in developing countries, reactive PBE is mostly caused by infections and particularly by tissue-invasive parasites (e.g., roundworms, tapeworms and flukes) [166].

Neoplastic PBE, also called clonal eosinophilia, is a phenotype of an underlying haematological neoplasm characterized by the presence of a histological, cytogenic or molecular marker of a myeloid malignancy in the bone marrow [164,166]. Myeloid disorders accompanied by clonal eosinophilia include acute myeloid leukaemia (AML), chronic myeloid leukaemia (CML) and Hodgkin lymphoma [94,162,166].

Idiopathic PBE is neither reactive of neoplastic, has no known cause and is only diagnosed when all alternative diagnosis have been ruled out [165]. HES is generally a subset of idiopathic PBE [165,166]. The clinical manifestations of idiopathic PBE and HES are heterogeneous as the disease can either be asymptomatic or can involve various organs such as the skin, the heart, the nervous system, the lung, the GI system, the hematopoietic system or the kidney [166]. HES can potentially be fatal with a 50% 10-year survival especially for corticoid-refractory cases that involve the heart [163,166].

2.4. Eosinophils and cancer

Eosinophilia can also be associated with several cancers (paraneoplastic eosinophilia) and presents itself either in the blood (PBE) or as tumour-associated tissue eosinophilia (TATE), or as eosinophilic pleural effusions (EPE) [167,168]. Paraneoplastic eosinophilia has been observed in various solid organ malignancies such as gastric, colorectal, oesophageal, lung, breast, ovary and uterine cancers, and represents 0.5 to 7% of the cases [165,167,169]. Eosinophil infiltration can vary extensively in the different tumour types, and even within a given tumour. However, tumour-infiltrating eosinophils often are a large proportion of the immune infiltration of the TME [129].

Multiple studies have shown an association between TATE, as well as PBE and EPE, and prognosis independently of other factors such as age or sex [168,170–174]. **Table 4** summaries the clinical correlations observed between cancer type and eosinophilia. The difference in results might be explained by eosinophils pleiotropy and heterogeneity (*see 2.3.1*), and by the fact that eosinophils might undergo phenotypic changes according to the TME they infiltrate.

Table 4 – Clinical correlation between cancer type and eosinophilia localization (adapted from Grisaru-Tal S. *et al*, 2020).

Cancer type	Localization	Clinical correlation
Bladder	Blood	Pro-tumorigenic *(Unfavourable)*
	Tumour	Both Pro- and Antitumorigenic
Cervical	Tumour	Pro-tumorigenic
Colorectal	Tumour	Antitumorigenic
Oesophageal	Tumour	Antitumorigenic *(Favourable)*
Gastric	Tumour	Antitumorigenic
Larynx	Tumour	Both Pro- and Antitumorigenic
Oral	Tumour	Both Pro- and Antitumorigenic
Breast	Blood	Antitumorigenic
Hodgkin lymphoma	Blood	Pro-tumorigenic
Primary Cutaneous T-cells lymphoma	Blood	Pro-tumorigenic
Melanoma	Blood	Antitumorigenic
Ovarian	Blood	Pro-tumorigenic
Liver	Blood	Antitumorigenic
Lung	Pleural effusion	Antitumorigenic

2.4.1. Eosinophil recruitment in the TME

The accumulation of eosinophils in various TME, including the lung, colorectal cancer (CRC) and melanoma, seems to be at least partially due to the IL-5, GM-CSF and CCR3 chemotactic pathway [167,169]. Indeed, several eosinophil chemokines have been shown to be produced by other leukocytes in the TME. In lung cancer and melanoma, several evidences show that ILCs produce IL-5 and GM-CSF [175,176]. Furthermore, tumour cells have been demonstrated to produce IL-5 and GM-CSF which recruit eosinophils in the peripheral blood stream or TME and activate them [151,177].

Besides chemokines, eosinophils can be recruited by VEGF and angiopoietin 1 (Ang1) produced either by tumour or tumour-infiltrating immune cells [178]. For example, in the TME macrophages and mast cells are potentiated to produce VEGF which can contribute to eosinophils recruitment [178].

In several cancers, such as CRC, Hodgkin's lymphoma and oral squamous cells, the expression of eotaxin-1, eotaxin-2 and RANTES in tumours and accumulation of eosinophils have a significant correlation [176,178–180]. In CRC patients, concentration of eotaxin-1 is elevated in both tissue and serum [179]. Furthermore, immunohistochemical staining of CRC tumour revealed that fibroblasts and lymphocytes in TME highly expressed eotaxin-1 and eotaxin-2 [181].

Finally, DAMPs such as HMGB1 and the alarmin IL-33 may recruit eosinophils in dying cells and hypoxia regions within tumours [167,182]. Of note, HMGB1 itself has no impact on eosinophils migration in physiological conditions *in vitro* but it can induce the expression of MCP-4 (CCL13) and MIP-1β (CCL4) which are directly involved in eosinophils chemotaxis [169]. As eosinophils express ST2, the IL-1R accessory protein, RAGE and may express TLR4 (*see 2.2.1*), they have the capacity to be stimulated by HMGB1 and IL-33 and thus, their role in eosinophils function in the TME cannot be excluded [169,178]. However, whether this phenomenon takes place *in vivo* remains to be elucidated.

2.4.2. Antitumorigenic roles

Eosinophils can exert antitumoral activities through either direct or indirect mechanisms. First, eosinophils can release their cationic proteins (MBP, EDN, ECP and EPX), granzymes and TNF-α that can induce tumour cell death by promoting ROS and oxidative stress (EPX), disrupting the integrity of the lipidic membrane (MBP) for example [167,178]. Importantly, several mediators including IFN-γ, IL-5, IL-33 and eotaxin-1 have been shown to increase this mode of eosinophil-related killing [169]. This phenomenon is also partially mediated by IL-18 that upregulates the expression of adhesion molecules LFA1 and ICAM1, which promotes contact between eosinophils and cancer cells [167]. Moreover, eosinophils can be a source of IL-10 and IL-12 that can decrease tumour metastatic migration by increasing their E-cadherin and thus strengthen their adhesion [169].

Regarding indirect mechanisms, it was highlighted that eosinophils attract $CD8^+$ T cells in the tumour polarize macrophages in a proinflammatory phenotype and improve normalization of the tumour vascularization which are associated with antitumorigenic activities [183]. Those effects are mediated by eosinophils-derived IFN-γ and TNF [169].

2.4.3. Pro-tumorigenic roles

Most of pro-tumorigenic roles of eosinophils are indirect. First, eosinophils can promote angiogenesis, which is the formation of new blood vessels and is essential for growing malignant tissues [178]. Indeed, eosinophils are a source of pro-angiogenic factors such as VEGF-A, fibroblast growth factor (FGF-2), TGF-β, IL-6, IL-8 and osteoponin [169]. Furthermore, it has been demonstrated that subtoxic doses of MBP can induce angiogenesis by promoting endothelial cell proliferation and enhancing VEGF effect [184].

Furthermore, eosinophils can also shape the TME by directing macrophages polarization towards M2-like immunosuppressive phenotype as they store IL-4 and IL-13 [151,167]. Furthermore, they can produce CCL22 which is involved in the recruitment of Treg, and are a source of indoleamine 2,3-dioxygenase which inhibits T and NK cells cytotoxic functions [151].

2.4.4. Eosinophils and MPM

Several factors associated with eosinophils have been found in patients who have been exposed to asbestos. Indeed, it was observed that eotaxin-1 and RANTEs, as well as the proinflammatory cytokines IL-5 and IL-6, are overexpressed in the pleura of some of these patients [167,185,186]. Moreover, it was demonstrated that IL-5 could have a pro-tumorigenic role on malignant pleural effusions [187]. Finally, Takeuchi *et al.* have highlighted a case of IL-5 producing MPM cells [188].

It is thus of particular interest to study the impact of eosinophils in MPM.

Chapter 2

Retrospective clinical study shows that excess of blood eosinophils prior mesothelioma therapy correlates with worse prognosis

1. Foreword

Considering that peripheral blood eosinophils can have different effects on patients OS and response to therapy according to the cancer type, we first studied their role in MPM. In the following article published in March 2023, we studied the data of 242 MPM patients and the mean AEC was determined in the month preceding chemotherapy administration. We determined if a mean AEC could split the cohort according to patients OS. Then, we analysed the progression-free survival (PFS), overall response rate (ORR) and disease control rate (DCR) of the patients with AEC $\geq$ 220/µL compared to patients with AEC < 220/µL.

frontiers | Frontiers in Immunology

TYPE Original Research
PUBLISHED 21 March 2023
DOI 10.3389/fimmu.2023.1148798

OPEN ACCESS

EDITED BY
Chiara Porta,
University of Eastern Piedmont, Italy

REVIEWED BY
Paolo Andrea Zucali,
Humanitas University, Italy
Elisa Giovannetti,
VU Medical Center, Netherlands

*CORRESPONDENCE
Luc Willems
luc.willems@uliege.be

†These authors have contributed equally to this work and share last authorship

SPECIALTY SECTION
This article was submitted to Cancer Immunity and Immunotherapy, a section of the journal Frontiers in Immunology

RECEIVED 20 January 2023
ACCEPTED 20 February 2023
PUBLISHED 21 March 2023

CITATION
Willems M, Scherpereel A, Wasielewski E, Raskin J, Brossel H, Fontaine A, Grégoire M, Halkin L, Jamakhani M, Heinen V, Louis R, Duysinx B, Hamaidia M and Willems L (2023) Excess of blood eosinophils prior to therapy correlates with worse prognosis in mesothelioma. *Front. Immunol.* 14:1148798. doi: 10.3389/fimmu.2023.1148798

Excess of blood eosinophils prior to therapy correlates with worse prognosis in mesothelioma

Mégane Willems[1], Arnaud Scherpereel[2], Eric Wasielewski[2], Jo Raskin[3], Hélène Brossel[1], Alexis Fontaine[1], Mélanie Grégoire[1], Louise Halkin[1], Majeed Jamakhani[1], Vincent Heinen[4], Renaud Louis[4], Bernard Duysinx[4], Malik Hamaidia[1†] and Luc Willems[1*†]

[1]Laboratory of Molecular and Cellular Epigenetics (GIGA at University of Liege), Sart-Tilman, Molecular Biology, Teaching and Research Centre (TERRA), Gembloux, Belgium, [2]Department of Pneumology and Thoracic Oncology, (CHU Lille) and INSERM (ONCOTHAI), Lille, France, [3]Department of Pulmonology and Thoracic Oncology, Antwerp University Hospital, Edegem, Belgium, [4]Department of Pneumology, University Hospital of Liege, Liege, Belgium

Background: Only a fraction of patients with malignant pleural mesothelioma (MPM) will respond to chemo- or immunotherapy. For the majority, the condition will irremediably relapse after 13 to 18 months. In this study, we hypothesized that patients' outcome could be correlated to their immune cell profile. Focus was given to peripheral blood eosinophils that, paradoxically, can both promote or inhibit tumor growth depending on the cancer type.

Methods: The characteristics of 242 patients with histologically proven MPM were retrospectively collected in three centers. Characteristics included overall survival (OS), progression-free survival (PFS), overall response rate (ORR) and disease control rate (DCR). The mean absolute eosinophil counts (AEC) were determined by averaging AEC data sets of the last month preceding the administration of chemo- or immunotherapy.

Results: An optimal cutoff of 220 eosinophils/µL of blood segregated the cohort into two groups with significantly different median OS after chemotherapy (14 and 29 months above and below the threshold, $p = 0.0001$). The corresponding two-year OS rates were 28% and 55% in the AEC ≥ 220/µL and AEC < 220/µL groups, respectively. Based on shorter median PFS (8 *vs* 17 months, $p < 0.0001$) and reduced DCR (55.9% vs 35.2% at 6 months), the response to standard chemotherapy was significantly affected in the AEC ≥ 220/µL subset. Similar conclusions were also drawn from data sets of patients receiving immune checkpoint-based immunotherapy.

Conclusion: In conclusion, baseline AEC ≥ 220/µL preceding therapy is associated with worse outcome and quicker relapse in MPM.

KEYWORDS

malignant pleural mesothelioma, eosinophils, chemotherapy, cisplatin, pemetrexed

Introduction

Malignant pleural mesothelioma (MPM) is a cancer associated with very poor prognosis mainly induced by occupational exposure to asbestos fibers (1). Despite the ban or limitation of asbestos use (2), incidence of MPM is still increasing worldwide (3) due to the long latency time between exposure and neoplasm development. There are 3 main histological subtypes of MPM: epithelioid (60–80% of cases), sarcomatoid (< 10%) and biphasic/mixed (10–15%) (4, 5). Therapeutic standard options include conventional treatments (surgery, radiotherapy, chemotherapy) and, more recently, immunotherapy (6–8). Thus, since 2003 the first-line standard-of-care for unresectable MPM has been chemotherapy based on the combination of a DNA cross-linking agent (cisplatin or carboplatin) and an antifolate (pemetrexed) (6). The median overall survival (mOS) obtained with this regimen ranges between 13 and 16 months (6, 9). Addition of an anti-VEGF antibody (bevacizumab) to cisplatin/pemetrexed improved mOS up to 18.8 months compared to 16.0 months in the control arm (9). As many MPM patients have a weakened immune system, chemotherapy initially seemed to be a better option than immunotherapy (10). However, the recent first-line dual immunotherapy by immune checkpoint inhibitors (ICIs) (nivolumab and ipilimumab, targeting PD-1 and CTLA-4, respectively) extended mOS from 14.1 months with standard chemotherapy to 18.1 months (11). Immunotherapy has only a limited benefit for the epithelioid subtype but is particularly effective for non-epithelioid MPM (12). Compared with chemotherapy, ICIs clearly provide much better OS rates at 4 years in non-epithelioid MPM (i.e., 14% *vs* 1%, respectively).

Despite these recent improvements, the prognosis of MPM remains globally poor. The biological mechanisms that drive the effectiveness of available therapies are still not well understood. However, the recent breakthroughs of ICIs indicate that the tumor microenvironment (TME) is a major parameter in cancer development and response to therapy. Even though mesothelioma was initially considered as a "cold" tumor (*i.e.*, absence of T cells within or at the edges of the tumor), the paradigm has recently been revisited (10). In the mesothelioma TME, tumor-associated macrophages (TAMs) are the most abundant immune infiltrating cells (13–18). The phenotype of these TAMs is shaped by mediators expressed by tumor cells. Therefore, the ability of TAMs to orchestrate the innate immune response and to modulate activation of effector T-cells is impaired in MPM. Among immune cells that regulate macrophage polarization, eosinophils favor the M1 phenotype through the production of IFN-γ and TNF-α. However, eosinophil-derived IL-4 and IL-13 can also promote suppressive TAMs and shape the TME (19, 20). The balance between Th1- and Th2-related cytokines modulates the migration and activation of $CD8^+$ T-cells and affects the local anti-tumor response. Among their pleiotropic activities, eosinophils also promote angiogenesis and tissue healing *via* VEGF, FGF and PDGF production. Besides their ability to shape the TME through the expression of cytokines, eosinophils display cytotoxic effects by secreting granule proteins and granzyme A.

Altogether, this evidence thus indicates that eosinophils exert both pro- and anti-tumorigenic activities. The final outcome will depend on a variety of parameters that include the cytokine balance, the interaction of eosinophils with other immune cells and the resulting cytotoxicity against the tumor. In this context, we investigated the correlation of blood eosinophil counts with mOS, progression-free survival (PFS) and duration of response in patients undergoing chemo- or immunotherapy.

Materials and methods

Patients' selection and data collection

Two hundred and forty-two eligible MPM patients were included in this study. Between January 2009 and December 2021, these patients were given chemo- or immunotherapy in 3 hospitals: 68 at the University Hospital of Liege (Belgium), 61 at the University Hospital of Antwerp (Belgium) and 101 at the University Hospital of Lille (France). According to standard guidelines, 230 patients received cisplatin or carboplatin and pemetrexed as first-line chemotherapy (4, 21). Among these, 32 patients also received 2^{nd} or 3^{rd} line immunotherapy with nivolumab and ipilimumab. Twelve patients were given ICIs in first-line therapy.

Exclusion criteria included autoimmune disease, congenital or acquired immunodeficiency including HIV, asthma, and active parasitic infection at diagnosis, requiring systemic treatment. Patients diagnosed less than a year before the study was initiated or who did not complete a full treatment plan were also excluded as the follow-up period was too short.

All data were collected for medical purposes and obtained retrospectively. The following data were collected from hospital databases: date of birth; date of diagnosis; sex; histological subtype; BAP-1 deletion; date and type of treatment; response to treatment at 3 months, 6 months and 1 year; hematological lab tests before, during and after treatment; smoking status; diabetes status; asbestos exposure information; comorbidity information; date of death if applicable. Clinical staging was not available for most patients.

This study was performed in compliance with the Helsinki Declaration and was approved by the local Ethics Committee with the reference 2020/45 (University Hospital of Liege) and 2022/1844 (University Hospital of Antwerp) and declared to the local Data Protection Officer (DPO), per General Data Protection Regulation (University Hospital of Lille). As this was a retrospective and non-interventional study, informed consent was not required. Medical records were analyzed pseudonymously.

Outcomes and statistical analysis

Absolute eosinophil counts (AEC) are routinely determined from hemograms collected at presentation. They were retrieved from the available medical records. Optimal AEC cutoff was determined with the X-tile 3.6.1 software (Yale University, New Heaven, CT) and validated by the receiver operating characteristics (ROC) curve. The analysis was based on the mean AEC, averaged during the last month preceding the administration of chemo- or immunotherapy.

10.3389/fimmu.2023.1148798

The primary studied endpoint was mOS, defined as the time from the diagnosis to the date of death due to any cause. Secondary endpoints included PFS, response rate, duration of response and disease control rate. The response was assessed with radiographic tumor assessment according to the modified Response Criteria (mRECIST) [version 1.1] (4, 22). PFS was defined as the time between diagnosis and first-documented tumor progression or death due to any cause, whichever came first. Response rate was defined as the best overall response of complete response (CR) or partial response (PR). Duration of response was defined as the time from the first response to the first documented tumor progression or death due to any cause, whichever occurred first. Disease control rate was defined as the best overall response of CR, PR, or stable disease (SD).

Hazard ratios (HRs) and confidence intervals (CIs) of 95% were assessed using an unstratified Cox proportional hazards regression model. Survival curves and rates were estimated with the Kaplan-Meier method and Log-Rank test. Patients with missing values were excluded from the analysis. For statistical purposes, age was categorized as less than 65 years and more or equal to 65 years, whereas subtype was classified as epithelioid and non-epithelioid (i.e., sarcomatoid, biphasic or desmoplastic).

Statistical analysis and graphs were performed by using Prism GraphPad 8 or RStudio 2022.07.1 + 554.

Results

A threshold of AEC at 220/µL splits the cohort into two groups with different overall survival

The X-tile software was used to identify the optimal AEC cutoff associated with survival in the cohort of 230 MPM patients receiving first-line chemotherapy. This bioinformatic tool is a graphical method for biomarker assessment and outcome-based cut-point optimization (23). The program provides the optimal division of the data by selecting significant uncorrected p-value and the highest Chi-square. An average AEC was calculated for each patient using the counts of the last month preceding the first administration of chemotherapy. The optimal AEC cutoff determined with the X-tile software was 220 eosinophils/µL of blood (Chi-square = 10.5992, uncorrected p = 0.00113, Figure 1A). This threshold divided the cohort into two groups of 169 (72.40%) and 61 (27.60%) subjects with AEC < 220/µL (in grey) and AEC ≥ 220/µL (in blue), respectively (Figure 1B). These settings optimally segregated the Kaplan-Meier survival curves of the two subsets (Figure 1C). The relative risk was estimated by dividing the death incidence corresponding to each AEC by that of the population (Figure 1D). The AEC 220/µL cutoff classified the patients into two populations with highly significant different distributions (p = 0.0005, Figure 1E). The ROC curve illustrating the true (sensitivity) and false (1-specificity) positive rates validated the cutoff of 220 eosinophils/µL of blood (AUC = 0.6475, p = 0.0006, Figure 1F).

To verify that the measured AEC levels did not result from an increase of all white blood cells, the average absolute counts of other leukocytes were calculated. In populations with AEC < 220/µL and AEC ≥ 220/µL, the absolute counts of lymphocytes, monocytes and neutrophils were similar (Figure 1G). Since the absolute counts of eosinophils differed significantly ($p < 0.0001$), it was concluded that high levels of AEC did not result from a general increase of all leukocyte subsets. Furthermore, X-tiles analysis of neutrophils, lymphocytes, monocytes and neutrophil-to-lymphocyte ratio (NLR) did not highlight any threshold or correlation with mOS.

This cut-point selection analysis thus indicated that a threshold of AEC ≥ 220/µL within the last month preceding the first administration of chemotherapy optimally divided the total population into two subsets displaying statistically significant different overall survival times.

Study population

Among the 230 eligible patients treated by chemotherapy, 53 males and 8 females' cases were above the threshold of AEC ≥ 220/µL (Table 1). The median age at the time of diagnosis of the patients with AEC < 220/µL and AEC ≥ 220/µL was similar (67 +/- 10.4 *vs* 67 +/- 10.9 years, respectively). In both categories, most patients were male (74.0% and 86.9%) and presented an epithelioid subtype of MPM (87.0% and 77.0%). These characteristics were thus representative of typical gender and histologic distributions of MPM (4).

Due to limitations of a retrospective study, only partial information was available for asbestos exposure, Eastern Cooperative Oncology Group (ECOG) performance status prior to chemotherapy, smoking status, diabetes, and BAP-1 expression (Table 1). Prior exposure to asbestos was confirmed in 28.4% and 34.4% of patients with AEC < and ≥ 220/µL, respectively. The proportions of patients presenting different ECOG performance status were similar. OS and AEC/µL were not statistically different in patients with ECOG status 0, 1 and 2 (Supplementary Figure 1). Both active tobacco consumption and diabetes affected a minority of patients. Loss of BAP-1 expression determined by immunohistochemistry was validated in 24.9% of AEC < 220/µL and 18.0% of AEC ≥ 220/µL subsets.

It thus appeared that the two populations split by the AEC 220/µL cutoff shared similar characteristics of age, gender and histological subtype.

AEC ≥ 220/µL is correlated with shorter overall survival

Kaplan-Meier analysis showed that patients characterized by AEC ≥ 220/µL during the month preceding their chemotherapy had a highly significant shorter OS compared to subjects with AEC < 220/µL (Figure 2A). The mOS of the 230 individuals enrolled in this study were 14 months and 29 months for AEC above or equal to and below 220/µL, respectively (p = 0.0001, HR of 2.063 [95% CI

10.3389/fimmu.2023.1148798

A

% Total	AEC Range (/µL)	Chi square	Uncorrected P
72.40 %	0 to 219	10.5992	0.00113
27.60 %	220 to 1,020		

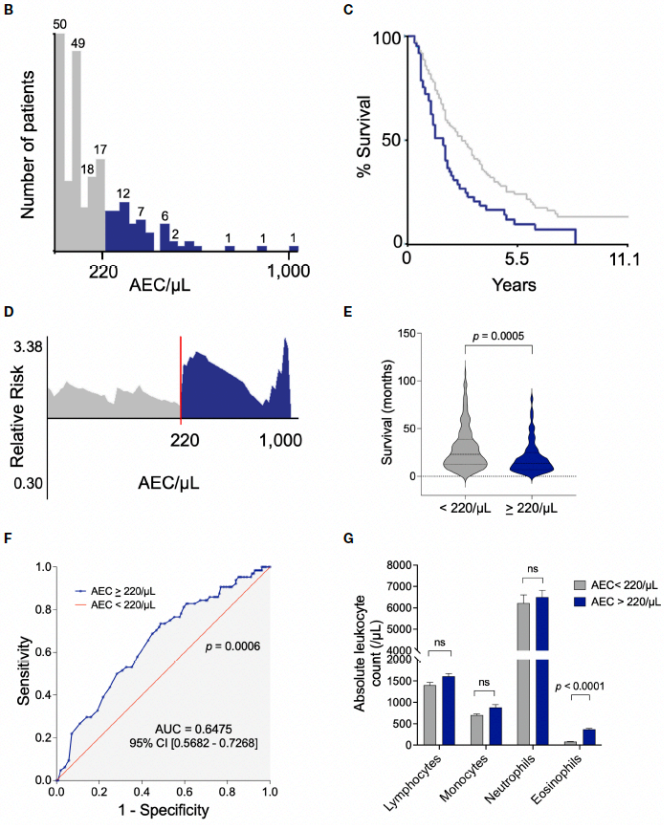

FIGURE 1
Determination of the AEC cutoff that optimally segregates the cohort according to OS. **(A)** An average AEC was calculated for each patient using the counts of the last month preceding the first administration of chemotherapy. The X-tile 3.6.1 software divided the data set into two populations by selecting significative uncorrected p-value and the highest Chi square. **(B)** Distribution of patients according to their AEC (below 219 per µl of blood in grey and 220-1,020 in blue). **(C)** Kaplan-Meier survival curve according to the AEC < 220/µL and AEC ≥ 220/µL. **(D)** The relative risk estimated by dividing the death incidence at each AEC by the death incidence of the population. **(E)** Median survival (in months) of the populations according to the AEC threshold. Normality of the populations was analyzed by the Shapiro-Wilk test and distributions were compared by Mann-Whitney test. **(F)** The ROC analysis of the true (sensitivity) and false (1-specificity) positive rates. **(G)** Absolute leucocyte counts (mean +/- standard deviation) in patients with AEC < 220/µL and AEC ≥ 220/µL. Statistical significance was calculated with the unpaired t-test. AEC, absolute eosinophil count; ROC, receiver operating characteristics; AUC, area under the curve.

1.420 – 2.998]). At 1 year, the OS rates were 58% [44.8 – 68.4] in subjects with AEC ≥ 220/µL compared to 79% [72.1 – 84.9] in the AEC < 220/µL group. The difference between the two categories was more pronounced at 2 years (28% [17.4 – 39.0] *vs* 55% [46.6 – 62.6]) corresponding to a 2.0-fold improvement in mOS when AEC < 220/µL. The lower mOS in the AEC ≥ 220/µL subset was observed independently of the histologic subtype (Figures 2B, C).

Although the proportion of patients with AEC ≥ 220/µL differed in the 3 hospitals (i.e., 17.8% in Lille, 32.35% in Liege and 34.4% in Antwerp; Supplementary Table 1), the mOS was significantly

10.3389/fimmu.2023.1148798

TABLE 1 Baseline characteristics of all patients receiving chemotherapy, segregated by the AEC cutoff of 220/µL.

	AEC < 220/µL		AEC ≥ 220/µL	
	N of patients (total 169)	% of patients	*N* of patients (total 61)	% of patients
Age at diagnosis:	67 ± 10.4 years		67 ± 10.9 years	
Sex				
Male	125	74.0%	53	86.9%
Female	44	26.0%	8	13.1%
Histological subtype				
Epithelioid	147	87.0%	47	77.0%
Sarcomatoid	10	5.9%	7	11.5%
Biphasic	6	3.6%	5	8.2%
Desmoplastic	3	1.8%	1	1.6%
Unknown	3	1.8%	1	1.6%
Known asbestos exposure				
Yes	48	28.4%	21	34.4%
No	91	53.8%	25	41.0%
Unknown	36	21.3%	15	24.6%
ECOG status prior to chemotherapy				
0	28	16.6%	8	13.1%
1	84	49.7%	26	42.6%
2	6	3.6%	2	3.3%
Unknown	57	33.7%	25	41.0%
Smoking status				
Smoking	25	14.8%	11	18.0%
Detoxed	56	33.1%	14	23.0%
No	78	46.2%	35	52.5%
Unknown	10	5.9%	4	6.6%
Diabetes				
Insulin-dependent	13	7.7%	5	8.2%
Non-insulin-dependent	19	11.2%	3	4.9%
No	128	75.7%	51	83.6%
Unknown	9	5.3%	2	3.3%
BAP-1 loss of expression				
Yes	42	24.9%	11	18.0%
No	17	10.1%	4	6.6%
Unknown	110	65.1%	46	75.4%

reduced from 36 to 17 months ($p = 0.0062$ for CHU of Lille) and from 29 to 16 months ($p = 0.0184$ for UZ Antwerp) (Supplementary Figure 2). However, there was no statistical difference in patients from the Liege CHU (17 vs 15 months, $p = 0.4610$) which may indicate a center bias. Furthermore, OS was shorter for patients with AEC ≥ 220/µL in predefined subgroups (Supplementary Figure 3).

Altogether, this retrospective observational study thus indicated that MPM patients with AEC ≥ 220/µL had a shorter mOS.

10.3389/fimmu.2023.1148798

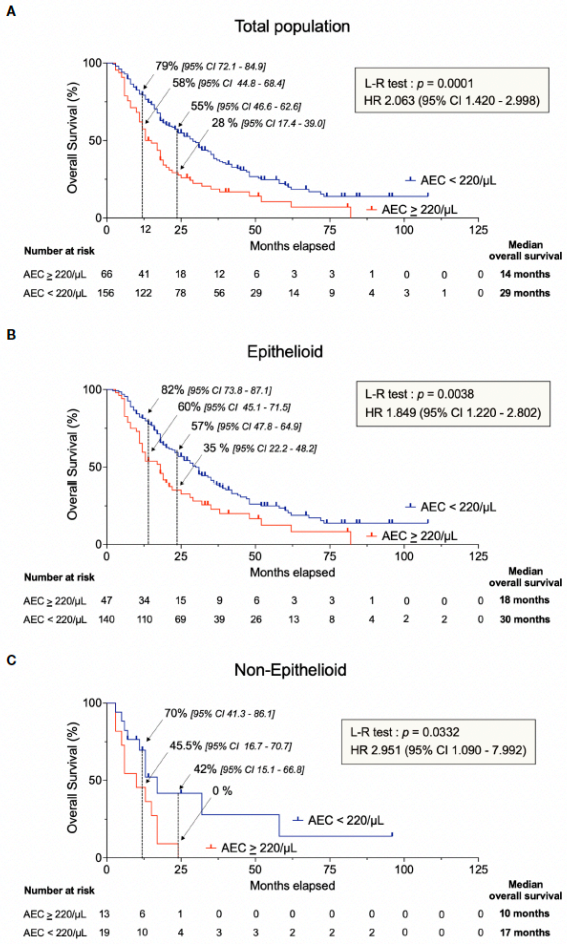

FIGURE 2
Kaplan-Meier analysis of OS in chemotherapy-treated patients with AEC ≥ 220/µL (in red) and AEC < 220/µL (in blue). **(A)** All patients of the cohort, **(B)** epithelioid MPM and **(C)** non-epithelioid MPM. AEC, absolute eosinophil count; OS, overall survival; L-R test; Log-Rank test; HR, hazard ratio; CI, confidence interval.

AEC superior or equal to 220/µL is associated with earlier relapse

The median PFS after chemotherapy was significantly lower in the AEC ≥ 220/µL group compared to the AEC < 220/µL subset (8 months *vs* 17 months; $p < 0.0001$, HR 2.589 [1.606 – 4.173]) (Figure 3A). Notably, PFS at 2 years was 13% [4.6 – 25.4] *vs* 42% [33.5 – 51.1] in patients with AEC ≥ 220/µL and AEC < 220/µL, respectively. Furthermore, the median time until progression or relapse differed significantly (7 months when AEC ≥ 220/µL *vs* 16 months when AEC < 220/µL; $p = 0.0011$, HR 1.950 [1.307 – 2.908]) (Figure 3B). Analysis of this retrospective dataset thus indicated that relapse after chemotherapy occurred more rapidly when AEC ≥ 220/µL.

Partial information on response to treatment was available in the retrospective data set (145 and 45 patients in the AEC < 220/µL and AEC ≥ 220/µL groups, respectively (Table 2). Information on response to treatment was missing in 31 patients. A single CR was

Willems et al.

10.3389/fimmu.2023.1148798

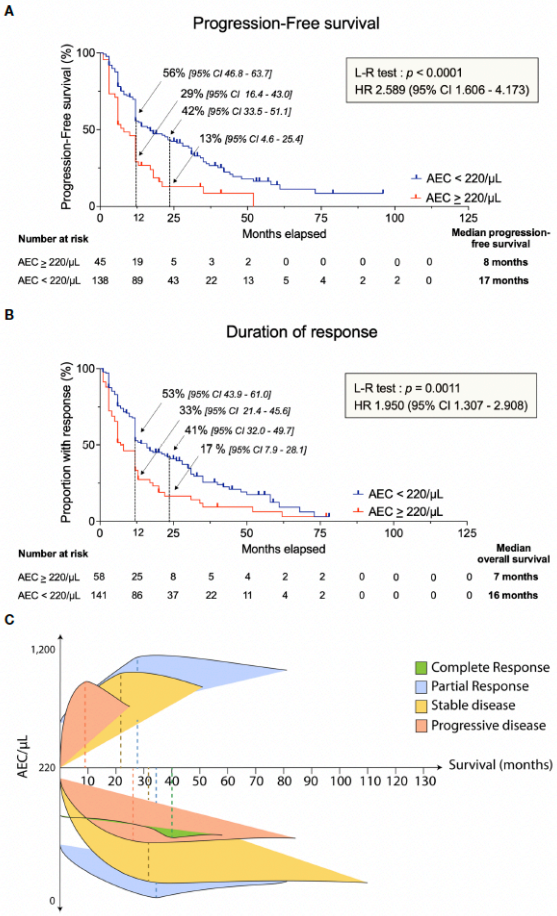

FIGURE 3
Response to chemotherapy according to AEC cutoff. **(A)** Progression-free survival in all randomized patients. **(B)** Duration of response in confirmed responders segregated by the AEC cutoff of 220/µL. **(C)** Schematic representation of response to chemotherapy, survival distribution and AEC. Dashed lines are the median survival (in months) corresponding to the type of response. L-R test, Log-Rank test; HR, hazard ratio; AEC, absolute eosinophil count.

observed in each category, consistently with other MPM trials (11, 24, 25). The objective response rate (ORR) combining CR and PR was similar in the 2 subsets (15.9% *vs* 20.4% at 3 months and 9.0% *vs* 9.3% at 6 months). In contrast, SD was significantly more common in patients with AEC < 220/µL (56.6%) than in those with AEC ≥ 220/µL (38.9%). This difference in SD was due to a higher proportion of patients with progressive disease (PD) in the AEC ≥ 220/µL subgroup (33.3%, *vs* 17.2%). Only 33% [21.4 – 45.6] of patients with AEC ≥ 220/µL displayed a disease control, including CR, PR and SD of at least 1 year, compared to 53% [43.9 – 61.0] in subjects with AEC < 220/µL. This difference was still observed after 2 years (17% in AEC ≥ 220/µL *vs* 41% in AEC < 220/µL).

Together, these data showed that the AEC cutoff of 220/µL identified groups of patients with different mOS (Figure 2A) and response to chemotherapy (Figure 3C). The same conclusion was drawn when the study was extended to patients who received immunotherapy (Supplementary Figures 4, 5). Indeed, Kaplan-Meier analysis highlighted that, patients with AEC ≥ 220/µL prior to immunotherapy had a shorter OS (p = 0.0022) and was characterized by a higher proportion of PD (42.9% *vs* 18.9%) compared with the AEC < 220/µL group.

10.3389/fimmu.2023.1148798

TABLE 2 Summary of patient's response in all randomized patients receiving chemotherapy, segregated by the AEC cutoff of 220/µL.

	AEC < 220/µL		AEC ≥ 220/µL	
	N of patients (total 145)	% of patients	*N* of patients (total 54)	% of patients
Best overall response				
Complete response	1	0.7%	1	1.9%
Partial response	37	25.5%	14	25.9%
Stable disease	82	56.6%	21	38.9%
Progressive disease	25	17.2%	18	33.3%
Disease control rate (CR + PR + SD)				
3 months	99	68.3%	29	53.7%
6 months	81	55.9%	19	35.2%
Objective response rate (CR + PR)				
3 months	23	15.9%	11	20.4%
6 months	13	9.0%	5	9.3%
Proportion of patients with a response of at least 1 year				
1 year	53%		33%	
95% CI	43.9 – 61.0		21.4 – 45.6	
2 years	41%		17%	
95% CI	32.0 – 49.7		7.9 – 28.1	

Responses were assessed accordingly to mRECIST v1.1 criteria. CR, complete response; PR, partial response; SD, stable disease; CI, confidence interval.

Discussion

In this report, we showed that patients with an AEC ≥ 220/µL prior to their therapy appear to have a worse outcome and relapse more rapidly. Importantly, we have considered the mean AEC value measured during the month preceding administration of chemo- or immunotherapy. In particular, the disease control rate was improved in chemotherapy-treated patients with AEC < 220/µL and, consistently, the proportion of subjects with a response at two years was increased by 2.4-fold (i.e., 41% *vs* 17%, Table 2). While the proportion of patients with objective response rate (CR + PR) was similar above and below the threshold of AEC 220/µL, there was a statistically significant difference of SD (Table 2; Supplementary Figures 4C and 5C).

It should be mentioned that, in this study, we excluded patients with hypereosinophilia induced by asthma, allergy, parasitic infection, autoimmune disease, and medication (26, 27). Indeed, these conditions require systemic treatments that would have affected the immune system. It should also be noted that, within the "normal" range (0-450 eosinophils/µL of blood), there is no clear mechanism that explains the fluctuations of eosinophil levels.

In this retrospective study, successive CT evaluations and over time distinguishable tumor margins were often missing. It should however be mentioned that multiple radiographic assessments are particularly challenging in MPM (28). Therefore, OS is preferred and considered to be a more objective and reliable endpoint compared to PFS, response rate and duration of response (11). In this perspective, we showed that the AEC 220/µL threshold predicted a significant difference in mOS (14 *vs* 29 months in patients treated with chemotherapy and 25 *vs* 48 months with immunotherapy, Figure 2 and Supplementary Figure 4). The significant association between AEC and OS does not preclude that eosinophilic MPM patients could still respond to chemotherapy or ICIs (29). Consistently, MPM case reports of poor response and fast deterioration have been described in eosinophilic patients (29–31). If validated by prospective and interventional studies, this conclusion could thus be of particular interest for MPM management.

In fact, the association of AEC and OS has been investigated in other cancers, yielding to opposite conclusions. Indeed, excess of eosinophils in the peripheral blood has been correlated with either a better or a worse prognosis depending on the cancer type (20, 32, 33). For example, in non-small cell lung cancer (NSCLC) and melanoma, an AEC equal or superior to 300/µL measured before therapy was associated with a better outcome (34–43). By contrast, the level of peripheral blood eosinophils is an independent prognostic factor for disease progression and disease-specific death in Hodgkin's lymphoma and primary cutaneous T-cell lymphoma (40, 44–46).

Due to the more recent advent of immunotherapy in MPM, the number of first-line immunotherapy-treated patients included in this study was limited. However, the difference of OS in the AEC ≥ 220/µL and AEC < 220/µL groups was nevertheless statistically significant (L-R test $p = 0.0022$; Supplementary Figure 4). This conclusion was valid providing that AECs were determined before, but not during or after, the initiation of therapy. In contrast, increase of peripheral blood eosinophils during treatment with ICIs is associated with better

response and clinical outcome in NSCLC, indicating that the correlation could be dependent on the tumor type (47, 48). Although the biological mechanisms underlying this difference are still not well understood, it is likely that the TME is a central parameter of this cancer specificity. The TME most likely shapes the phenotype of eosinophils into diverse subpopulations with opposite functions, as illustrated in asthma (49–51). In MPM, the interaction of eosinophils with other immune cells such as macrophages, monocytes and neutrophils may direct pro- or anti-tumor functions as well as response to therapy (13–18). Consistently, inflammation markers such as lymphocyte predominance, NLR and absolute monocyte count (AMC) have been correlated with poor survival (52–57). Analysis of the data set of our cohort did not reveal any association of OS with NLR, AMC and monocyte-to-lymphocyte ratios.

Although a causal link still needs to be demonstrated, the correlation between AEC and OS possibly opens direct prospects for therapeutic intervention. Indeed, our report suggests that there might be a benefit to decrease the AEC below the 220/µL threshold before initiating the chemo- or immunotherapy. For example, glucocorticoids (e.g., methylprednisolone) used to prevent pemetrexed-associated rash, emesis and inflammation (58–60) are able to induce apoptosis of eosinophils (61). In our study, a single dose of methylprednisolone at 48mg effectively reduced inflammation but did not reduce myeloid cell counts as numbers remained approximately constant before and after administration. More specific approaches targeting eosinophils have recently been developed in the treatment of asthma (62). Monoclonal antibodies interacting with cytokines associated with eosinophilia (e.g., IL-5, IL-33) are currently evaluated in clinical trials to treat eosinophilic COPD patients: Mepolizumab (anti-IL-5; NCT04075331), MEDI3506 (anti-IL-33; NCT04570657), REGN3500 (anti-IL-33; NCT04701983 and NCT04751487) and Astegolimab (anti-ST2; NCT03615040). Whether these targeted approaches are effective as add-on therapy in MPM could thus merit further evaluation.

Conclusion

In summary, this retrospective study shows that an AEC threshold of 220/µL measured prior to therapy identifies populations with distinct outcomes in mesothelioma, supporting further prospective analysis and possibly interventional trials.

Data availability statement

The original contributions presented in the study are included in the article/Supplementary Material. Further inquiries can be directed to the corresponding author.

Ethics statement

The studies involving human participants were reviewed and approved by University Hospital of Liège Ethical Committee, reference 2020/45 University Hospital of Antwerp Ethical Committee, reference 2022/1844. Written informed consent for participation was not required for this study in accordance with the national legislation and the institutional requirements.

Author contributions

MW, AS and EW collected the dataset in Lille CHU. JR collected the dataset in Antwerp CHU. MW, AF and MH collected the dataset in Liege CHU. AF, AS, EW, HB, JR, MG, LH, MJ, VH, RL participated in data interpretation and manuscript reviewing. MW, LW and MH designed the study. MW and LW drafted the manuscript. All authors contributed to the article and approved the submitted version.

Funding

This work was supported by the Belgian Foundation against Cancer, the Fonds National de la Recherche Scientifique (FNRS), the Télévie, and the Fondation Léon Fredericq.

Acknowledgments

The authors thank the GIGA Platforms (ULiège, Belgium) for support, help and advice. We gratefully acknowledge Ramatou Sare (Gembloux Agro Bio-Tech) for the collection of data in Lille CHU. We also thank Jan Van Meerbeeck for making this study possible.

Conflict of interest

Beyond the scope of this study, AS participated to clinical trials and expert boards with Amphera, AstraZeneca, BMS, MSD, Regeneron/Sanofi, Roche and Trizell. VH declares consultancy fees from AstraZeneca and Chiesi.

The remaining authors declare that the research was conducted in the absence of any commercial or financial relationships that could be construed as a potential conflict of interest.

Publisher's note

Supplementary material

The Supplementary Material for this article can be found online at: https://www.frontiersin.org/articles/10.3389/fimmu.2023.1148798/full#supplementary-material

References

1. Asciak R, George V, Rahman NM. Update on biology and management of mesothelioma. *Eur Respir Rev* (2021) 30:1–13. doi: 10.1183/16000617.0226-2020

2. Kazan-Allen L. *Current asbestos bans* (2022). Available at: http://www.ibasecretariat.org/alpha_ban_list.php (Accessed September 14, 2022).

3. Bray F, Ferlay J, Soerjomataram I, Siegel RL, Torre LA, Jemal A. Global cancer statistics 2018: GLOBOCAN estimates of incidence and mortality worldwide for 36 cancers in 185 countries. *CA Cancer J Clin* (2018) 68:394–424. doi: 10.3322/caac.21492

4. Popat S, Baas P, Faivre-Finn C, Girard N, Nicholson AG, Nowak AK, et al. Malignant pleural mesothelioma: ESMO clinical practice guidelines for diagnosis, treatment and follow-up. *Ann Oncol* (2022) 33:129–42. doi: 10.1016/j.annonc.2021.11.005

5. Ali G, Bruno R, Fontanini G. The pathological and molecular diagnosis of malignant pleural mesothelioma: A literature review. *J Thorac Dis* (2018) 10:S276–84. doi: 10.21037/jtd.2017.10.125

6. Vogelzang NJ, Rusthoven JJ, Symanowski J, Denham C, Kaukel E, Ruffie P, et al. Phase III study of pemetrexed in combination with cisplatin versus cisplatin alone in patients with malignant pleural mesothelioma. *J Clin Oncol* (2003) 21:2636–44. doi: 10.1200/JCO.2003.11.136

7. Fennell DA, Ewings S, Ottensmeier C, Califano R, Hanna GG, Hill K, et al. Nivolumab versus placebo in patients with relapsed malignant mesothelioma (CONFIRM): A multicentre, double-blind, randomised, phase 3 trial. *Lancet Oncol* (2021) 22:1530–40. doi: 10.1016/S1470-2045(21)00471-X

8. Baas P. Nivolumab plus ipilimumab should be the standard of care for first-line unresectable epithelioid mesothelioma. *J Thorac Oncol* (2022) 17:30–3. doi: 10.1016/j.jtho.2021.07.029

9. Zalcman G, Mazieres J, Margery J, Greillier L, Audigier-Valette C, Moro-Sibilot D, et al. Bevacizumab for newly diagnosed pleural mesothelioma in the mesothelioma avastin cisplatin pemetrexed study (MAPS): A randomised, controlled, open-label, phase 3 trial. *Lancet* (2016) 387:1405–14. doi: 10.1016/S0140-6736(15)01238-6

10. Désage AL, Karpathiou G, Peoc'h M, Froudarakis ME. The immune microenvironment of malignant pleural mesothelioma: A literature review. *Cancers (Basel)* (2021) 13:1–31. doi: 10.3390/cancers13133205

11. Baas P, Scherpereel A, Nowak AK, Fujimoto N, Peters S, Tsao AS, et al. First-line nivolumab plus ipilimumab in unresectable malignant pleural mesothelioma (CheckMate 743): a multicentre, randomised, open-label, phase 3 trial. *Lancet* (2021) 397:375–86. doi: 10.1016/S0140-6736(20)32714-8

12. Fennell DA, Dulloo S. Chemotherapy with or without bevacizumab should be the standard of care for first-line unresectable epithelioid mesothelioma. *J Thorac Oncol* (2022) 17:34–7. doi: 10.1016/j.jtho.2021.08.004

13. Chénè AL, D'Almeida S, Blondy T, Tabiasco J, Deshayes S, Fonteneau JF, et al. Pleural effusions from patients with mesothelioma induce recruitment of monocytes and their differentiation into M2 macrophages. *J Thorac Oncol* (2016) 11:1765–73. doi: 10.1016/j.jtho.2016.06.022

14. Lievense LA, Cornelissen R, Bezemer K, Kaijen-Lambers MEH, Hegmans JPJJ, Aerts JGJV. Pleural effusion of patients with malignant mesothelioma induces macrophage-mediated T cell suppression. *J Thorac Oncol* (2016) 11:1755–64. doi: 10.1016/j.jtho.2016.06.021

15. Hamaidia M, Gazon H, Hoyos C, Hoffmann GB, Louis R, Duysinx B, et al. Inhibition of EZH2 methyltransferase decreases immunoediting of mesothelioma cells by autologous macrophages through a PD-1-dependent mechanism. *JCI Insight* (2019) 4:1–17. doi: 10.1172/jci.insight.128474

16. Gauttier V, Pengam S, Durand J, Biteau K, Mary C, Morello A, et al. Selective SIRPα blockade reverses tumor T cell exclusion and overcomes cancer immunotherapy resistance. *J Clin Invest* (2020) 130:6109–23. doi: 10.1172/JCI135528

17. Mola S, Pinton G, Erreni M, Corazzari M, De Andrea M, Grolla AA, et al. Inhibition of the histone methyltransferase EZH2 enhances protumor monocyte recruitment in human mesothelioma spheroids. *Int J Mol Sci* (2021) 22:1–25. doi: 10.3390/ijms22094391

18. Hoyos C, Fontaine A, Jacques JR, Heinen V, Louis R, Duysinx B, et al. HDAC inhibition with valproate improves direct cytotoxicity of monocytes against mesothelioma tumor cells. *Cancers (Basel)* (2022) 14:1–19. doi: 10.3390/cancers14092164

19. Reichman H, Karo-atar D, Munitz A. Emerging roles for eosinophils in the tumor microenvironment. *Trends Cancer* (2016) 2:664–75. doi: 10.1016/j.trecan.2016.10.002

20. Varricchi G, Galdiero MR, Loffredo S, Lucarini V, Marone G, Mattei F, et al. Eosinophils: The unsung heroes in cancer? *Oncoimmunology* (2018) 7:1–14. doi: 10.1080/2162402X.2017.1393134

21. Scherpereel A, Opitz I, Berghmans T, Psallidas I, Glatzer M, Rigau D, et al. ERS/ESTS/EACTS/ESTRO guidelines for the management of malignant pleural mesothelioma. *Eur Respir J* (2020) 55:1–31. doi: 10.1183/13993003.00953-2019

22. Byrne MJ, Nowak AK. Modified RECIST criteria for assessment of response in malignant pleural mesothelioma. *Ann Oncol* (2004) 15:257–60. doi: 10.1093/annonc/mdh059

23. Camp RL, Dolled-Filhart M, Rimm DL. X-Tile: A new bio-informatics tool for biomarker assessment and outcome-based cut-point optimization. *Clin Cancer Res* (2004) 10:7252–9. doi: 10.1158/1078-0432.CCR-04-0713

24. Santoro A, O'Brien ME, Stahel RA, Nackaerts K, Baas P, Karthaus M, et al. Pemetrexed plus cisplatin or pemetrexed plus carboplatin for chemonaïve patients with malignant pleural mesothelioma: Results of the international expanded access program. *J Thorac Oncol* (2008) 3:756–63. doi: 10.1097/JTO.0b013e31817c73d6

25. Van Meerbeeck JP, Gaafar R, Manegold C, Van Klaveren RJ, Van Marck EA, Vincent M, et al. Randomized phase III study of cisplatin with or without raltitrexed in patients with malignant pleural mesothelioma: An intergroup study of the European organisation for research and treatment of cancer lung cancer group and the national cancer institute. *J Clin Oncol* (2005) 23:6881–9. doi: 10.1200/JCO.20005.14.589

26. Kovalszki A, Weller PF. Eosiniophilia. *Prim Care* (2016) 43:607–17. doi: 10.1016/j.pop.2016.07.010.Eosinophilia

27. Kovalszki A, Weller PF. "Eosinophils and eosinophilia", In: Rich RR, Fleisher TA, Shearer WT, Schroeder HW, Frew A, Weyand CM, editors. *Clinical Immunology Principles and Practices (Fifth Edition)* (2019), p. 349–61. doi: 10.1016/B978-0-7020-6896-6.00024-7

28. U.S. Food and Drug Administration. *Clinical trial endpoints for the approval of cancer drugs and biologics: Guidance for industry* (Rockville: U.S. Food and Drug Administration) (2018). pp. 1–16.

29. Yamazoe M, Ozasa H, Kim YH. Effectiveness of nivolumab on sarcomatoid malignant pleural mesothelioma with eosinophilia and eosinophilic pleural effusion. *J Thorac Oncol* (2019) 14:e251–3. doi: 10.1016/j.jtho.2019.06.007

30. Takeuchi E, Takahashi N, Morizumi S, Tamiya H, Matsuoka H, Kuroda N, et al. Interleukin-5-producing malignant pleural mesothelioma with eosinophilic pleural effusion. *Thorac Cancer* (2020) 11:3043–6. doi: 10.1111/1759-7714.13652

31. Yamazaki M, Ohwada A, Miyaji A, Yamazaki H, Nara T, Hirai S, et al. Pulmonary paragonimiasis with coincidental malignant mesothelioma. *Intern Med* (2008) 47:1027–31. doi: 10.2169/internalmedicine.47.0852

32. Grisaru-Tal S, Itan M, Klion AD, Munitz A. A new dawn for eosinophils in the tumour microenvironment. *Nat Rev Cancer* (2020) 20:594–607. doi: 10.1038/s41568-020-0283-9

33. Simon SCS, Utikal J, Umansky V. Opposing roles of eosinophils in cancer. *Cancer Immunol Immunother* (2019) 68:823–33. doi: 10.1007/s00262-018-2255-4

34. Wu HX, Zhuo KQ, Cheng DY. Peripheral blood eosinophil as a biomarker in outcomes of acute exacerbation of chronic obstructive pulmonary disease. *Int J COPD* (2019) 14:3003–15. doi: 10.2147/COPD.S226783

35. Zhang Y, Liang LR, Zhang S, Lu Y, Chen YY, Shi HZ, et al. Blood eosinophilia and its stability in hospitalized COPD exacerbations are associated with lower risk of all-cause mortality. *Int J COPD* (2020) 15:1123–34. doi: 10.2147/COPD.S245056

36. Reichman H, Itan M, Rozenberg P, Yarmolovski T, Brazowski E, Varol C, et al. Activated eosinophils exert antitumorigenic activities in colorectal cancer. *Cancer Immunol Res* (2019) 7:388–400. doi: 10.1158/2326-6066.CIR-18-0494

37. Onesti CE, Josse C, Boulet D, Thiry J, Beaumecker B, Bours V, et al. Blood eosinophilic relative count is prognostic for breast cancer and associated with the presence of tumor at diagnosis and at time of relapse. *Oncoimmunology* (2020) 9:1–11. doi: 10.1080/2162402X.2020.1761176

38. Günduz S, Göksu SS, Arslan D, Tatli AM, Uysal M, Gündüz UR, et al. Factors affecting disease-free survival in patients with human epidermal growth factor receptor 2-positive breast cancer who receive adjuvant trastuzumab. *Mol Clin Oncol* (2015) 3:1109–12. doi: 10.3892/mco.2015.610

39. Steel JL, Kim KH, Dew MA, Unruh ML, Antoni MH, Olek MC, et al. Cancer-related symptom clusters, eosinophils, and survival in hepatobiliary cancer: An exploratory study. *J Pain Symptom Manag* (2010) 39:859–71. doi: 10.1016/j.jpainsymman.2009.09.019

40. Davis BP, Rothenberg ME. Eosinophils and cancer. *Cancer Immunol Res* (2014) 2:1–9. doi: 10.1158/2326-6066.CIR-13-0196

41. Simon SCS, Hu X, Panten J, Grees M, Renders S, Thomas D, et al. Eosinophil accumulation predicts response to melanoma treatment with immune checkpoint inhibitors. *Oncoimmunology* (2020) 9:1–12. doi: 10.1080/2162402X.2020.1727116

42. Moreira A, Leisgang W, Schuler G, Heinzerling L. Eosinophilic count as a biomarker for prognosis of melanoma patients and its importance in the response to immunotherapy. *Immunotherapy* (2017) 9:115–21. doi: 10.2217/imt-2016-0138

43. Wei Y, Zhang X, Wang G, Zhou Y, Luo M, Wang S, et al. The impacts of pretreatment circulating eosinophils and basophils on prognosis of stage I–III colorectal cancer. *Asia Pac J Clin Oncol* (2018) 14:e243–51. doi: 10.1111/ajco.12871

44. Tancrède-Bohin E, Ionescu MA, de la Salmonière P, Dupuy A, Rivet J, Rybojad M, et al. Prognostic value of blood eosinophilia in primary cutaneous T-cell lymphomas. *Arch Dermatol* (2004) 140:1057–61. doi: 10.1001/archderm.140.9.1057

45. Utsunomiya A, Ishida T, Inagaki A, Ishii T, Yano H, Komatsu H, et al. Clinical significance of a blood eosinophilia in adult T-cell leukemia/lymphoma: A blood eosinophilia is a significant unfavorable prognostic factor. *Leuk Res* (2007) 31:915–20. doi: 10.1016/j.leukres.2006.10.017

46. Bishara S, Griffin M, Cargill A, Bali A, Gore ME, Kaye SB, et al. Pre-treatment white blood cell subtypes as prognostic indicators in ovarian cancer. *Eur J Obstet Gynecol Reprod Biol* (2008) 138:71–5. doi: 10.1016/j.ejogrb.2007.05.012

47. Okauchi S, Shiozawa T, Miyazaki K, Nishino K, Sasatani Y, Ohara G, et al. Association between peripheral eosinophils and clinical outcomes in patients with non-small cell lung cancer treated with immune checkpoint inhibitors. *Polish Arch Intern Med* (2021) 131:152–60. doi: 10.20452/pamw.15776

48. Alves A, Dias M, Campainha S, Barroso A. Peripheral blood eosinophilia may be a prognostic biomarker in non-small cell lung cancer patients treated with immunotherapy. *J Thorac Dis* (2021) 13:2716–27. doi: 10.21037/jtd-20-3525

49. Januskevicius A, Jurkeviciute E, Janulaityte I, Kalinauskaite-Zukauske V, Miliauskas S, Malakauskas K. Blood eosinophils subtypes and their survivability in asthma patients. *Cells* (2020) 9:1–17. doi: 10.3390/cells9051248

50. Mesnil C, Raulier S, Paulissen G, Xiao X, Birrell MA, Pirottin D, et al. Lung-resident eosinophils represent a distinct regulatory eosinophil subset. *J Clin Invest* (2016) 126:3279–95. doi: 10.1172/JCI85664

51. Percopo CM, Brenner TA, Ma M, Kraemer LS, Hakeem RMA, Lee JJ, et al. SiglecF + Gr1 hi eosinophils are a distinct subpopulation within the lungs of allergen-challenged mice. *J Leukoc Biol* (2017) 101:321–8. doi: 10.1189/jlb.3a0416-166r

52. Gutierrez-Sainz L, Cruz P, Martinez-Recio S, Higuera O, Esteban-Rodriguez MI, Arias-Lotto F, et al. Malignant pleural mesothelioma: clinical experience and prognostic value of derived neutrophil-to-lymphocyte ratio and PD-L1 expression. *Clin Transl Oncol* (2021) 23:2030–5. doi: 10.1007/s12094-021-02605-w

53. Urso L, Silic-Benussi M, Boscolo A, Lorenzi M, Bonanno L, Lunardi F, et al. Detection of circulating immunosuppressive cytokines in malignant pleural mesothelioma patients for prognostic stratification. *Cytokine* (2021) 146:155622. doi: 10.1016/j.cyto.2021.155622

54. De Fonseka D, Arnold DT, Morley AJ, Brett M, Bhatt N, Edey A, et al. Lymphocyte predominance in blood, pleural fluid, and tumour stroma; a prognostic marker in pleural mesothelioma. *BMC Pulm Med* (2022) 22:1–6. doi: 10.1186/s12890-022-01968-2

55. Cimen F, Agackiran Y, Düzgün S, Aloglu M, Senturk A, Atikcan S. Factors affecting the life expectancy in malignant pleural mesothelioma: Our 10 years of studies and experience. *Med (Baltimore)* (2022) 101:e30711. doi: 10.1097/md.0000000000030711

56. Okita R, Okada M, Inokawa H, Murakami T, Ikeda E. Prognostic values of preoperative c-reactive protein, albumin, and neutrophil ratios in patients with malignant pleural mesothelioma who underwent extrapleural pneumonectomy. *Surg Oncol* (2022) 43:101813. doi: 10.1016/j.suronc.2022.101813

57. Fournel L, Charrier T, Huriet M, Iaffaldano A, Lupo A, Damotte D, et al. Prognostic impact of inflammation in malignant pleural mesothelioma: A large-scale analysis of consecutive patients. *Lung Cancer* (2022) 166:221–7. doi: 10.1016/j.lungcan.2022.03.014

58. Hazarika M, White RM, Booth BP, Wang Y, Ham DYL, Liang CY, et al. Pemetrexed in malignant pleural mesothelioma. *Clin Cancer Res* (2005) 11:982–92. doi: 10.1158/1078-0432.982.11.3

59. Sakurada T, Kakiuchi S, Tajima S, Horinouchi Y, Konaka K, Okada N, et al. Pemetrexed-induced rash may be prevented by supplementary corticosteroids. *Biol Pharm Bull* (2015) 38:1752–6. doi: 10.1248/bpb.b15-00435

60. Sakurada T, Nokihara H, Koga T, Zamami Y, Goda M, Yagi K, et al. Prevention of pemetrexed-induced rash using low-dose corticosteroids: A phase II study. *Oncologist* (2022) 27:e554–60. doi: 10.1093/oncolo/oyab077

61. Cook AM, McDonnell AM, Lake RA, Nowak AK. Dexamethasone co-medication in cancer patients undergoing chemotherapy causes substantial immunomodulatory effects with implications for chemo-immunotherapy strategies. *Oncoimmunology* (2016) 5:1–11. doi: 10.1080/2162402X.2015.1066062

62. Cusack RP, Whetstone CE, Xie Y, Ranjbar M, Gauvreau GM. Regulation of eosinophilia in asthma–new therapeutic approaches for asthma treatment. *Cells* (2021) 10:1–23. doi: 10.3390/cells10040817

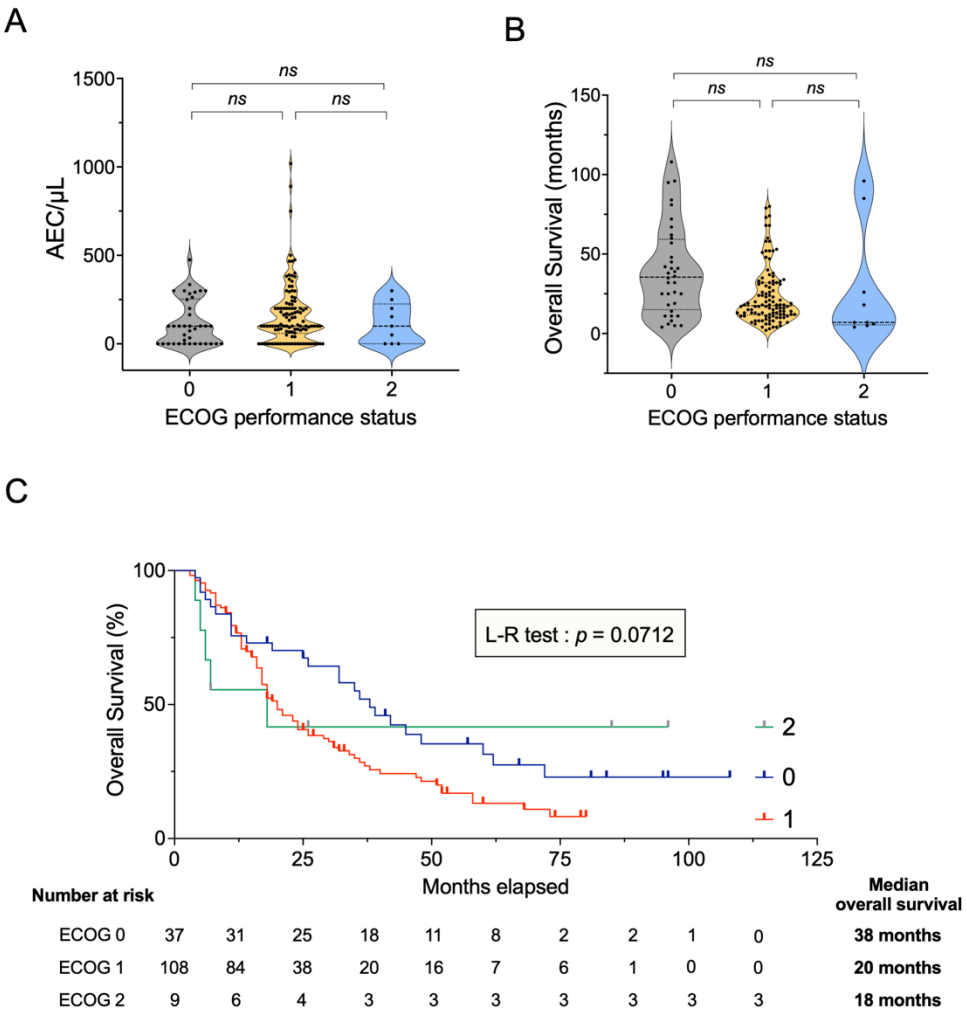

Supplementary Figure 1: Populations' distribution and Kaplan-Meier analysis of overall survival by ECOG status

(A) Distribution of AEC per µL of blood according to the ECOG performance status of 0, 1 and 2. **(B)** Distribution patients' survival (in months) according to their ECOG performance status. **(C)** Kaplan-Meier survival curve according to the ECOG performance status. Normality of the populations was analyzed by the Shapiro-Wilk test. The variance of the means was compared by one-way ANOVA followed by Tukey's multiple comparison test (A,B). ECOG: European Cooperative Oncology Group; AEC: Absolute Eosinophil Count; L-R test: Log-Rank Test. *ns*: not significant

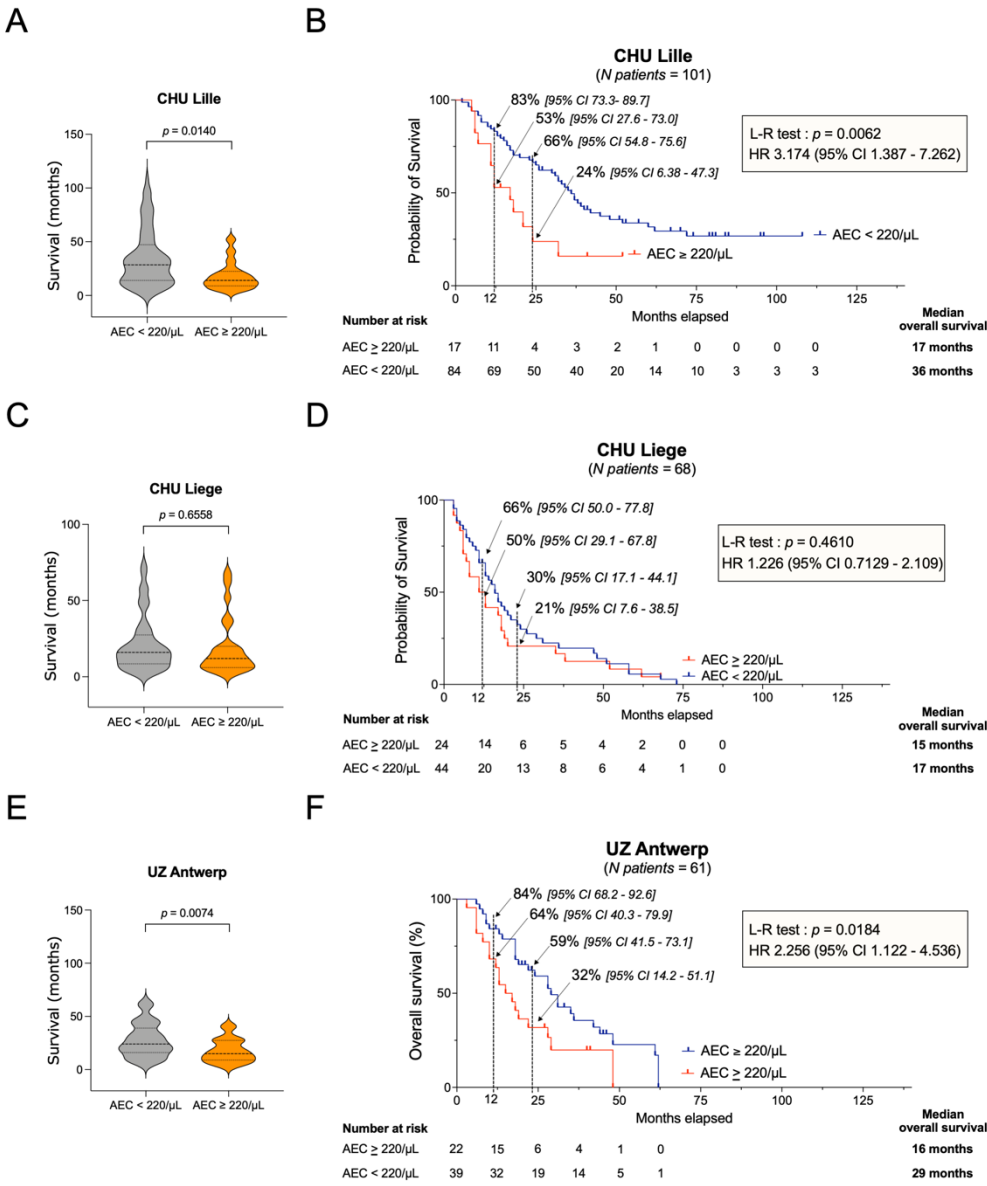

Supplementary Figure 2: Median survival and Kaplan-Meier analysis of overall survival in the three cohorts

Survival in months (**A,C,E**) and overall survival in % (**B,D,F**) were calculated from data sets of the CHU of Lille **(A,B),** the CHU of Liege **(C,D)** and UZ Antwerp **(E,F)**. Normality of the populations was analyzed by the Shapiro-Wilk test and distributions were compared by Mann-Whitney (A,C,E). Overall survival (y axis) during the study (x axis, in months) are presented in Kaplan-Meier graphs and survival curves are compared by Log-Rank test (B,D,F).

AEC: absolute eosinophil count; L-R test: Log-Rank test; HR: hazard ratio; CI: confidence interval.

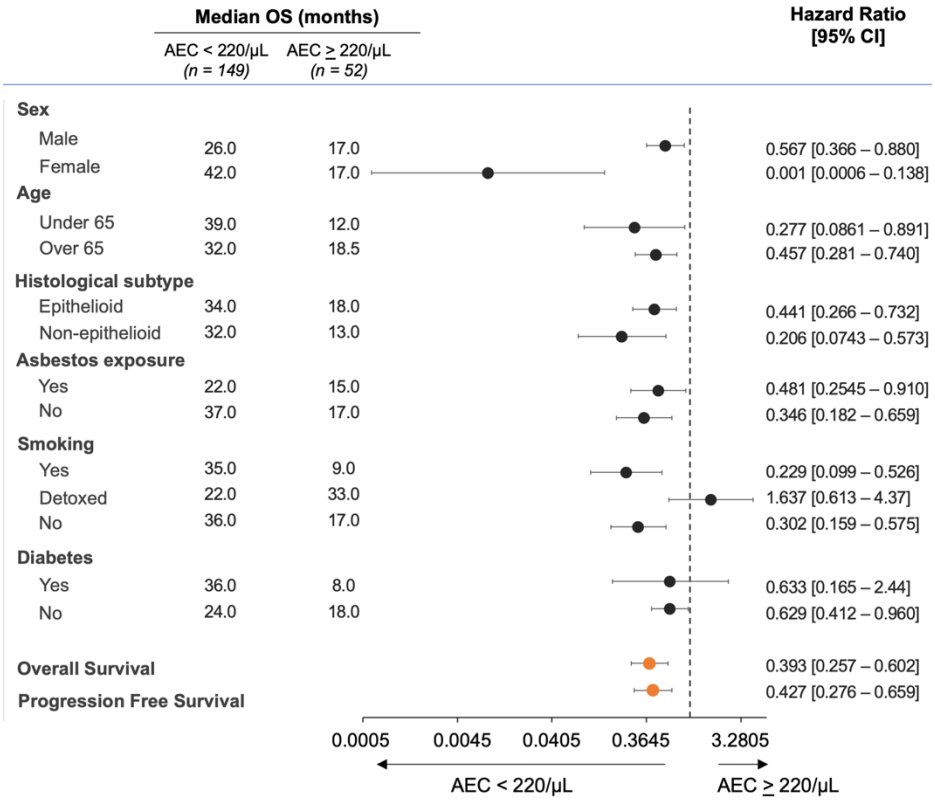

Supplementary Figure 3: Hazard ratios and overall survival of predefined subgroups
Overall survival and hazard ratios were generated by Kaplan-Meier analysis of subgroups divided by the AEC cutoff.
AEC: absolute eosinophil count; OS: overall survival; CI: confidence interval.

A

	AEC < 220/µL		AEC ≥ 220/µL	
	N of patients (total 37)	% of patients	N of patients (total 7)	% of patients
Age at diagnosis	65.8 ± 8.5 years		69.0 ± 8.0 years	
Line of treatment				
1st line immunotherapy	8	21.6 %	4	57.1 %
2nd or 3rd line immunotherapy	29	78.4 %	3	42.9 %
Best overall response				
Complete response	0	0.0%	0	0.0%
Partial response	6	16.2%	1	14.3%
Stable disease	24	64.9%	3	42.9%
Progressive disease	7	18.9%	3	42.9%

B

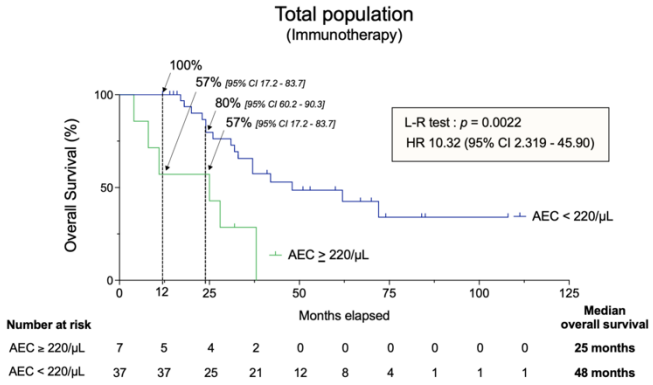

C

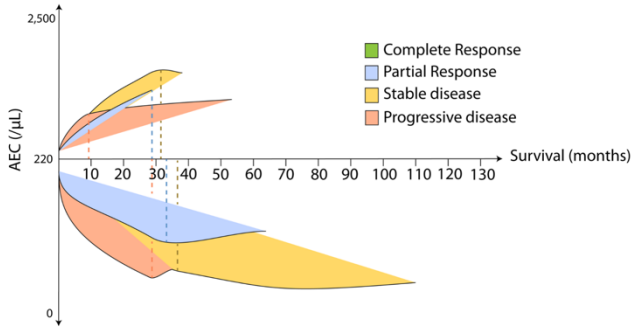

Supplementary Figure 4: Response to immunotherapy and OS according to AEC cutoff
(A) Age at diagnosis, line of treatment and type of response to immunotherapy determined accordingly to mRECIST v1.1 criteria. **(B)** Kaplan-Meier analysis of OS in groups of patients with AEC ≥ 220/µL (in blue) and AEC < 220/µL (in green) determined before immunotherapeutic treatment. **(C)** Schematic representation of response to immunotherapy, survival distribution and AEC. Dashed lines are the median survival times (in months) corresponding to the type of response. L-R test: Log-Rank test; HR: hazard ratio; AEC: absolute eosinophil count.

A

	AEC < 220/µL		AEC ≥ 220/µL	
	N of patients (total 193)	% of patients	N of patients (total 70)	% of patients
Best overall response				
Complete response	1	0.5%	1	1.'%
Partial response	40	20.7%	14	20.0%
Stable disease	100	51.8%	23	32.9%
Progressive disease	33	17.1%	21	30.0%
Response at 3 months				
Disease control rate (CR + PR + SD)	123	63.7%	28	40.0%
Objective response rate (CR + PR)	29	15.0 %	5	7.1%

B

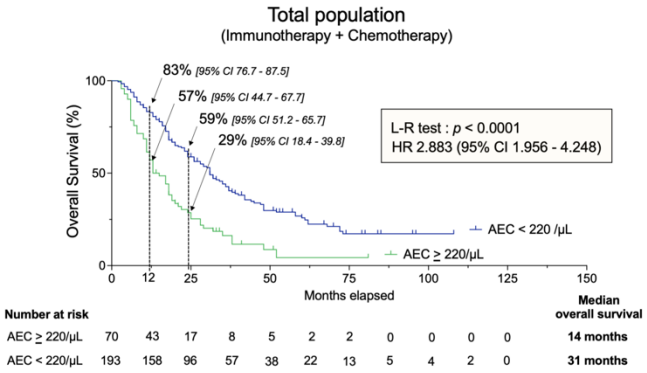

C

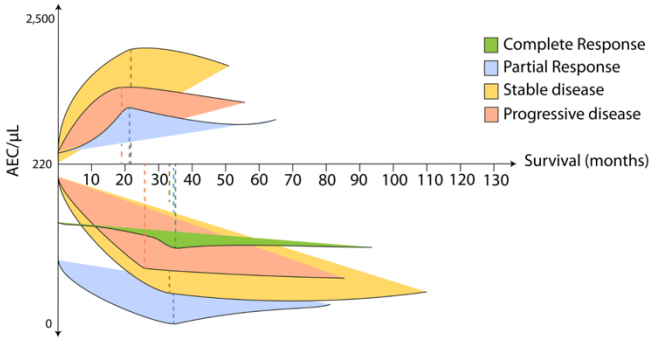

Supplementary Figure 5: **Response to therapy and OS of all randomized patients segregated according to the AEC cutoff of 230/µL**

(A) Type of response determined according to mRECIST v1.1 criteria. Objective response rate is defined as the sum of patients with either complete or response. Disease control rate is defined as the sum of patients with either complete response, partial response, or stable disease. **(B)** Kaplan-Meier analysis of OS in groups of patients with AEC ≥ 220/µL (in blue) and AEC < 220/µL (in green) before treatment. (**C**) Schematic representation of AEC, survival distribution and response to all therapies. Dashed lines are the median survival times (in months) corresponding to the type of response. CR: complete response; PR: partial response; SD: stable disease.

In addition to the European Cooperative Oncology Group (ECOG) status, the AEC/µL and OS were not statistically significant according to primary tumor (cT) status 1, 2, 3 and 4 (**Figure 14**).

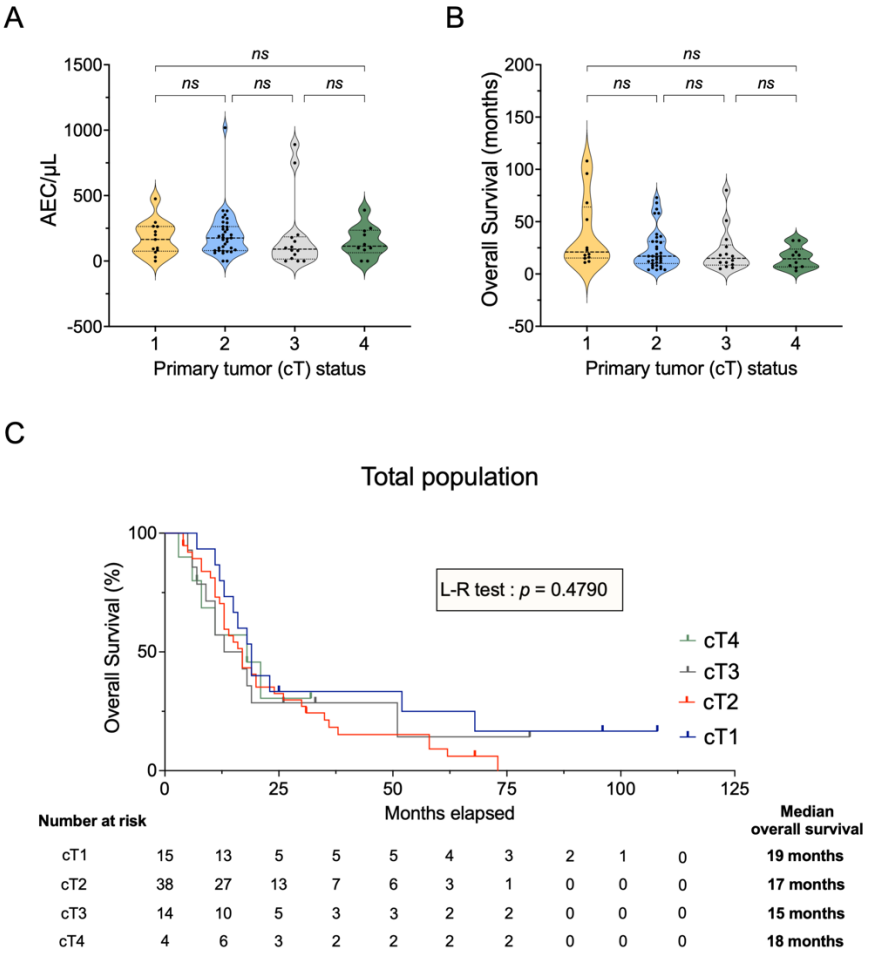

Figure 14 - Populations' distribution and Kaplan-Meier analysis of overall survival by tumor status. (A) Distribution of AEC/µL of blood according to the primary tumor (cT) status of 1, 2, 3 and 4. **(B)** Distribution of patients' survival (in months) according to cT status. **(C)** Kaplan-Meier survival curve according to cT status

Chapter 3

Eosinophil-derived Charcot-Leyden crystal protein mediates mesothelioma chemoresistance in the tumour macroenvironment

1. Foreword

Considering the results obtained in the retrospective study, which show an association between AEC and MPM patients OS and response to treatment, understanding the role of eosinophils in MPM response to treatment could lead to the identification of a novel prognostic and predictive biomarker but, more importantly to the identification of a novel therapeutic target. To achieve these objectives, we designed *in vitro* and mice experiments.

In the following article (manuscript in preparation), we based *in vitro* experiments on the human eosinophilic cell line EOL1, and primary eosinophils isolated from healthy donors' blood. The aim of these experiments was to confirm that eosinophils inhibit MPM tumour cells response to cisplatin and pemetrexed and identify the mechanisms involved. As we showed a correlation between peripheral blood eosinophils, and not an eosinophil infiltration in the tumour, we used cell culture supernatant to assess MPM chemoresistance in 2D monolayer and 3D spheroids culture. The same model was used to understand the mechanisms involved in chemoresistance.

We further assessed whether tumour development is impacted by the number of circulating eosinophils in a mouse model. We compared the tumour growth of mice having normal and elevated eosinophil counts. These comparisons were made in different conditions: *i.e.,* (i) non-treated mice, (ii) mice treated with cisplatin and pemetrexed, (iii) mice receiving anti-eosinophil treatment before administration of cisplatin and pemetrexed.

Eosinophil-derived Charcot Leyden Crystal protein mediates mesothelioma chemoresistance in the tumor macroenvironment

Mégane Willems [1,*], Malik Hamaidia [1,*], Alexis Fontaine [1], Mélanie Grégoire [1], Louise Halkin [1], Majeed Jamakhani [1], Christophe Blanquart [2], Vincent Heinen [3], Renaud Louis [3], Bernard Duysinx [3], Eric Wasielewski [4], Arnaud Scherpereel [4], Luc Willems [1,5]

[1] Molecular and Cellular Epigenetics (GIGA-Cancer), Liege and Molecular Biology (TERRA), Gembloux – Belgium

[2] Université de Nantes, CNRS, INSERM, CRCINA, Nantes, France, 2 Labex IGO, Immunology Graft Oncology, Nantes, France

[3] Department of Pneumology (University Hospital of Liege), Liege, Belgium

[4] Department of Pneumology and Thoracic Oncology (CHU Lille) and INSERM U1189 (ONCOTHAI), Lille, France

[*] co-first authors

Address correspondence to: Luc Willems, Molecular and Cellular Epigenetics, Interdisciplinary Cluster for Applied Genoproteomics (GIGA), University of Liège, B34, 1 avenue de l'Hôpital, 4000 Sart-Tilman Liège, Belgium. Phone: 32.81.622152; Email: luc.willems@uliege.be.

Emails:

megane.willems@uliege.be ; alexis.fontaine@uliege.be ; m.gregoire@uliege.be ; louise.halkin@uliege.be ; majeed.jamakhani@uliege.be ; christophe.blanquart@inserm.fr ; V.Heinen@chuliege.be ; R.Louis@chuliege.be ; bduysinx@chuliege.be ; arnaud.scherpereel@chru-lille.fr ; eric.wasielewski@chru-lille.fr ; mhamaidia@uliege.be ; luc.willems@uliege.be

AUTHOR'S CONTRIBUTION

MW and LH performed the experiments. AF and MG participated in mice experiments. AF and MW designed bioinformatic analysis. MW, MH and LW designed the project. AF, AS, EW, MG, LH, MJ, VH, RL, BD participated in data interpretation and manuscript reviewing. MW and LW drafted the manuscript.

ABSTRACT:

The role of eosinophils in asthma, allergy and parasite immunity has been widely documented. Their involvement in tumor progression and response to therapy is by far less well understood. Indeed, eosinophils can both promote or inhibit tumor growth depending on the cancer type. In mesothelioma, clinical evidence indicates that the absolute eosinophil count in the peripheral blood negatively correlates with overall survival and response to standard chemotherapy. Since eosinophils poorly infiltrate mesothelioma tumors, we hypothesized that endocrine rather than paracrine pathways mediate the therapeutic response. In this study, we thus studied the effect of eosinophils and eosinophils-associated factors on mesothelioma response to chemotherapy.

Our data show that supernatant of eosinophils differentiated from progenitor cells or directly isolated from peripheral blood inhibit apoptosis induced by cisplatin and pemetrexed in 2D cultures and in spheroids. Transcriptomic analysis indicates that the anti-apoptotic effect of culture media conditioned by eosinophils involves molecular interactions with the Charcot-Leyden Crystal protein or Galectin-10 (CLC-P/Gal10). The functional relevance of CLC-P/Gal10 is demonstrated by pharmacological inhibition and antibody-mediated depletion experiments. A recombinant CLC-P/Gal10 protein also mimics the anti-apoptotic activity of eosinophil-derived supernatants. In a preclinical mouse model, eosinophilia does not significantly affect tumor growth of implanted mesothelioma cells but alter the response to the cisplatin + pemetrexed regimen. Finally, pretreatment of eosinophilia with the anti-Siglec-F antibody before chemotherapy restores the efficacy of the cisplatin + pemetrexed regimen.

In summary, this study provides a mechanistic rationale to clinical evidence correlating the poor outcome of mesothelioma patients with their eosinophil levels. Besides the tumor microenvironment, macroenvironmental factors mediate the therapeutic response, opening new prospects for intervention in this fatal solid tumor.

Keywords:
Pleural mesothelioma, eosinophils, Charcot-Leyden crystal, chemotherapy

2. Introduction

Malignant mesothelioma, a rare but aggressive cancer, is mainly induced by chronic inflammation and oxidative stress caused by inhaled asbestos fibers. It can affect serous membranes of the pleura, the peritoneum, the pericardium and, less frequently, the tunica vaginalis testis [12]. Histologically, pleural mesothelioma (MPM) can be classified as epithelioid (the most frequent subtype, accounting for 60-80% of cases), sarcomatoid (~10%) and biphasic (10-15%). Despite the progressive ban of asbestos use in most countries, incidence of MPM is still increasing worldwide [13,14]. In principle, MPM patients may be eligible for a standard multimodal treatment including surgery, radiotherapy and/or chemotherapy [61,63]. Since 2003, the standard-of-care for unresectable MPM has been a combination of a DNA cross-linking agent (cisplatin or carboplatin) and an antifolate (pemetrexed) [63]. With an increase of median overall survival (OS) from 9.1 to 13-16 months, the benefit of this treatment remains nevertheless modest [63]. Combination of an anti-VEGF antibody (bevacizumab) to the cisplatin/pemetrexed regimen slightly improves the median OS up to 18.8 months (*vs* 16.0 months in the control arm) [61]. In addition, immune checkpoint inhibitors (ICIs) targeting PD-1 (nivolumab) and CTLA-4 (ipilimumab) are particularly effective in the sarcomatoid subset of MPM and are now incorporated in practice guidelines [4,60]. Despite these recent improvements, the prognosis of MPM patients remains usually poor.

Increasing evidence indicates that the immune tumor microenvironment (TME) is a major parameter that orients the outcome of cancer patient [32,189,190]. Although MPM has been initially considered as a cold tumor [2,35], a significant proportion of cases are characterized by an infiltration of tumor-associated macrophages (TAMs) and Tregs [36,41,190–194]. The presence of these immunosuppressive cells in MPM tumors or in the pleural fluid of MPM patients correlates with poor therapeutic response and bad prognosis. In addition, TAMs and monocyte myeloid-derived immunosuppressive cells (M-MDSCs) constitute a major fraction of the TME [33,34]. The selective depletion of myeloid cells in a knockout mouse model of MPM promotes tumor rejection, indicating the role of monocyte-derived TAMs in MPM development [195]. In contrast, targeting tissue-resident large peritoneal/pleural macrophages abrogates the antitumoral memory immunity. Besides phagocytosis, cytokine production and antibody-dependent cell-mediated cytotoxicity (ADCC), macrophages also exert a cytotoxic activity by cell-to-cell contact with MPM cells. Consistently, tumoricidal macrophages exert immunoediting activity against mesothelioma tumors in the absence of adaptive immunity [190,192].

It is widely accepted that macrophages are essential mediators of MPM tumor growth. However, the mechanisms underlying their role in MPM remain unknown. The current hypotheses are even complexified by their phenotypic diversity, their interplay with other immune cells and by the fact that immune cells are not directly infiltrating the TME [196,197]. The prognosis of MPM is indeed negatively influenced by systemic inflammation markers such as the C-reactive protein (CRP) [198]. In this

context, we recently provided clinical evidence indicating that blood eosinophils inversely correlate with response to chemotherapy and patient's overall survival. Excess of absolute eosinophil counts in the peripheral blood prior to chemotherapy is associated with worse outcome and quicker relapse in MPM [199].

By releasing cytokines, including chemokines, growth factors and enzymes, eosinophils mediate well-characterized immune-related mechanisms such as allergic disorders and pathogen infections [89,92,95]. The role of eosinophils in tumor development is far from being well understood. Eosinophils produce both anti- (*e.g.,* TNF-α, granzyme, cationic proteins and IL-12) and pro-tumorigenic molecules (*e.g.,* TGF-β1, VEGF) [169]. In the TME, eosinophils interact with macrophages, dendritic cells, T-lymphocytes and mast cells [167,169,200]. IL-4, IL-13 and IL-10 produced by eosinophils lead to the differentiation of macrophages into the M2/TAM phenotype [151,200]. Eosinophils also promote T-cell proliferation and activation via Th1 (*e.g.,* IFN-γ, IL-2 and IL-12) and Th2 (*e.g.,* IL-4, IL-5, IL-6, IL-10 and IL-13) cytokines [89,152]. As antigen presenting cells (APCs), eosinophils can directly modulate the adaptive T cell response [152]. Finally, eosinophils induce angiogenesis by promoting endothelial cell proliferation and by producing VEGF, FGF and PDGF [162,169]. The functional complexity of eosinophils and their interplay with multiple immune cells likely explain their pro- and anti-tumorigenic effects, as well as their association with both good (*e.g*., melanoma and colorectal cancer) and poor prognosis (*e.g.,* Hodgkin's lymphoma, cervical carcinoma) depending on the cancer type [151].

Based on the correlation observed in the retrospective analysis, the objectives of the present study are (i) to investigate the impact of eosinophils on response to therapy in cell culture and mouse models and (ii) to characterize the mechanisms involved and identify the factors that mediate eosinophil activity.

3. Materials and methods

3.1. Differentiation of the EOL1 progenitor cell line into eosinophils

The EOL1 cell line (Cellosaurus_CVCL_0258) was cultured in RPMI-1640 (Lonza) supplemented with 10% heat-inactivated fetal bovine serum (FBS, Lonza), 1% penicillin and streptomycin (10,000 U/ml, BioWhittaker), 1% sodium pyruvate (Gibco) and 1% amphotericin B (Gibco) (*i.e.,* complete RPMI) at 37°C in a humidified atmosphere containing 5% CO_2. EOL1 (2 x 10^5 cells/well in a 24-well plate) were differentiated into eosinophil-like cells using 2 mM sodium valproate (Sigma) in complete RPMI-1640 medium for 8 days. To reach further maturation, differentiated EOL1 (Dif-EOL1) were incubated with 100 ng/mL interleukin-5 (IL-5) for 48 hours. Cell culture supernatants from progenitors (EOL1) and differentiated EOL1 were collected, cleared by centrifugation, aliquoted and stored at -80°C for further experiments.

To control for adequate differentiation, the ability of Dif-EOL1 to express CCR3, IL-5Rα, CD63 and CLC-P/Gal10 was determined by flow cytometry immunophenotyping and confocal microscopy (see M&M paragraphs below). To quantify eosinophil peroxidase activity, 5 x 10^5 EOL1 and Dif-EOL1 cells were incubated in 500 µL of a substrate solution containing o-phenylenediamine (Sigma, OPD; 0.4 mM), Tris-HCl (Sigma, 0.4 M, pH 8.0) and H_2O_2 (1.25 x 10^{-3} % v/v) [201]. After 30 minutes at room temperature in the dark and addition of an equal volume of HCl 4N, the optical density was determined at λ = 492 nm (SpectraMax Plus, Molecular Devices).

3.2. Isolation of primary human eosinophils

To isolate primary human eosinophils, buffy coats were obtained from healthy donors (Red Cross of Belgium). The use of human samples was approved by the institutional ethic committee of the University Hospital (CHU, Sart-Tilman) under the reference #2012/8. Granulocytes were isolated by gradient centrifugation on lymphoprep (1.077 g/ml, Stemcell Technologies). Erythrocytes were lysed with RBC lysis buffer (BioLegend). Granulocytes (10 x 10^6 cells) were washed in PBS before labelling with 1 µg/mL anti-CCR3 antibody (Fisher Scientific, #15297277) for 30 minutes at 4°C. Eosinophils were purified by magnetic cell sorting using microbeads coupled with anti-mouse IgG2a+b (Miltenyi Biotec). $CCR3^+$ primary human eosinophils were then cultured in RPMI supplemented with 1% sodium pyruvate at 37°C for 24 hours and their supernatant (SN Eos) was stored in aliquots at -80°C. The purity of isolated primary human eosinophils was evaluated by flow cytometry immunophenotyping (see M&M paragraph below).

3.3. Culture of MM cells in 2D and in spheroids

The epithelioid M14K (Cellosaurus CVCL_8102) and biphasic ZL34 (CVCL_5906) human MPM cell lines were cultured in 2D at 37°C in DMEM medium (Lonza) containing 2mM L-glutamine, supplemented with 10% heat inactivated FBS (Lonza) and 1% penicillin and streptomycin (10,000 U/ml, BioWhittaker) (*i.e.,* complete DMEM). Spheroids were generated using the liquid overlay method according to the protocol as described by Friedrich *et al*. [202]. Briefly, 96-well plates were coated with 50 µl agarose (Sigma) dissolved in DMEM (1.5% w/v) to render plates non-adhesive. M14K and ZL34 cells were added to the wells at a density of 1.5 x 10^4 /well and cultured for 72 hours in presence of differentiated EOL1 supernatant (25% v/v SN Dif-EOL1). Spheroid growth and response to cisplatin (10 µM; VWR) and pemetrexed (10 µM; Sigma-Aldrich) were recorded daily with a CKX41 inverted microscope (Olympus). After transfer into a 24-well plate, spheroid adherence and cell migration (surface occupied by cells in mm^2) were recorded with the CKX41 inverted microscope and quantified with the ImageJ software.

3.4. Flow cytometry immunophenotyping

Dif-EOL1 cells were collected in PBS-FBS 2%. After 2 washes with PBS-FBS 2%, cells were labelled for 1 hour on ice with 1 µg/mL of anti-IL-5Rα antibody (Invitrogen, #PA525159). After 2 washes, cells were incubated for 45 minutes with 2 µg/mL AlexaFluor488 anti-mouse IgG1 (Invitrogen, #A11001) conjugate as well as with 1 µg/mL anti-CD193 (CCR3) antibody coupled with allophycocyanin (APC) (eBioscience, clone 5E8-G9-B4, #15518046).

Alternatively, $CCR3^+$ Primary human eosinophils were fixed in the dark in PBS containing 4% paraformaldehyde (PFA, Sigma, #1004960700) for 10 minutes at room temperature. After 2 washes in PBS-FBS 2%, cells were labelled for 1 hour at room temperature with 1 µg/mL anti-IL-5Rα (Invitrogen, PA525159) and anti-Siglec-8 (Miltenyi Biotec, clone 7C9, #130-108-015) antibodies. After 2 washes, cells were incubated for 45 minutes with 2 µg/mL AlexaFluor488 anti-rabbit IgG (Invitrogen, #A11008) and AlexaFluor647 anti-mouse IgG1 (Invitrogen, #A21240) conjugates.

For CLC-P/Gal10 detection, primary eosinophils and Dif-EOL1 cells were fixed in PBS containing 4% PFA and 0.5% Tween 20 overnight at 4°C. After 2 washes with PBS containing 3% FBS and 0.5% Tween 20, cells were labelled for 1 hour at room temperature with 10 µg/mL anti-CLC-P/Gal10 (clone B-F42, Diaclone, #852.960.000). After two washes, cells were incubated for 45 minutes with 2 µg/mL AlexaFluor488 anti-mouse IgG1 (Invitrogen, #A21121) conjugate.

The labelled cells were recorded by flow cytometry (Cytoflex, Beckman Coulter) and analyzed with the Cytexpert software (Beckman Coulter).

3.5. Confocal microscopy and live imaging

For confocal microscopy, CFSE-labelled M14K or ZL34 cells were co-cultured with primary eosinophils on coverslips for 24 hours at a 1:1 ratio and fixed with 4% PFA for 10 minutes at room temperature in the dark. After permeabilization with 1% Triton X-100 in PBS for 10 minutes, cells were incubated in PBS containing 10% FBS for 30 minutes. After 1 wash with PBS, cells were labelled with 1 µg/mL APC-coupled anti-human tetraspanin (CD63) conjugate (Immunotools, #21270636) for 1 hour at room temperature. Cells were stained with 5 µM DAPI (BioLegend, #422801) and coverslips were mounted with Fluoroshield (Sigma-Aldrich, #F6182). Images were acquired with a Zeiss LSM 880 AiryScan Elyra S1 confocal microscope equipped with x40 and x63-1.4 oil immersion objectives (Zeiss).

Primary eosinophils and Dif-EOL1 cells were washed in PBS and fixed with 4% PFA for 10 minutes at room temperature in the dark. After 2 washes and permeabilization with PBS - 0.5% Triton X-100 for 10 minutes, samples were incubated overnight at 4°C with 15 µg/mL anti-CLC-P/Gal10 monoclonal antibody (clone B-F42, Diaclone, #852.960.000) and 1 µg/mL rabbit antiserum specific for the major basic protein (MBP) (also called Proteoglycan 2 PRG2; Invitrogen, #PA5102628). After 2 washes with PBS, cells were labelled with 2 µg/mL AlexaFluor488 goat anti-mouse IgG1 (Invitrogen) and TexasRed goat anti-Rabbit IgG (Molecular Probes) conjugates for 30 minutes at room temperature. After mounting with Fluoroshield-DAPI (Sigma-Aldrich), images were acquired with a Zeiss LSM 980 AiryScan Elyra S2 confocal microscope equipped with x40 and x63-1.4 oil immersion objectives (Zeiss).

For time-lapse imaging, Dif-EOL1 cells (1 x 10^6 cells/mL) were washed in RPMI-1640 medium supplemented with 1% penicillin and streptomycin (10,000 U/ml). Dif-EOL1 cells (10^6 cells) were labelled with 10 µM carboxyfluorescein succinimidyl ester (CFSE, Abcam) for 7 minutes at 37°C and washed in complete RPMI. CFSE-labelled Dif-EOL1 cells (1 x 10^5 cells/well) were then co-cultured with M14K or ZL34 (ratio 1:1) MPM cells in a 96-well plate at 37°C. Cells were monitored hourly by Incucyte imaging S3 Live-Cell system equipped with a 20X objective (Sartorius).

3.6. Analysis of apoptosis by flow cytometry

M14K and ZL34 cells were cultured for 48 hours in 2D monolayers in a 24-well plate (2.5 x 10^4 cells/well) in the presence of 25% eosinophil supernatant (SN Dif-EOL1 or SN Eos) or N-terminal His-tag recombinant human CLC-P/Gal10 (0.1, 1 and 5 µg/ml; Novus Biological, #NBP1-51096). Experimental conditions also included 4-hour pre-inhibition with N-ethylmaleimide (at 10^{-7} M; Sigma) and antibody-mediated depletion of CLC-P/Gal10. For this purpose, SN Dif-EOL1 and SN Eos were incubated with 1 µg/mL anti-CLC-P/Gal10 antibody (clone B-F42, Diaclone) for 1 hour at room temperature. SN Dif-EOL1 and SN Eos were then incubated with anti-mouse IgG magnetic microbeads (Miltenyi Biotec) for 30 minutes. CLC/Gal10 was depleted by magnetic sorting.

Apoptosis was evaluated by phosphatidylserine exposure and plasma membrane integrity using Annexin V-FITC and propidium iodide (PI) as described by the manufacturer (Immunotools). Ten thousand events were recorded by flow cytometry (FacsCanto II, BD Bioscience) and analyzed with the FlowJo software (version 7, BD Bioscience). Annexin V^+ PI^- and Annexin V^+ PI^+ cells were considered as undergoing early and late apoptosis, respectively.

Apoptosis was also evaluated based on DNA fragmentation, quantified by cell cycle analysis upon ethanol fixation and PI staining. After overnight permeabilization with absolute ethanol at -20°C, M14K and ZL34 cells were digested with 100 µL RNAse A (50 µg/ml; Sigma-Aldrich) and 0.1% Tween-20 in PBS for 30 minutes at 37°C and stained with PI (20 µg/ml) for 10 minutes in the dark at room temperature. Ten thousand events were recorded by flow cytometry (Cytoflex, Beckman Coulter) and, after doublet exclusion, analyzed with the CytExpert software (version 2.4, Beckman Coulter).

3.7. RNA sequencing and bioinformatics

RNA was extracted from M14K and ZL34 cells using the NucleoSpin RNA Plus kit as described by the manufacturer (Macherey-Nagel) and quantified with a Nanodrop 2000 spectrophotometer. Sequencing of the libraries (2 x150 bp) with a depth of 30M paired reads per sample was performed by Macrogen Europe on a NovaSeq 6000 system (Illumina, San Diego, CA, USA).

Quality controls of FASTQ reads included base quality, sequence duplications and adapter contents (FASTQ tools version 0.11.9). Illumina universal adapters as well as low quality and short reads were filtered out with Trimmomatic (version 0.39). Reads corresponding to rRNA were removed with bwa mem (version 0.7.17). rRNA-free and trimmed reads were mapped to the human genome (hg18, Genome Reference Consortium GRCh38) using STAR (version 2.7.9.a). Aligned reads were further marked for duplicates with MarkDuplicates (version 2.26.3). The read count table was eventually generated using Featurecounts (version 2.0.1).

Differential expression analysis between experimental conditions was performed using the R/Bioconductor DESeq2 package (version 1.34.0). Differentially expressed genes (DEGs) (p-adj ≤ 0.05 and $|Log_2FC| > 1$) were obtained in each comparison and ranked according to adjusted p-values. Enriched pathway analysis of significant genes (p-adj ≤ 0.05) against Gene Ontology (GO) for molecular function (GO:MF), Biological Process (GO:BP) and Kyoto Encyclopedia for Genes and Genomes (KEGG) were performed using the gprofiler2 package (version 0.2.1).

3.8. Mouse model

All procedures were approved by the Ethical Review Board (protocol #2366) and performed according to the Federation of Laboratory Animal Science Association (FELASA) guidelines.

Six-week-old C57BL/6 mice (Janvier Labs) were inoculated subcutaneously in both flanks with 1.5 x 10^6 syngeneic AK7 epithelioid mesothelioma cells. When the tumor reached ~150 mm^3, eosinophilia was induced by daily intraperitoneal (i.p.) injections of recombinant mouse IL-5 and IL-33 at 5 and 20 ng/g of body weight (gbw), respectively (Immunotools). Upon regular blood sampling from the tail vein, eosinophil counts were measured with an hematocytometer (Advia 2120i; Siemens Healthineers). After 5 days, eosinophilia was maintained with i.p. injections of either IL-5+IL-33 or IL-5 alone. When the tumor volume reached ~500 mm^3, mice were treated i.p. with PBS (mock) or with 6 µg/gbw cisplatin (VWR) and 150 µg/gbw pemetrexed (Sigma-Aldrich). Two days before this chemotherapy, eosinophils were depleted with 15 µg of anti-Siglec-F monoclonal antibody given i.p. (clone 238074, Bio-Techne). Tumor dimensions (L=length, W=width, H=height) were measured tri-weekly and volumes were calculated using the hemi-ellipsoid formula $V = LxWxHx\pi/6$.

3.9. Statistical analysis

Statistical analyses were performed using GraphPad Prism 9.5.0 for *in vitro* experiments or R (v4.1.1) and RStudio 2022.07.1+554 for mice experiments. The Shapiro-Wilk test was used to verify if continuous variables followed a normal distribution. For comparisons between 2 populations, in case of normal distribution, the variance of the means was compared by t-test. If populations were not following a normal distribution, the variance of the means was compared with a Welch's test.

For comparisons between more than 2 populations, the homogeneity of the group variances was evaluated with the Brown-Forsythe test. When populations followed normal distributions and had similar variances, the variance of the means was compared by one-way ANOVA followed by Tukey's multiple comparison test. If the variances were significantly different, the variance of the means was compared by one-way ANOVA followed by Brown-Forsythe and Welch. Finally, if populations were not following a normal distribution, the variance of the means was compared with the nonparametric one-way ANOVA followed by Dunnett's T3 multiple comparison test.

For mice experiments, growth indexes were calculated using the formula $((V_F - V_{C+P})/V_{C+P})$ where V_F is the tumor volume at the end of the experiment and V_{C+P} is the tumor volume at the time of cisplatin and pemetrexed injection. Based on these growth indexes, two-way ANOVA with categorical variables "eosinophilia" and "chemotherapy" for the first experiment, or "eosinophilia" and "anti-Siglec-F" for the second experiment was performed. After checking if the populations were following a normal distribution with Shapiro-Wilk and evaluating the variance homogeneity

with Levene's test, the variance of the means was compared with two-way ANOVA. Finally, the effect size was calculated by calculating the partial η^2 for the interaction between "eosinophilia" and "chemotherapy" and for the interaction between "eosinophilia" and "anti-Siglec-F". The power of the analysis was calculated using G*Power 3.1.9.6.

4. Results

4.1. The culture supernatant from differentiated EOL1 impacts the response of mesothelioma cells to cisplatin and pemetrexed

An experimental model *in cellulo* was designed to evaluate the effect of eosinophils on mesothelioma chemotherapy. EOL1 eosinophilic cells were differentiated (Dif-EOL1) for 8 days with valproate, a histone deacetylase (HDAC) inhibitor (**Figure 15A**). An optimal concentration of 2 mM valproate promoted the expression of two characteristic eosinophil markers: IL5-Rα (**Figure 15B**) and CCR3 (**Figure 15C-D**). Upon differentiation, the actin cytoskeleton underwent depolymerization as revealed by lack of phalloidin labelling (**Figure 15D**). Dif-EOL1 cells were more granular and smaller than EOL1, as indicated by the side (SSC) and forward (FSC) scatters (**Figure 15E**). Consistent with their phenotype, Dif-EOL1 also demonstrated higher levels of eosinophil peroxidase activity (**Figure 15F**). Furthermore, live cell imaging demonstrated that IL-5 increased the expression of CD63 thereby indicating eosinophil activation and functional degranulation (**Figure 15G**). These results confirmed that Dif-EOL1 cells were phenotypically representative of functional human eosinophils.

To study the impact of eosinophils on chemotherapy, M14K mesothelioma cells were cultured in with 25% v/v of Dif-EOL1 cell supernatant (SN Dif-EOL1) for 48 hours and treated with 10 µM cisplatin and pemetrexed (C+P) for 48 additional hours (**Figure 15A**). Flow cytometry revealed that the percentages of Annexin V^+ $PI^{+/-}$ cells increased in presence of the C+P regimen indicating, as expected, the onset of apoptosis (**Figure 15H**). Preincubation of M14K cells with SN Dif-EOL1 significantly attenuated the proapoptotic effect of the C+P regimen compared to the control medium ($p < 0.0001$). As another hallmark of apoptosis, DNA fragmentation reflected by the proportion of Sub-G1 cells was also reduced in presence of SN Dif-EOL1 (**Figure 15I**). To extend these conclusions obtained in 2D cultures, the effect of the Dif-EOL1 supernatant was evaluated in spheroids. In this 3D model, the SN Dif-EOL1 significantly decreased apoptosis induced by the C+P regimen (**Figure 15J** Upon transfer into a C+P free medium, adherence and outgrowth of the spheroids precultured with SN Dif-EOL1 (blue) was improved compared to the mock control (gray). Outgrowth of the spheroids pre-treated with C+P in presence of SN Dif-EOL1 (yellow) was also improved compared to spheroids pre-treated with C+P in absence of SN Dif-EOL1 (red) (**Figure 15K-L**).

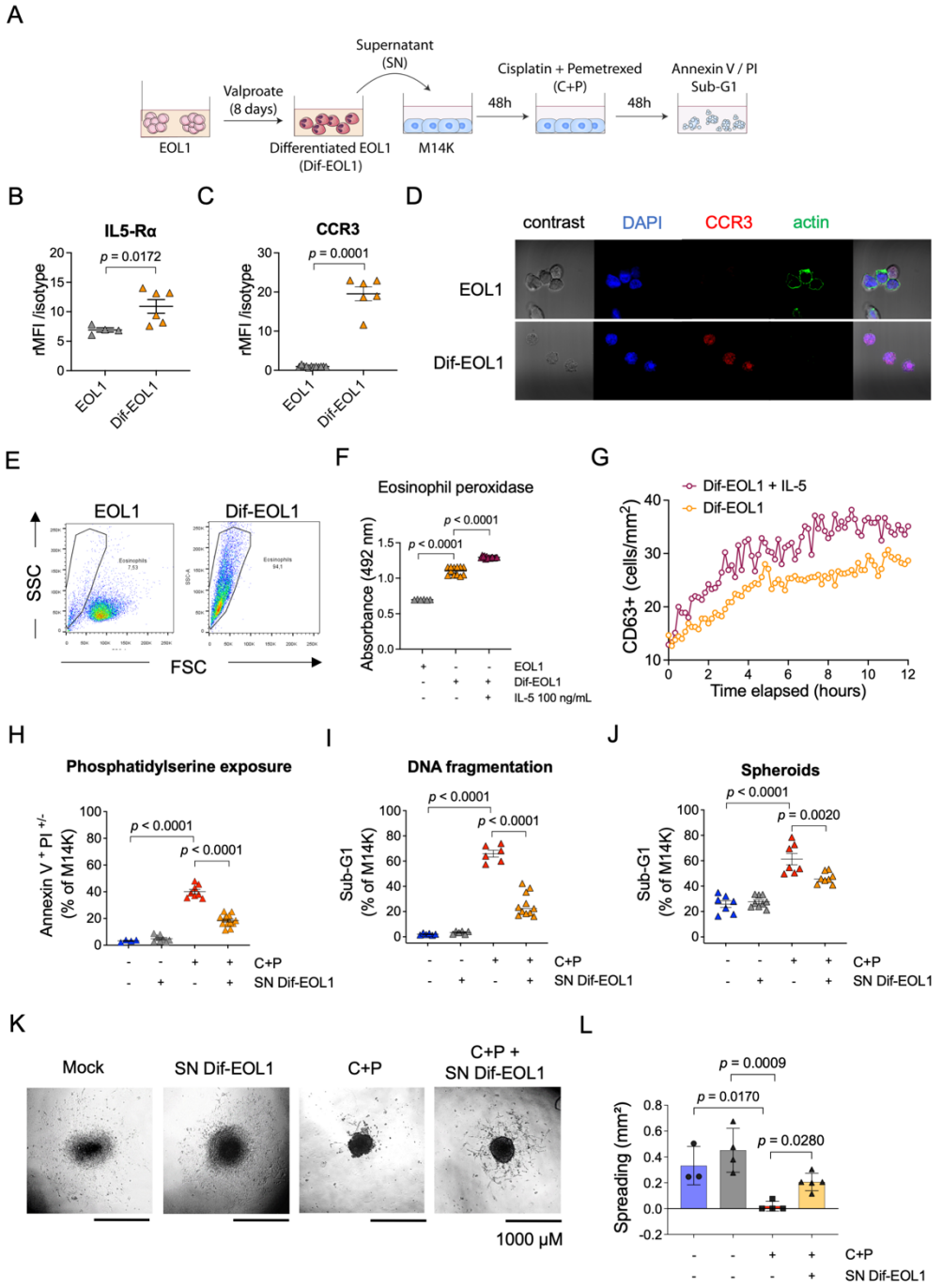
A
Supernatant (SN)
Valproate (8 days)
Cisplatin + Pemetrexed (C+P)
48h
48h
Annexin V / PI Sub-G1
EOL1
Differentiated EOL1 (Dif-EOL1)
M14K
B
IL5-Rα
p = 0.0172
rMFI /isotype
EOL1
Dif-EOL1
C
CCR3
p = 0.0001
rMFI /isotype
EOL1
Dif-EOL1
D
contrast
DAPI
CCR3
actin
EOL1
Dif-EOL1
E
EOL1
Dif-EOL1
SSC
FSC
F
Eosinophil peroxidase
p < 0.0001
p < 0.0001
Absorbance (492 nm)
EOL1
Dif-EOL1
IL-5 100 ng/mL
G
Dif-EOL1 + IL-5
Dif-EOL1
CD63+ (cells/mm²)
Time elapsed (hours)
H
Phosphatidylserine exposure
p < 0.0001
p < 0.0001
Annexin V⁺ PI⁺/⁻ (% of M14K)
C+P
SN Dif-EOL1
I
DNA fragmentation
p < 0.0001
p < 0.0001
Sub-G1 (% of M14K)
C+P
SN Dif-EOL1
J
Spheroids
p < 0.0001
p = 0.0020
Sub-G1 (% of M14K)
C+P
SN Dif-EOL1
K
Mock
SN Dif-EOL1
C+P
C+P + SN Dif-EOL1
1000 µM
L
p = 0.0009
p = 0.0170
p = 0.0280
Spreading (mm²)
C+P
SN Dif-EOL1

Figure 15 – Eosinophils differentiated from EOL1 cells inhibit the response to cisplatin and pemetrexed. (**A**) EOL1 progenitors were differentiated with 2 mM valproate for 8 days. The culture supernatant (SN) of the differentiated EOL1 (Dif-EOL1) was added to M14K mesothelioma cells at 25% v/v for 48 hours. M14K were then treated with 10 µM cisplatin and 10 µM pemetrexed (C+P) for 48 hours. After fluorescent labelling of IL-5Rα **(B)** and CCR3 **(C)**, EOL1 and Dif-EOL1 were analyzed by flow cytometry. The relative Mean Fluorescence Intensity (rMFI) corresponds to the ratio of fluorescence intensities associated with IL-5Rα **(B)** and CCR3 **(C)** with control isotypes. Bars represent mean ± standard deviation (SD) from 6 independent experiments. **(D)** Dif-EOL1 were labelled for CCR3 and actin, stained with DAPI and analyzed by confocal microscopy (magnification 40x). **(E)** Flow cytometry was used to discriminate EOL1 progenitors from Dif-EOL1 based on size (forward scatter; FSC) and granulometry (side scatter; SSC). **(F)** Eosinophil peroxidase activity in EOL1 and Dif-EOL1 cells (stimulated with mock or IL-5; 100 ng/mL). Absorbance of the chromogenic substrate (OPD) was measured at 492 nm with a spectrophotometer. **(G)** CD63-positive cells (number/mm^2) were recorded by time-lapse microscopy (Incucyte imaging S3 Live-Cell system equipped with a 20X objective) in Dif-EOL1 cultures in presence of mock or IL-5 (100 ng/mL). **(H)** Percentages of apoptotic M14K cells (2D) were determined by flow cytometry after Annexin V/ propidium iodide (PI) staining. Early (Annexin V^+ PI^-) and late (Annexin V^+ PI^+) apoptotic cells were counted for each condition. **(I)** After ethanol permeabilization and PI staining, the cell cycle profiles (2D) were analyzed by flow cytometry. The percentages of cells with fragmented genomic DNA (*i.e.,* Sub-G1) were evaluated. **(J)** M14K spheroids were generated by the liquid overlay method for 72 hours in presence or absence of Dif-EOL1 supernatant. After treatment with C+P for 48 hours, the proportion of M14K cells in Sub-G1 was determined by flow cytometry after spheroid dissociation, cell permeabilization and PI staining. **(K)** After transfer of the spheroids into an adherent 24-well plate, cell migration was monitored with an Olympus CKX41 microscope. **(L)** The surface occupied by the cell culture in mm^2 was measured after 24 hours. Data are expressed as means ±SD, each point representing an independent test. Normality was checked by Shapiro-Wilk and equality of the variances was checked by Brown-Forsythe. Variance of the means was compared by t-test (Panels B and C) or by one-way ANOVA followed by Tukey's multiple comparison test (Panels F, H, I, J and L).

Together, these experiments thus demonstrate that the supernatant of Dif-EOL1 attenuated the pro-apoptotic effect of C+P in the epithelioid M14K cell line. The effect of Dif-EOL1 supernatant was also evaluated on the ZL34 non-epithelioid cell line, which modeled a refractory form of mesothelioma (**Supplementary Figure 1A**). Based on phosphatidylserine exposure and DNA fragmentation, the conclusion was partly extended, as ZL34 underwent only limited DNA fragmentation that was not further decreased by the SN Dif-EOL1 in 2D cultures and spheroids (**Supplementary Figure 1B-D**). Instead of undergoing apoptosis, ZL34 cells mainly arrested in S phase in presence of C+P (**Supplementary Figure 2B**). The S phase blockade induced by C+P was significantly reduced in presence of SN Dif-EOL1.

Altogether, these data reveal that the culture supernatant from differentiated EOL1 impacted mesothelioma cell response to C+P chemotherapy.

4.2. Eosinophil-associated factors affect binding functions of the mesothelioma transcriptome

To characterize the mechanisms promoted by the eosinophil-conditioned medium, the kinetics of the experimental protocol was modified. When the SN Dif-EOL1 and the C+P regimen were added concomitantly to the M14K or ZL34 mesothelioma cells, the anti-apoptotic effect of the eosinophilic supernatant was lost, as reflected by the percentage of Annexin V^+ $PI^{+/-}$ cells (**Supplementary Figure 3A-B**). In the spheroid model, DNA fragmentation in M14K and S phase arrest in ZL34 were also unaffected by SN Dif-EOL1 (**Supplementary Figure 3D-F**, respectively**).** This result indicated that preincubation of mesothelioma cells with the SN Dif-EOL1 was required to attenuate the effect of C+P. This delay suggested that the eosinophilic supernatant promoted molecular changes in mesothelioma cells.

To get deeper insight into the mechanisms promoted by the eosinophil-conditioned medium, the transcriptome of M14K cells cultured in presence of the SN Dif-EOL1 and/or C+P regimen was evaluated by RNA sequencing. The heatmap of differentially expressed genes (DEG) indicated that the SN Dif-EOL1 and/or C+P regimen significantly modified in mesothelioma cell transcription (**Figure 16A, Supplementary Figure 4**). In particular, the volcano plot highlighted specific changes (DEG at p-adj < 0.05 and $|Log_2FC| > 1$) that correlated with the effect of the Dif-EOL1-conditioned medium upon C+P treatment of M14K cells (**Figure 16B**). Among these, 137 unique DEG were associated with SN Dif-EOL1+C+P *vs* SN Dif-EOL1 as illustrated by the Venn diagram (**Figure 16C**).

To obtain a comprehensive view of the underlying mechanisms, an unsupervised analysis of the transcriptomic data set was performed. Gene Ontology (GO) comparison and pathway enrichment analysis revealed that protein binding (GO:0005515, p-adj = 9.59×10^{-150}), ion binding (GO:0043167, p-adj = 1.63×10^{-44}), organic cyclic compound binding (GO:0097159, p-adj = 2.09×10^{-22}), heterocyclic compound binding (GO:1901363) p-adj = 2.19×10^{-21}), hydrolase activity (GO:0016787, p-adj = 2.71×10^{-20}), small molecule binding (GO:0036094, p-adj = 5.68×10^{-19}) and transferase activity (GO:0016740, p-adj = 4.36×10^{-16}) characterized the impact of the SN Dif-EOL1 on the C+P response (**Figure 16D**). This analysis suggested that a soluble factor secreted in the SN Dif-EOL1 primarily affected the binding functions in mesothelioma cells. In particular, pathways associated with the Charcot-Leyden Crystal protein / galectin-10 (CLC-P/GAL10), a protein predominant in human eosinophils, were included in the top list of the GO analysis. Indeed, a series of molecular functions of the CLC-P/Gal10 protein (*i.e.*, GO:0005515, GO:0042802, GO:0043281, GO:0030246 and GO:0016936) closely characterized the effect of the SN Dif-EOL1 on the C+P response (**Figure 16E**).

These transcriptomic analyses indicated that the SN Dif-EOL1 significantly affected the binding functions in mesothelioma cells, possibly via soluble mediators such as CLC-P/Gal10.

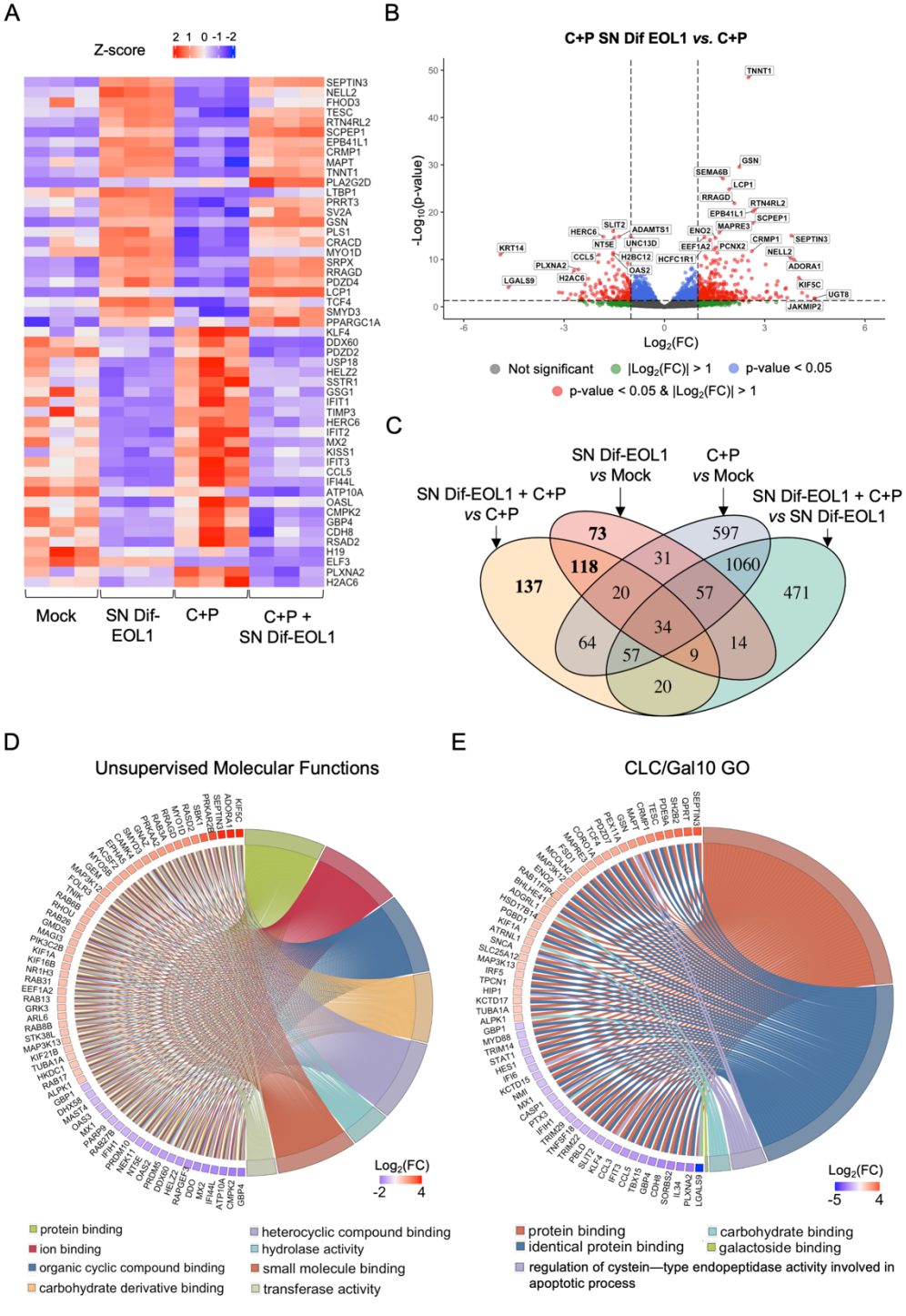
A
Z-score
2 1 0 -1 -2
SEPTIN3
NELL2
FHOD3
TESC
RTN4RL2
SCPEP1
EPB41L1
CRMP1
MAPT
TNNT1
PLA2G2D
LTBP1
PRRT3
SV2A
GSN
PLS1
CRACD
MYO1D
SRPX
RRAGD
PDZD4
LCP1
TCF4
SMYD3
PPARGC1A
KLF4
DDX60
PDZD2
USP18
HELZ2
SSTR1
GSG1
IFIT1
TIMP3
HERC6
IFIT2
MX2
KISS1
IFIT3
CCL5
IFI44L
ATP10A
OASL
CMPK2
GBP4
CDH8
RSAD2
H19
ELF3
PLXNA2
H2AC6
Mock
SN Dif-EOL1
C+P
C+P + SN Dif-EOL1
B
C+P SN Dif EOL1 vs. C+P
-Log10(p-value)
Log2(FC)
TNNT1
GSN
SEMA6B
LCP1
RRAGD
RTN4RL2
EPB41L1
SCPEP1
MAPRE3
CRMP1
SEPTIN3
NELL2
ADORA1
KIF5C
UGT8
JAKMIP2
SLIT2
ADAMTS1
HERC6
NT5E
UNC13D
KRT14
CCL5
H2BC12
HCFC1R1
PLXNA2
OAS2
H2AC6
LGALS9
ENO2
EEF1A2
PCNX2
Not significant
|Log2(FC)| > 1
p-value < 0.05
p-value < 0.05 & |Log2(FC)| > 1
C
SN Dif-EOL1 vs Mock
C+P vs Mock
SN Dif-EOL1 + C+P vs C+P
SN Dif-EOL1 + C+P vs SN Dif-EOL1
73
597
31
118
1060
137
20
57
471
34
64
14
57
9
20
D
Unsupervised Molecular Functions
Log2(FC)
protein binding
ion binding
organic cyclic compound binding
carbohydrate derivative binding
heterocyclic compound binding
hydrolase activity
small molecule binding
transferase activity
E
CLC/Gal10 GO
Log2(FC)
protein binding
identical protein binding
regulation of cystein—type endopeptidase activity involved in apoptotic process
carbohydrate binding
galactoside binding

Figure 16 - Conditioned media of differentiated EOL1 cultures induce transcriptomic changes in M14K cells. (A) Unsupervised heatmap of the 25 most significant up-regulated (red) and down-regulated (blue) genes in the transcriptome of M14K cells. Experimental data with the control (Mock), Dif-EOL1 supernatant (SN) and/or cisplatin + pemetrexed (C+P) were deduced from 3 independent replicates. **(B)** Volcano plot of differentially expressed genes (DEGs) in conditions C+P and SN Dif-EOL1 *vs.* C+P. Genes with $Log_2(FC) > 1$ and $-Log_{10}pvalue > 1.3$ (p-adj threshold: 0.05) are marked in red. **(C)** Venn diagram of significant DEGs in the different conditions (Mock, C+P, Dif-EOL1 SN, C+P and Dif-EOL1). The numbers of genes impacted by SN Dif-EOL1 are in bold. **(D)** Representative chord diagram of the most significant pathways affected in Gene Ontology Molecular Functions (GO:MF) in conditions C+P and SN Dif-EOL1 *vs.* C+P. Pathways (right side) are linked to the genes (left side) according to their $Log_2(FC)$. The names of the pathways are provided below the diagram **(E)** Representative chord diagram of the most significant pathways associated with CLC-P/Gal10 in GO:MF.

C+P: cisplatin + pemetrexed; DEGs: differentially expressed genes; GO: Gene ontology.

4.3. Dif-EOL1-derived CLC-P/Gal10 affects MPM cells response to C+P chemotherapy

To further characterize the interplay between eosinophils and mesothelioma cells, cocultures of Dif-EOL1 and M14K cells were analyzed by time-lapse imaging. To trace eosinophilic factors, the protein content of Dif-EOL1 cells was labeled with CFSE prior to the coculture. Fluorescence microscopy showed that Dif-EOL1 cells interacted with M14K cells (**Figure 17A**). In addition, CFSE-stained components migrated from the Dif-EOL1 to the M14K cells, suggesting secretion and transfer of eosinophilic protein factors. This interpretation was validated by confocal microscopy upon tetraspanin labelling **(**CD63 in red; **Figure 17B)**. Representing approximately 7-10% of eosinophil cytoplasmic proteins, CLC-P/Gal10 was reported to be a main component of the granules [89,90,203]. Consistently, confocal microscopy and flow cytometry showed that Dif-EOL1 indeed expressed large amounts of CLC-P/Gal10 (**Figure 17C and D**).

To test whether resistance to C+P chemotherapy involved CLC-P/Gal10, a compound binding to its carbohydrate recognition domain, N-ethylmaleimide, was added to the SN Dif-EOL1 before culture with the M14K cells. At a subtoxic dose of 10^{-7} M, N-ethylmaleimide impaired the effect of SN Dif-EOL1 on M14K apoptosis induced by C+P (**Figure 17E**).

As an irreversible thiol-alkylating agent, N-ethylmaleimide could possibly affect a number of other targets, including cysteine peptidases. Therefore, CLC-P/Gal10 was also directly removed from the Dif-EOL1-conditioned medium by antibody-mediated depletion. In the absence of CLC-P/Gal10, the Dif-EOL1 SN did not impair C+P-induced apoptosis of M14K cells (**Figure 17F**). Finally, the addition of a recombinant human CLC-P/Gal10 protein (0.1 to 5 µg/ml) reduced the proapoptotic activity of C+P regardless of the dose, thereby mimicking the effect of SN Dif-EOL1 (**Figure 17G**).

These results demonstrated that CLC-P/Gal10 protein expressed by EOL1-derived eosinophils affected MPM cells response to C+P chemotherapy.

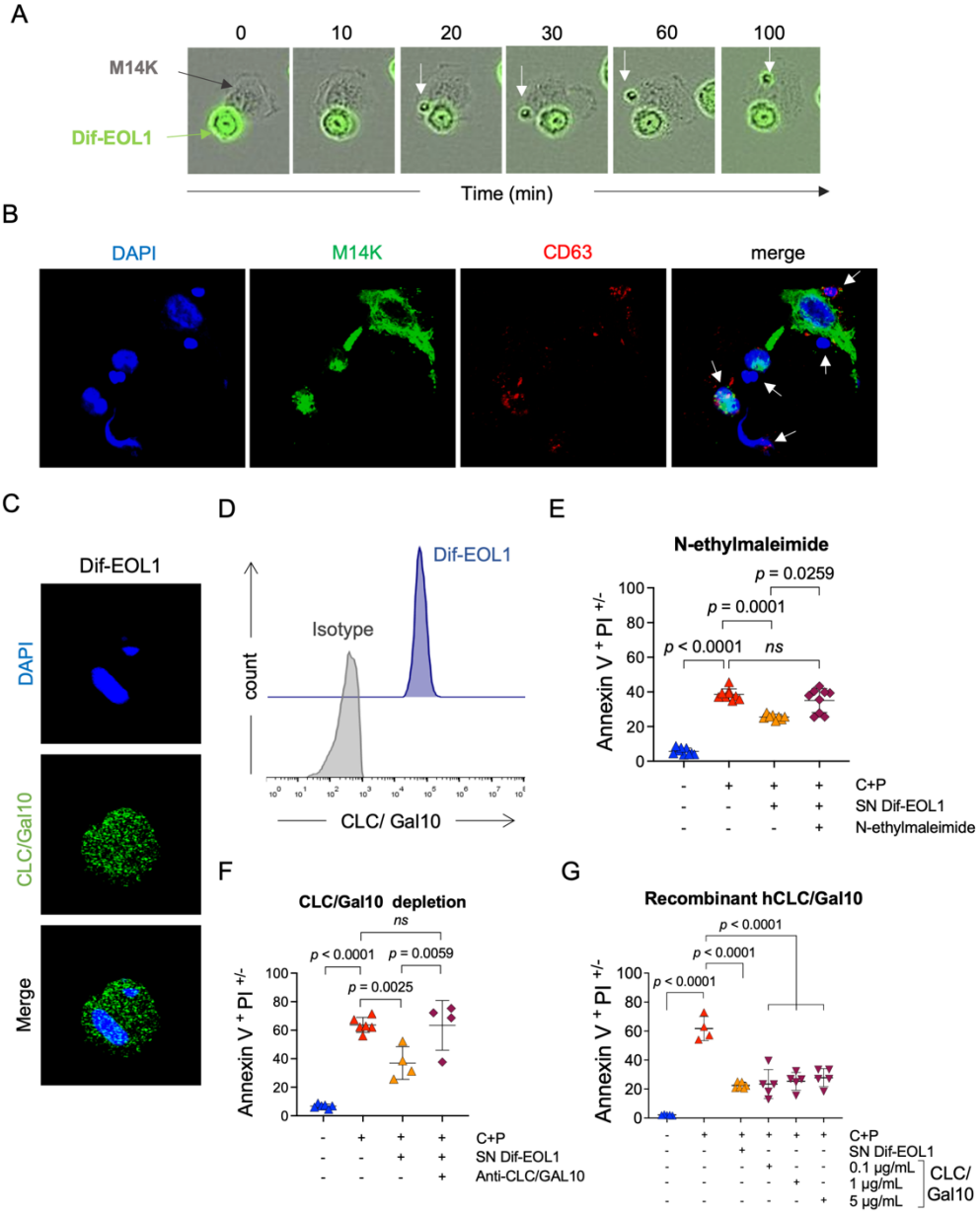

Figure 17 – CLC-P/ Gal10 inhibits MPM response to chemotherapy. (A) Incucyte time-lapse imaging of M14K cells (black) and CFSE-stained Dif-EOL1 cells (green). The white arrow shows a CFSE-labelled granule migrating inside M14K cells. **(B)** Confocal microscopy of primary human eosinophils co-cultured with CFSE-labelled M14K cells. After 24 hours, cells were fixed, permeabilized, stained with DAPI and labeled with an anti-CD63 APC conjugate (in red). Images were acquired using a Zeiss LSM 880 AiryScan Elyra confocal microscope equipped with a x63-1.4 oil immersion objective. White arrows indicate eosinophils. **(C)** Confocal analysis of Dif-EOL1 cells labeled with DAPI (blue), with an anti-CLC-P/Gal10 antibody and with an AlexaFluor488 conjugate (green). Images were acquired using a Zeiss 980 Airyscan Elyra confocal microscope equipped with a x63-1.4 oil immersion objective. **(D)** Representative histogram plot of CLC-P/Gal10 expression acquired by flow cytometry. Dif-EOL1 cells were labeled as described in Panel C. **(E)** Apoptosis of M14K cells in presence of SN Dif-EOL1, N-ethylmaleimide and/or C+P. M14K cells were preincubated with 10^{-7} M N-ethylmaleimide for 4 hours and cultured with SN Dif-EOL1 for 48 hours. After treatment with C+P for 48 hours, cells were labeled with Annexin V/PI and analyzed by flow cytometry. **(F)** Same as in Panel E except that CLC-P/Gal10 was removed from SN Dif-EOL1 by antibody-mediated depletion. **(G)** Recombinant human CLC-P/Gal10 (0.1, 1 and 5 µg/ml) was added in M14K culture medium for 48 hours before treatment with C+P. Apoptosis of M14K cells was determined by flow cytometry after Annexin V/PI labeling. Data are expressed as mean ±SD, each dot representing an independent test. Normality was checked by Shapiro-Wilk and equality of the variances was verified by Brown-Forsythe and Welch. Variance of the means was compared by one-way ANOVA followed by either Tukey's (Panels E and F) or Sidak's (Panel G) multiple comparison test.

4.4. CLC-P/Gal10 expressed by primary human eosinophils mediate chemoresistance

The advantage of EOL1 progenitors-derived eosinophils is that, although not all cells undergo terminal differentiation, they belong to the same eosinophil-committed lineage. However, the EOL1 cell line derives from a chronic eosinophilic leukemia. Therefore, primary eosinophils (Eos) were isolated from peripheral blood of healthy donors using magnetic-activated cell sorting with an anti-CCR3 antibody (**Figure 18A**). The purity of the isolated population was controlled by flow cytometry using Siglec-8 and IL-5Rα markers, as illustrated in **Figure 18B**. Confocal microscopy confirmed that purified Eos staining positive major basic protein (MBP) also expressed CLC-P/Gal10 (**Figure 18C and 18D**).

Based on the observations obtained with Dif-EOL1 cells, the involvement of CLC-P/Gal10 expressed by primary eosinophils in MPM chemoresistance was also investigated. Culture medium was conditioned overnight with Eos and the primary eosinophil supernatant (SN Eos) was added to M14K cells 48 hours before C+P treatment. The apoptotic response of M14K cells to C+P was significantly reduced in presence of the SN Eos (**Figure 18E)**. Compilation of 6 independent experiments with primary cells from different donors confirmed this conclusion statistically (**Figure**

18F). Antibody-mediated depletion of CLC-P/Gal10 reverted the anti-apoptotic activity of the SN Eos in presence of C+P (**Figure 18G**, $p = 0.0007$)

These data demonstrated that CLC-P/Gal10 produced by primary human eosinophils impaired the chemotherapeutic response of MPM cells.

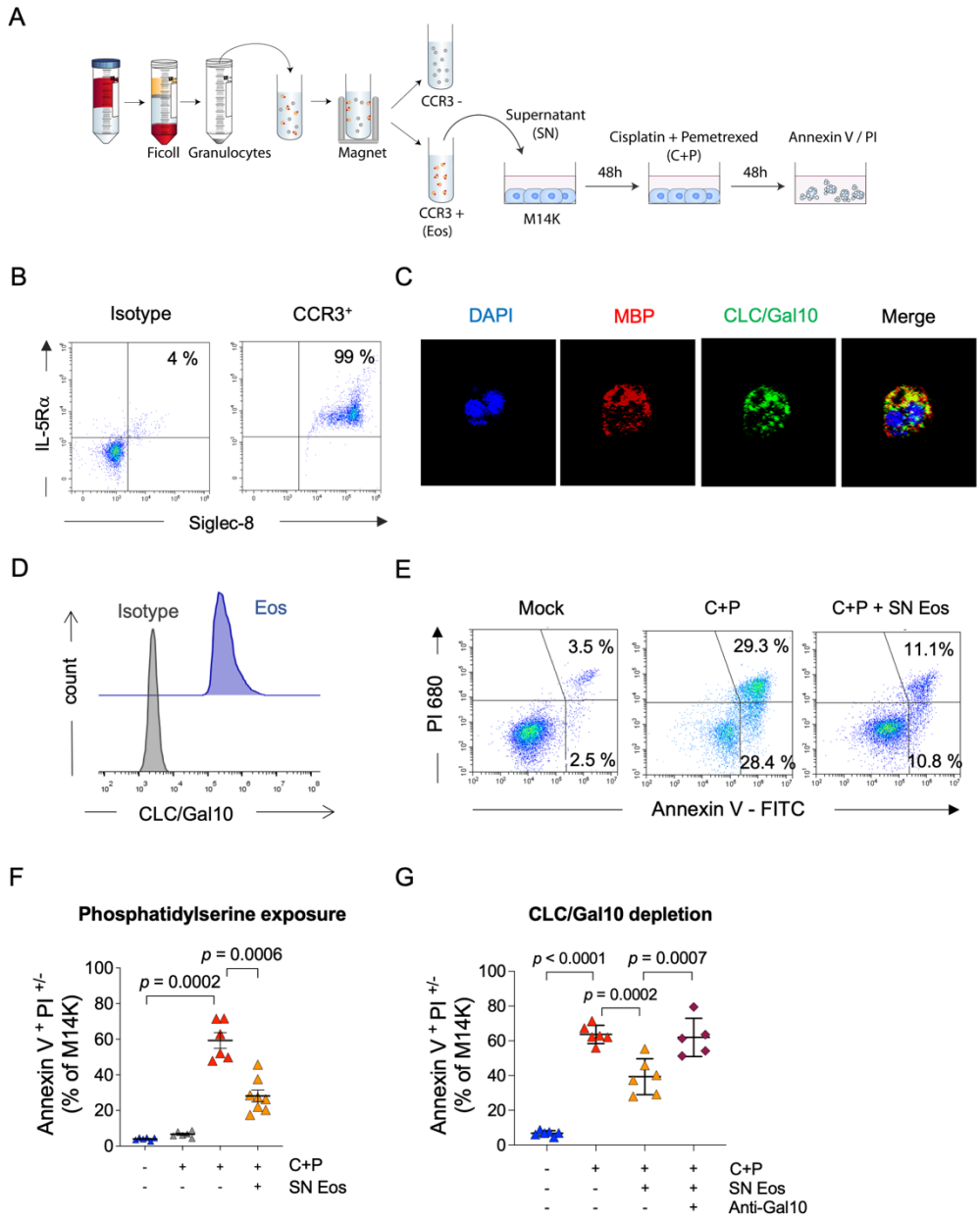

Figure 18 - CLC-P/Gal10 expressed by primary eosinophils impairs the cytotoxic activity of cisplatin and pemetrexed. (A) Schematic representation of the experimental protocol for the isolation of primary human eosinophils. Primary eosinophils were purified from the polymorphonuclear cell (granulocytes)-rich fraction of peripheral blood by Ficoll gradient centrifugation and positively selected by magnetic-activated cell sorting using an anti-CCR3 antibody. The culture supernatant of CCR3-positive eosinophils (SN Eos) was collected after 24 hours and added at a ratio of 25% (v/v) to M14K cells for 48 hours. Then, M14K cells were treated with C+P for 48 hours and analyzed by flow cytometry after Annexin V/PI labeling. **(B)** Representative dot plot of isolated $CCR3^+$ cells labeled with antibodies directed against Siglec-8 and IL-5Rα. **(C)** Purified $CCR3^+$ eosinophils were fixed, permeabilized and labeled with DAPI (blue), CLC-P/Gal10 (AlexaFluor488 in green) and MBP (TexasRed in red). Images were acquired using a Zeiss 980 Airyscan Elyra confocal microscope equipped with a x63-1.4 oil immersion objective. **(D)** Representative histogram plot of CLC-P/Gal10 expression acquired by flow cytometry. Primary eosinophils were labeled with an anti-CLC-P/Gal10 antibody and an AlexaFluor488 conjugate. (**E**) Representative flow cytometry dot plot of M14K cells cultured with C+P and/or SN Eos (25% v/v) and labeled with Annexin V/PI. **(F)** Apoptosis of M14K cells in presence of SN Eos and/or C+P. M14K cells were cultured with SN Eos for 48 hours. After treatment with C+P for 48 hours, cells were labeled with Annexin V/PI and analyzed by flow cytometry. **(G)** Same as in Panel F except that CLC-P/Gal10 protein was depleted from SN Eos by using an anti-Gal10 antibody. Data are expressed as mean +/- SD, each dot representing an independent test. Normality was checked by Shapiro-Wilk and equality of the variances were determined by Brown-Forsythe and Welch. Variance of the means was compared by Brown-Forsythe and Welch ANOVA followed by Dunnett's T3 multiple comparison test.

4.5. An anti-eosinophilic treatment restores the effectiveness of chemotherapy in mice

To investigate the role of eosinophils in response to chemotherapy in a preclinical mouse model, the epithelioid mesothelioma AK7 cell line was inoculated into syngeneic C57BL/6 mice [204]. At an early stage of tumor growth (~150 mm^3), eosinophilia was induced by IL-5 and/or IL-33 treatment (Day 0) in half of the mice [169,205] (**Figure 19A**). When the tumors reached approximately ~500 mm^3, mice were treated with the C+P chemotherapeutic regimen (**Supplementary Figure 5**). In these experimental settings, the absolute eosinophil count (in blood samplings from the tail vein) at Day 10 significantly increased upon administration of IL-5 or IL-5 + IL-33, while the count of other leukocyte populations (*i.e.*, monocytes, lymphocytes and neutrophils) remained unaffected (**Figure 19B**). In eosinophilic mice (induced by IL-5 or IL-5+IL-33), mesothelioma tumors were unresponsive to an effective dose of C+P ($p < 0.0001$, **Figure 19C, Supplementary Figure 5**). It was therefore deduced that eosinophilia impaired the response to the C+P regimen.

To investigate the efficacy of an anti-eosinophilic treatment, mice were treated with the anti-Siglec-F antibody two days before chemotherapy (D8). A single dose of the

neutralizing anti-Siglec-F antibody restored the baseline eosinophil counts (**Figure 19D**) as well as the response to the C+P regimen (**Figure 19E**).

In conclusion, preclinical data in a syngeneic mouse model demonstrated that the excess of peripheral blood eosinophils impaired the response to the C+P chemotherapy. Antibody-mediated ablation of eosinophils restored the efficacy of the C+P regimen, providing preclinical evidence for an improved therapy of mesothelioma based on an anti-eosinophilic treatment.

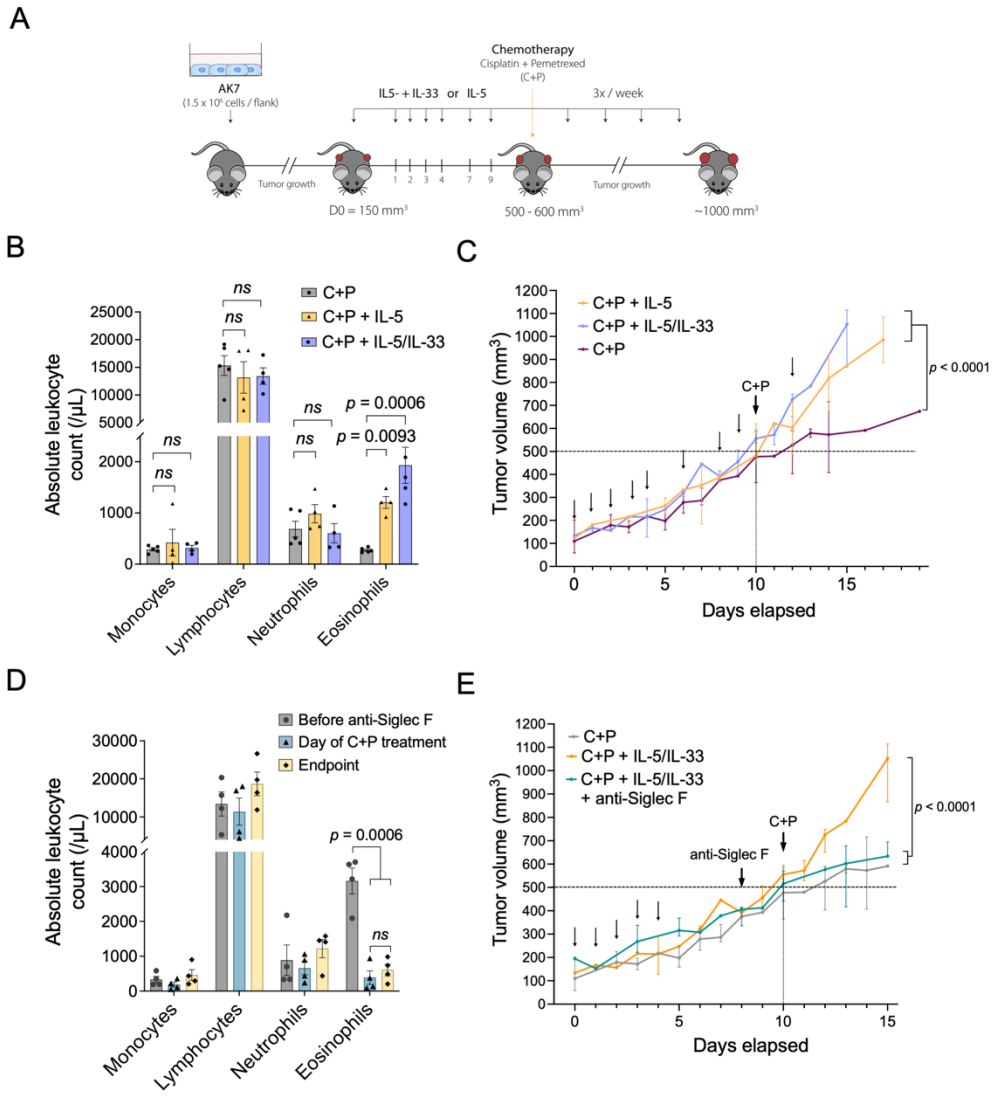

Figure 19 – Peripheral blood eosinophilia inhibits chemotherapy in mice while an anti-eosinophilic treatment restores effectiveness. (A) Experimental design. C57/BL6 mice were implanted subcutaneously with epithelioid AK7 mesothelioma cells (1.5 x 10^6 cells/flank). When the tumor reached ~150 mm^3, eosinophilia was increased with IP injections of IL-5 and/or IL-33 as indicated. When the tumor reached ~500 mm^3, mice were given C+P chemotherapy and tumor growth was assessed until tumor reached 1000 mm^3. **(B)** Absolute counts (number of cells/µL of blood collected from the tail vein) at Day 10 of the different leukocyte populations measured with an hematocytometer just before C+P treatment. **(C)** The tumor volume (mm^3) was regularly determined by using the hemi-ellipsoid formula (L x l x W x π/6), where L=length, W=width, H=height. **(D)** Eosinophilic mice were injected with anti-Siglec-F antibody 2 days prior to chemotherapy administration. Absolute leukocyte counts were measured before (grey), concomitantly (blue) and at the end of the experiment (yellow). **(E)** Tumor growth was determined as in Panel C. Normality of the populations and homogeneity of variances were checked by Shapiro-Wilk and by Levene's test, respectively. Growth curves were compared by using the "growth index" method followed by two-way ANOVA.

5. Discussion

In mesothelioma, several examples illustrate the involvement of the local microenvironment in tumor growth and response to therapy [32,40,206]. The role of the macroenvironment is by far more controversial although the prognostic impact of systemic inflammation achieves a broader consensus [197]. Blood inflammatory markers such as total leucocyte count, neutrophil/lymphocyte ratio (NLR) and C-reactive protein (CRP) have been inversely correlated with survival [206]. Recently, we added an additional layer of complexity by including another cell type of the myeloid lineage. Indeed retrospective data sets from 230 mesothelioma patients collected in 3 clinical centers indicated that an excess of peripheral blood eosinophils prior to chemotherapy was associated with worse outcome and quicker relapse [199]. Since this correlation did not imply causation, we have investigated here the mechanism mediating the interplay between eosinophils and response to chemotherapy. Based on experimental evidence in cell culture and mice, we demonstrated in this study that eosinophils-derived CLC-P/Gal10 promotes resistance to the standard chemotherapy of mesothelioma (*i.e.,* the C+P regimen) and, more importantly, that an anti-eosinophilic treatment allows to improve the therapeutic response in a preclinical mouse model.

Besides chemotherapy, immunotherapy represents the other standard first-line treatment of mesothelioma. Whether the efficacy of ICIs could be improved by combination with anti-eosinophilic therapy is unknown but deserves further investigation. Interestingly, a threshold in absolute eosinophil counts allows to identify ICI-treated patients who have a better prognosis, although the correlation was based on a limited number of patients and needs to be validated with other cohorts [199].

An important aspect of mesothelioma clinical management is the tumor cell phenotype. In this study, 2 cell lines modeling the epithelioid and non-epithelioid subtypes displayed different responses to C+P chemotherapy, reflecting similar disparities observed in clinical settings. The M14K cell line is undoubtedly of epithelial origin but the phenotype of ZL34 is unclear [207–210]. A consensus is that ZL34 is predominantly of sarcomatoid morphology with a biphasic component. Of note, examination of stress fibers, lamellipodia and perinuclear actin arcs revealed a wide diversity in the cytoskeleton organization of mesothelioma cell lines [211]. It would thus be interesting to analyze a broader range of cell lines, short-term cultures of patient's derived biopsies or possibly implanted tumors in patient-derived xenograft models. The behavior of the 2 cell types used in this study nevertheless reveals that response to chemotherapy may imply apoptosis as well as S phase arrest. Transcriptomic analyzes highlight a series of shared DEG between the 2 cell lines, but also marked differences that may reflect their response to eosinophil-derived factors (**Supplementary Figure 4**).

The paradigm is even more complicated by the ability of mesothelioma cells to undergo senescence upon chemotherapy [212]. Platinum-based compounds induce extensive genomic lesions through covalent adducts and intra- or inter-strand DNA cross-linking. Consequently, damaged tumor cells undergo senescence to avoid

further genomic instability and accumulation of DNA lesions [213]. Eosinophil-conditioned media increases C+P-induced senescence of M14K cells, which is consistent with their effects on apoptosis and cell cycle (**Supplementary Figure 6**). Detailed kinetics of proliferation, apoptosis and senescence of mesothelioma cells associated to chemoresistance should therefore be investigated dynamically at the single cell level.

Experimental evidence obtained in this study also demonstrates that CLC-P/Gal10 is a central mediator of eosinophil-mediated chemoresistance. Deprivation of CLC-P/Gal10 from the eosinophil supernatant and addition of the recombinant protein have consistently opposite effects on C+P-induced apoptosis. It remains nevertheless possible that other eosinophil components such as citrullinated chromatin from eosinophil extracellular traps (EETs), which are associated with CLC-P/Gal10 [124,127], are involved in this process. However, a direct interaction between EETs and mesothelioma cells is unlikely due to the infrequent infiltration of eosinophils in tumors or pleural fluid. Alternatively, CLC-P/Gal10 could be produced by distant eosinophils and act in an exocrine manner on mesothelioma tumors. The CLC-P/Gal10 protein is a small hydrophobic polypeptide of 142 amino acids that interacts with a lysophospholipase inhibitor and promotes lysophosphatidylcholine hydrolysis [121,125]. In its insoluble form, crystalized CLC-P has been recognized as a classical hallmark of eosinophilic inflammation in tissues and body fluids. Charcot-Leyden crystal results from non-covalent aggregation of Galectin-10 leading to highly insoluble and remarkably stable crystals. Although its ligands have not yet been identified, it is known that CLC-P/Gal10 is externalized to sites of inflammation, possibly via extracellular vesicles generated by EETosis [124,127]. Our current experiments show that CLC-P/Gal10 can be detected in the sera and pleural fluids of mesothelioma patients. A 2-day pre-incubation of mesothelioma cells with the eosinophil-derived supernatant or with the recombinant CLC-P/Gal10 protein is required to attenuate the effect of C+P, thereby excluding a direct quenching by the cytotoxic compounds (**Figure 15** and **Supplementary Figure 3**). Transcriptomic analyzes further support that molecular changes (binding) indeed occur in mesothelioma cells in response to eosinophil-derived factors (**Figure 16** and **Supplementary Figure 4**). Charcot-Leyden crystal or soluble Galectin-10 likely interact with a still unidentified membrane cell receptor to modify the cell phenotype and lead to chemoresistance. Since recombinant, purified and soluble (*i.e.*, His-tagged) human Galectin-10 mimics the effect of the eosinophil-conditioned medium, the anti-apoptotic activity does not result from other associated proteins such as granule cationic ribonucleases (RNases). Whatever the mechanism, CLC-P/Gal10 may be a novel therapeutic target to reduce chemoresistance in mesothelioma. Interestingly, In this context, camelid antibodies able to dissolve CLC/Gal10 crystals have shown therapeutic value in Th2-type inflammatory airway diseases [124].

In addition to a CLC-P/Gal10-specific therapy, it may be useful to evaluate alternative options targeting eosinophils. However, particular attention should be paid to the indirect effects of anti-eosinophilic treatment as eosinophils release cytotoxic

factors (granzyme, MBP, ECP and EDN) that can destroy tumors [169]. Eosinophil-derived cytokines IL-12 and IL-10 decrease metastasis by enhancing E-cadherin expression on tumor cells. Eosinophils also release IFN-γ, which acts in an autocrine fashion or in combination with $CD8^+$ T cells. Finally, TNFα and IFN-γ-activated eosinophils polarize macrophages towards an anti-tumorigenic M1 phenotype. Therefore, a therapy targeting eosinophils may also favor tumor growth and be detrimental to patients' outcome. However, there is no data supporting the anti-tumorigenic role of eosinophils in mesothelioma. Furthermore, our data shows that 2 central cytokines modulating eosinophil fate (*i.e.*, IL-5 and IL-33) do not significantly modify tumor growth kinetics in our mouse model of mesothelioma (**Supplementary Figure 7**). However, a trend for a slightly accelerated tumor growth upon administration of both IL-5 and IL-33 cytokines compared to control mice. Our data also shows that IL-5 does not affect apoptosis or cell cycle in response to C+P M14K and ZL34 cells (**Supplementary Figure 8**). In addition, the effect of an anti-eosinophilic therapy would also deserve further investigation is mesothelioma patients.

Another question worth discussing is the dose of C+P that was specifically selected to stabilize but not completely clear the tumor in the preclinical model (**Figure 19** and **Supplementary Figure 5**). Although this experimental design mirrors the partial response to platinum-based regimen in mesothelioma patients, we are aware that the pharmacokinetics of the chemotherapeutic compounds are different in mice and humans. This trivial statement is becoming a particularly hot topic for targeted immunotherapies. In a perspective of metronomic therapy that would better preserve the host immunity, further experiments are needed to broaden the conclusions in clinical settings. Notwithstanding, there is concordance between evidence obtained in cell cultures, mouse models and clinical datasets that support the detrimental role of eosinophils in mesothelioma. A strategy aimed at reducing the eosinophil counts just prior to chemotherapy is therefore predicted to provide a clinical benefit to mesothelioma patients.

There is a number of strategies for reducing the number of eosinophils. Although this question has not been specifically studied, it is still unclear why methylprednisolone, a glucocorticoid frequently combined with chemotherapy to limit inflammation, does not improve the effectiveness of chemotherapy. Among different hypotheses, it is possible that the kinetics of administration is inappropriate because methylprednisolone doses are given the day before, concomitantly with, and the day after chemotherapy. The anti-inflammatory activity of methylprednisolone may also affect other immune cell types that modulate patient's response. It is also conceivable that similar approaches focusing on identical targets may have different outcomes as illustrated by the non-overlapping effects of PD-1 and PDL-1 immunotherapies. In the same line, therapies targeting eosinophil-modulating cytokines such as IL-5, IL-33 or their receptors may have more specific effects than broad anti-inflammatory drugs, such as methylprednisolone. A series of monoclonal antibodies interacting with these cytokines, such as the anti-IL-5 antibodies mepolizumab and reslizumab, and the anti-IL5-Rα antibody benralizumab, are readily

available for clinical use to treat eosinophil-associated diseases [156]. Based on the findings reported here and promising observations in eosinophilic gastritis/duodenitis [214], we propose that Siglec-8, the human ortholog of mouse Siglec-F which induce eosinophil apoptosis, may be a priority candidate to target in mesothelioma therapy.

AUTHOR'S NOTE

AF (Télévie Fellow), LH (research fellow), LW (research director), MJ and MH (postdoctoral researchers) are members of the FNRS. MG and MW are supported by grants of ULiege. Clinicians are AS and EW (CHU Lille), VH, RL and BD (University Hospital of Liege).

ACKNOWLEDGEMENTS

This work was supported by the Belgian Foundation against Cancer, the Fonds National de la Recherche Scientifique (FNRS), the Télévie, and the Fondation Léon Fredericq. We are very grateful to the Red Cross of Belgium for providing the buffy coats. We thank Claire Josse and Christophe Desmet for their advice with mice experiments. We thank the GIGA Imaging technological platform for advice and support, especially Alexandre Hego and Gaëtan Lefevre for confocal microscopy as well as Raafat Stephan and Céline Vanwinge for flow cytometry. We thank Hélène Hiertz for her experimental contribution on the spheroid model and to Jean-Rock Jacques for his technical expertise.

CONFLICTS OF INTEREST

The authors declare no conflict of interest.

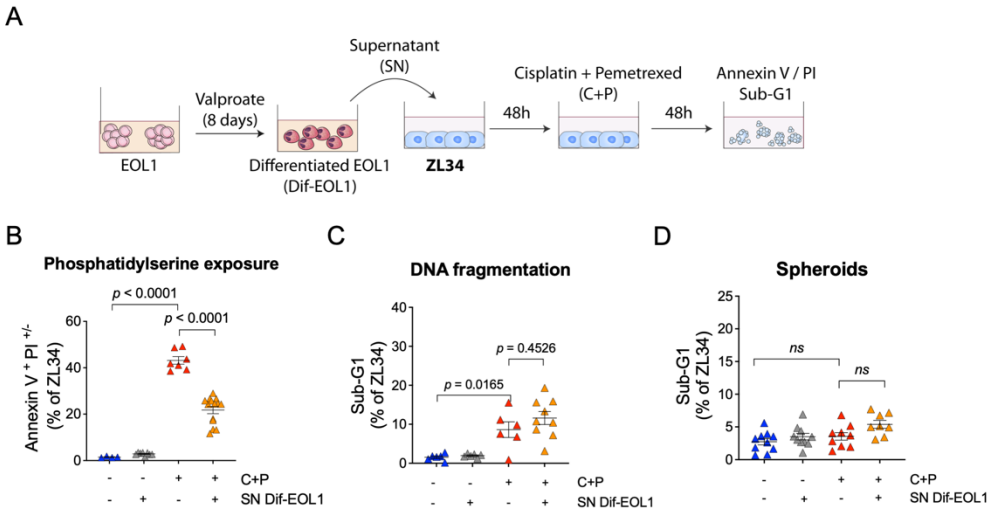

Supplementary Figure 1 – EOL1-conditioned medium affects the apoptotic response of non-epithelioid ZL34 cells to chemotherapy. (A) Experimental design. EOL1 progenitors were differentiated in eosinophils (Dif-EOL1) with valproate for 8 days. Supernatant from differentiated cells (SN Dif-EOL1) was added at 25% v/v to the medium of ZL34 cell cultures for 48 hours. After treatment with 10 µM cisplatin and 10 µM pemetrexed (C+P) for 48 hours, the rates of apoptosis were quantified by Annexin V/PI labeling and cell cycle analysis (Sub-G1). **(B)** Percentages of apoptotic ZL34 cells evaluated by flow cytometry analysis of annexin/PI labeled cells. **(C)** After ethanol permeabilization and PI staining, the proportion of cells with fragmented DNA (*i.e.*, Sub-G1) was determined by flow cytometry. **(D)** ZL34 cells were cultured for 72 hours in a 96-well plate coated with DMEM-agarose 1.5% in presence of SN Dif-EOL1 and then treated with C+P for 2 days. The proportion of ZL34 cells with fragmented DNA (i.e., Sub-G1) was analyzed after spheroid dissociation, cell permeabilization and propidium iodide staining. Data are expressed as means +/- SD, each dot representing an independent test. Normality was checked by Shapiro-Wilk and equality of the variances was analyzed by Brown-Forsythe. The variance of the means was compared by one-way ANOVA followed by Tukey's multiple comparison test.

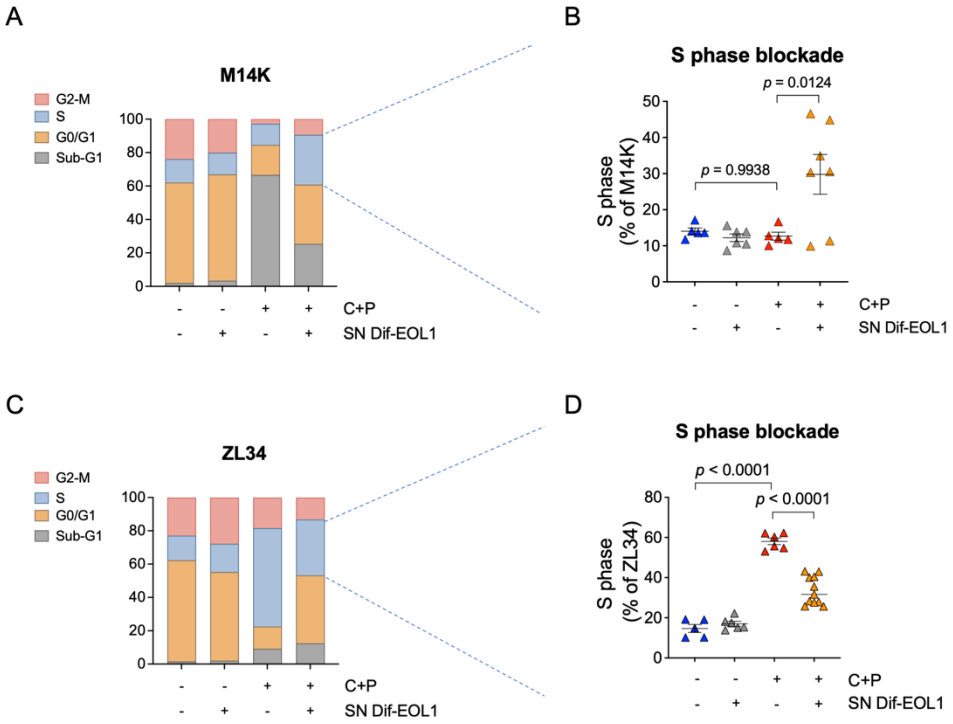

Supplementary Figure 2 – Compared to M14K, non-epithelioid ZL34 cells preferably undergo S phase arrest in presence of C+P. Representative cell cycle profiles of M14K **(A)** and ZL34 **(B)** cells. The proportion of cells in each phase of the cell cycle (Sub-G1, G0, S and G2-M) in the different conditions are indicated. Statistical analysis of S-phase blockade in M14K **(B)** and ZL34 **(D)**. Data are expressed as mean +/- SD, each point representing an independent test. Normality was checked by Shapiro-Wilk and equality of the variances was checked by Brown-Forsythe. Variance of the means was compared by one-way ANOVA followed by Tukey's multiple comparison test.

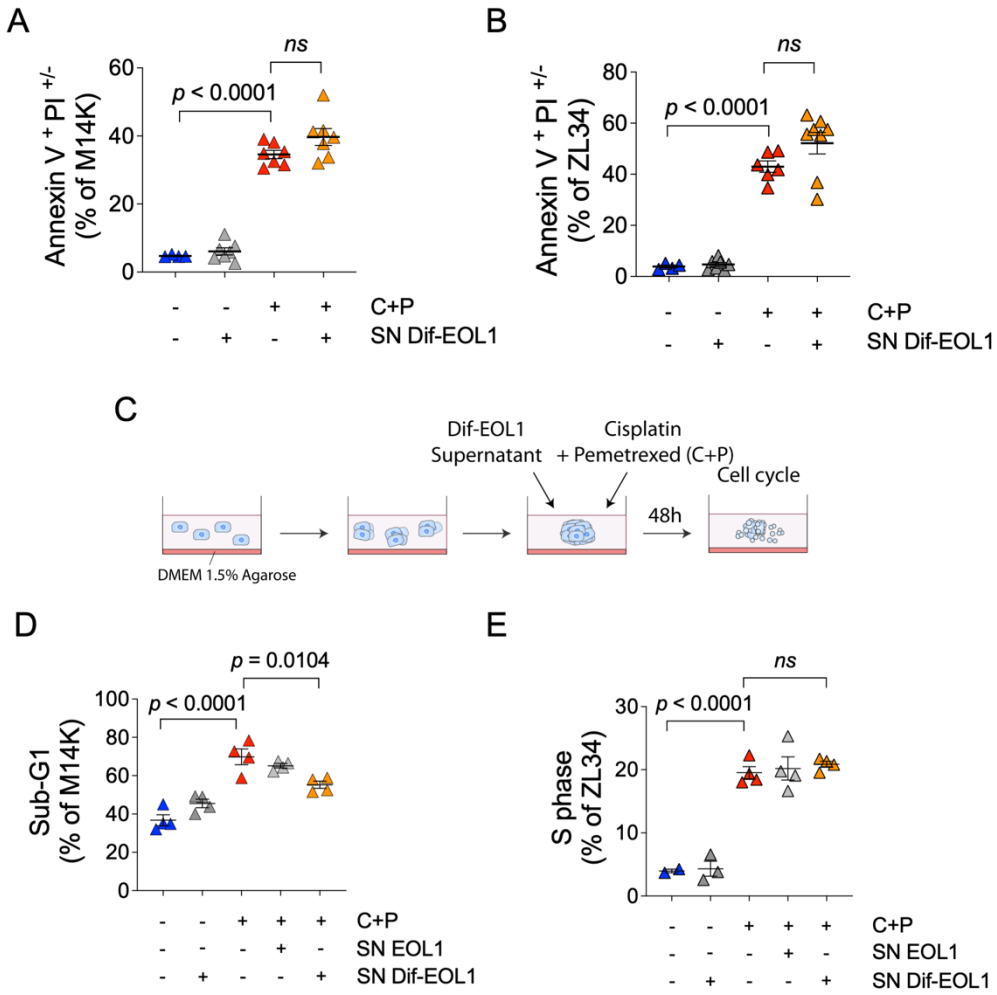

Supplementary Figure 3 – Co-administration of SN Dif-EOL1 and C+P does not affect apoptosis. MPM cells were cultured in presence of differentiated EOL-1 supernatant (SN Dif-EOL1) at 25% v/v, 10µM cisplatin and 10 µM pemetrexed (C+P) for 48 hours. After labeling with Annexin V/PI, apoptosis was evaluated by flow cytometry. Apoptotic rates in M14K **(A)** and ZL34 **(B)** were then analyzed by flow cytometry. **(C)** MPM cells were cultured in a 96-well plate coated with DMEM-agarose 1.5% for 72 hours. Spheroids were then cultured for 48 hours in presence or absence of SN Dif-EOL1 and 10µM C+P. After spheroid dissociation, ethanol permeabilization and propidium iodide staining, the proportion of M14K cells with fragmented DNA (*i.e.,* Sub-G1) **(D)** and ZL34 cells in S phase **(E)** were analyzed by flow cytometry. Data are expressed as mean +/- SD, each dot representing an independent test. Normality was checked by Shapiro-Wilk and equality of the variances was determined by Brown-Forsythe. The variance of the means was compared by one-way ANOVA followed by Tukey's multiple comparison test.

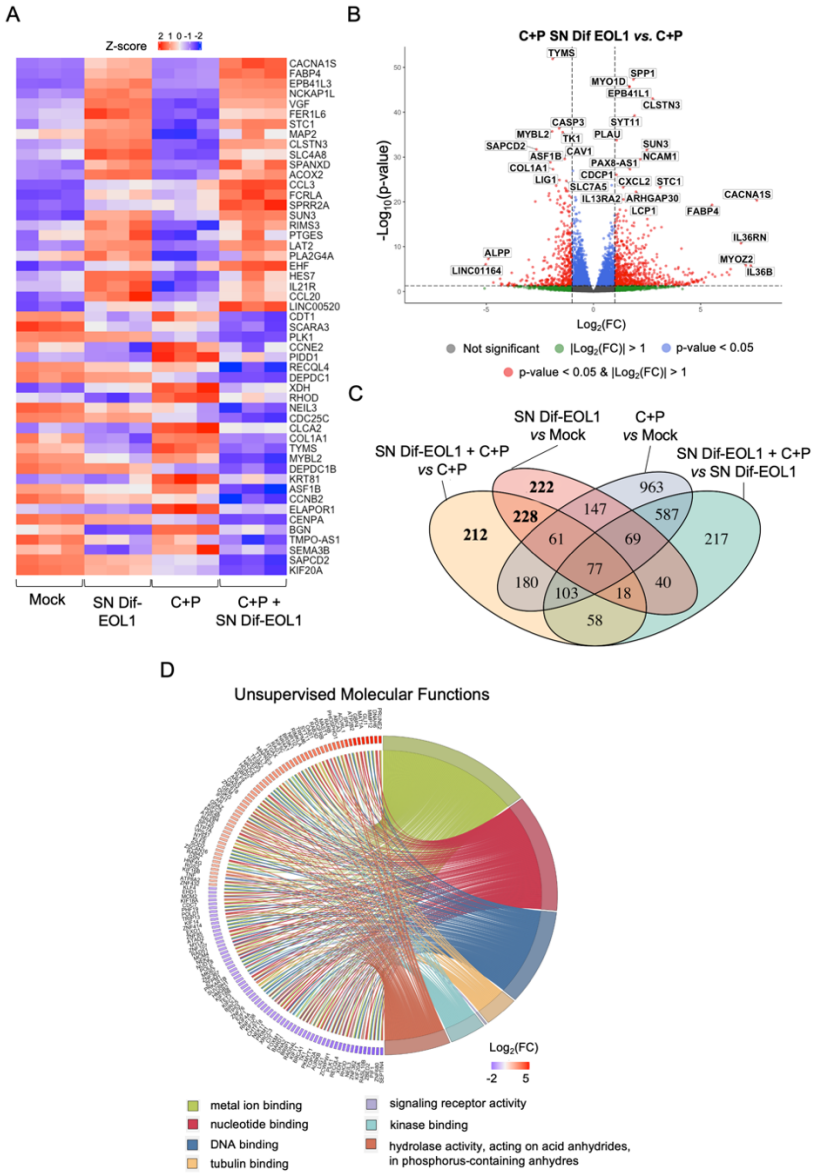

Supplementary Figure 4 – Transcriptomic profiles of ZL34 cells in response to Dif-EOL1 supernatant. (A) Unsupervised heatmap of the top 25 up- and down-regulated most significant genes deduced from 3 independent experiments. **(B)** Volcano plot of DEGs in M14K treated with C+P with or without conditioned medium of differentiated EOL1 (SN Dif-EOL1). DEGs $Log_2(FC) > 1$ and p-adj > 0.05 are colored in red. **(C)** Venn diagram of significant DEGs in the different conditions. Numbers of genes impacted by SN Dif-EOL1 are in bold. **(D)** Representative chord diagram of the most significative pathways affected in GO Molecular Functions (GO:MF) in conditions C+P+SN Dif-EOL1 and C+P. Pathways (right half of the diagram) are linked to the genes (on the left side) according to their $Log_2(FC)$.

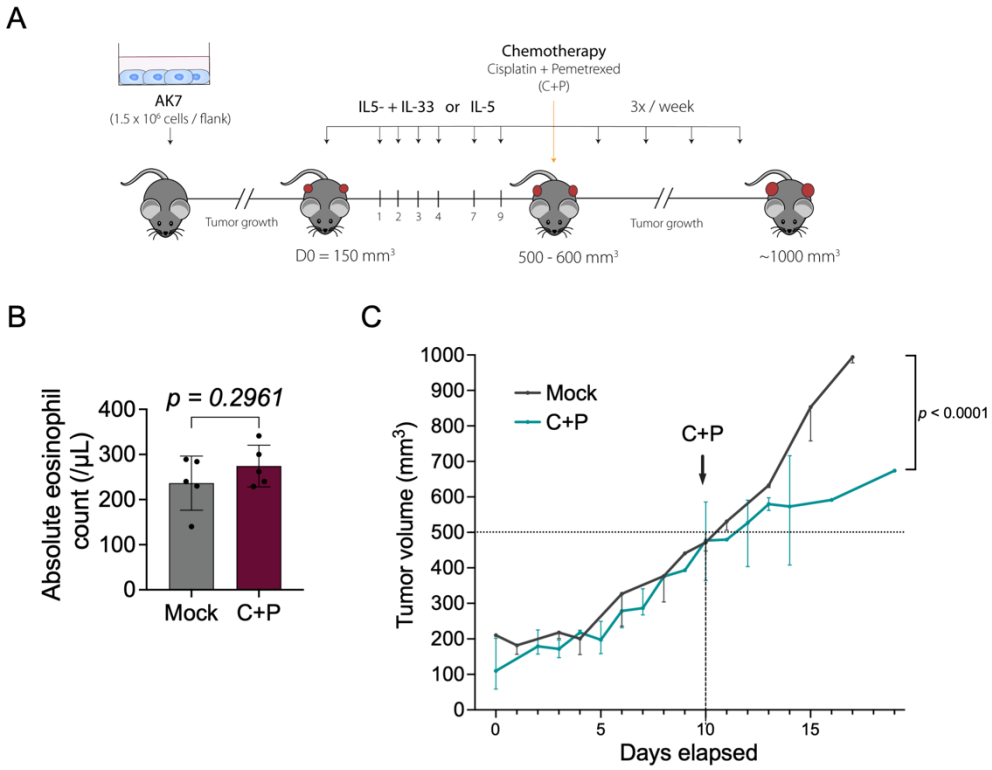

Supplementary Figure 5 - The cisplatin+pemetrexed regimen reduces tumor growth in C57BL/6 mice. (A) C57BL/6 mice were inoculated subcutaneously with syngeneic AK7 cells. When the tumor reached 500 mm3, mice were injected with cisplatin (6 µg /gbw) and pemetrexed (150 µg/gbw). **(B)** Absolute eosinophil counts (number of cells / µL of blood) measured with an hematocytometer just before C+P treatment. **(C)** The tumor volume was regularly determined by using the hemi-ellipsoid formula (L x l x W x π/6), where L=length, W=width, H=height.

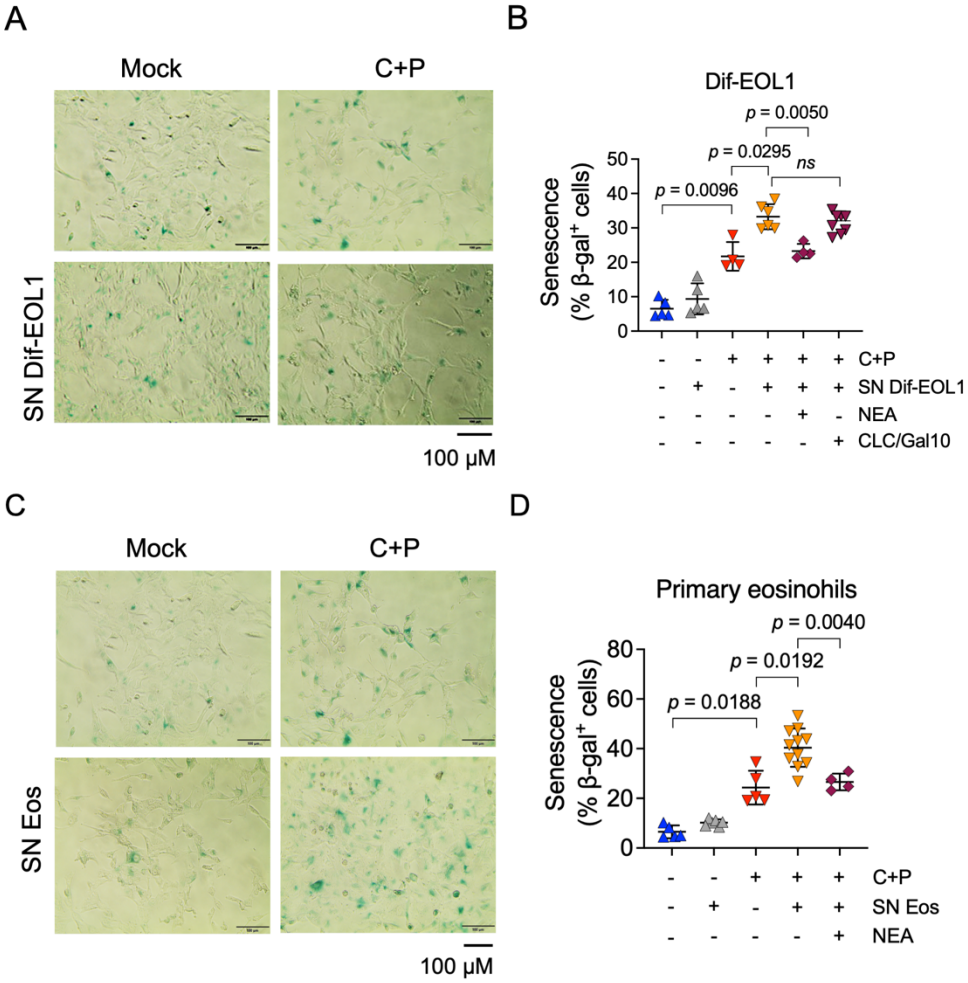

Supplementary Figure 6 – The C+P regimen and eosinophil-conditioned media promote senescence in M14K cells. (A and **C)** Representative images of senescent M14K cells in presence of conditioned medium of differentiated EOL1 (SN Dif-EOL1) or primary eosinophils (SN Eos), respectively. M14K cells were cultured for 48 hours in presence of mock, SN Dif-EOL1 (25% v/v), SN Eos (25% v/v) or recombinant human CLC-P/GAL10 (1 µg/mL). In condition NEA, the eosinophil supernatants were pre-incubated for 4 hours with N-ethylmaleimide (at 10^{-7} M; Sigma). M14K cells were then incubated with 10 µM cisplatin and 10 µM pemetrexed for an additional 2 days. Senescence-associated β-galactosidase (SA-β-gal) activity at pH 6.0 was visualized with an Olympus CKX41 inverted microscope equipped with a 20X objective. (**B** and **D**) The percentages of SA-β-gal positive cells were counted in ten different fields. Data are the means +/- SD experiments. Normality of the populations was checked by Shapiro-Wilk and means were compared by one-way ANOVA followed by Tukey's multiple comparison test.

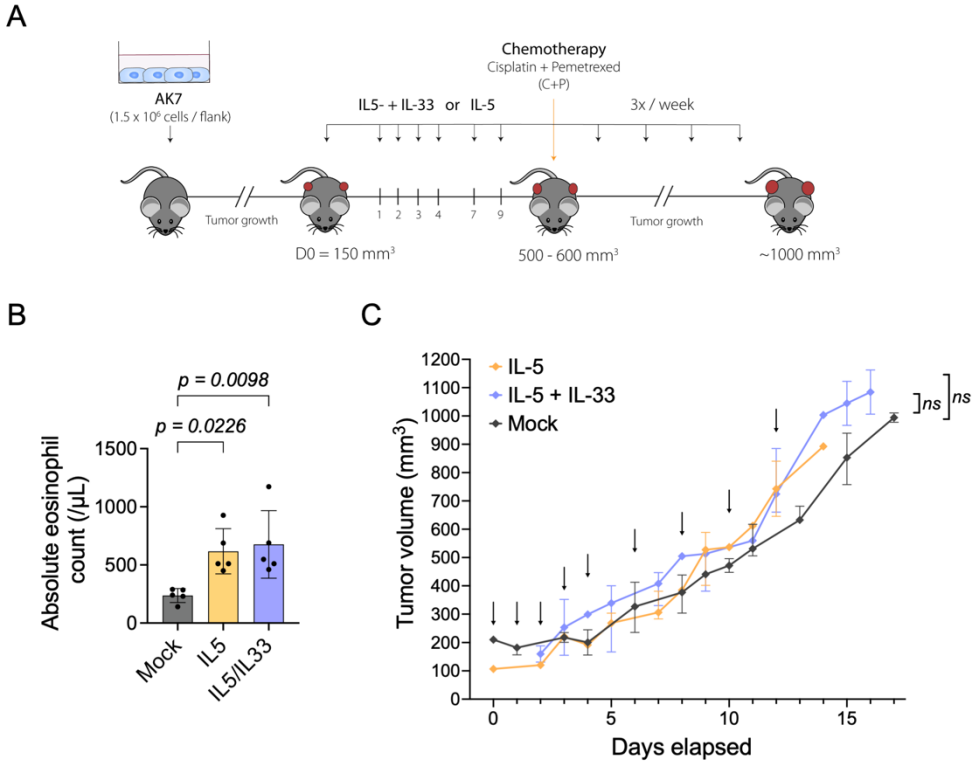

Supplementary Figure 7 – Cytokine-induced blood eosinophilia does not influence tumor growth in C57BL/6. (A) C57BL/6 mice were inoculated subcutaneously in both flanks with syngeneic AK7 cells. When the tumor reached 200 mm3, mice were injected intraperitoneally with IL-5 (5 ng /gbw) and IL-3 (20 ng/gbw) as indicated by the arrows. **(B)** Absolute eosinophil counts were determined with an hematocytometer when the tumor reached 500 mm3, before chemotherapy administration. Normality of the populations was checked by Shapiro-Wilk and homogeneity of the variances by Brown-Forsythe. Variance of the means were compared by one-way ANOVA followed by Tukey's multiple comparison test. **(C)** Kinetics of the tumor volume (in mm3). The tumor volume was regularly determined by using the hemi-ellipsoid formula (L x l x W x π/6), where L=length, W=width, H=height. Normality of the populations was checked by Shapiro-Wilk and homogeneity of the variances was checked by Levene's test. Growth curves were compared by using the "growth index" method followed by two-way ANOVA.

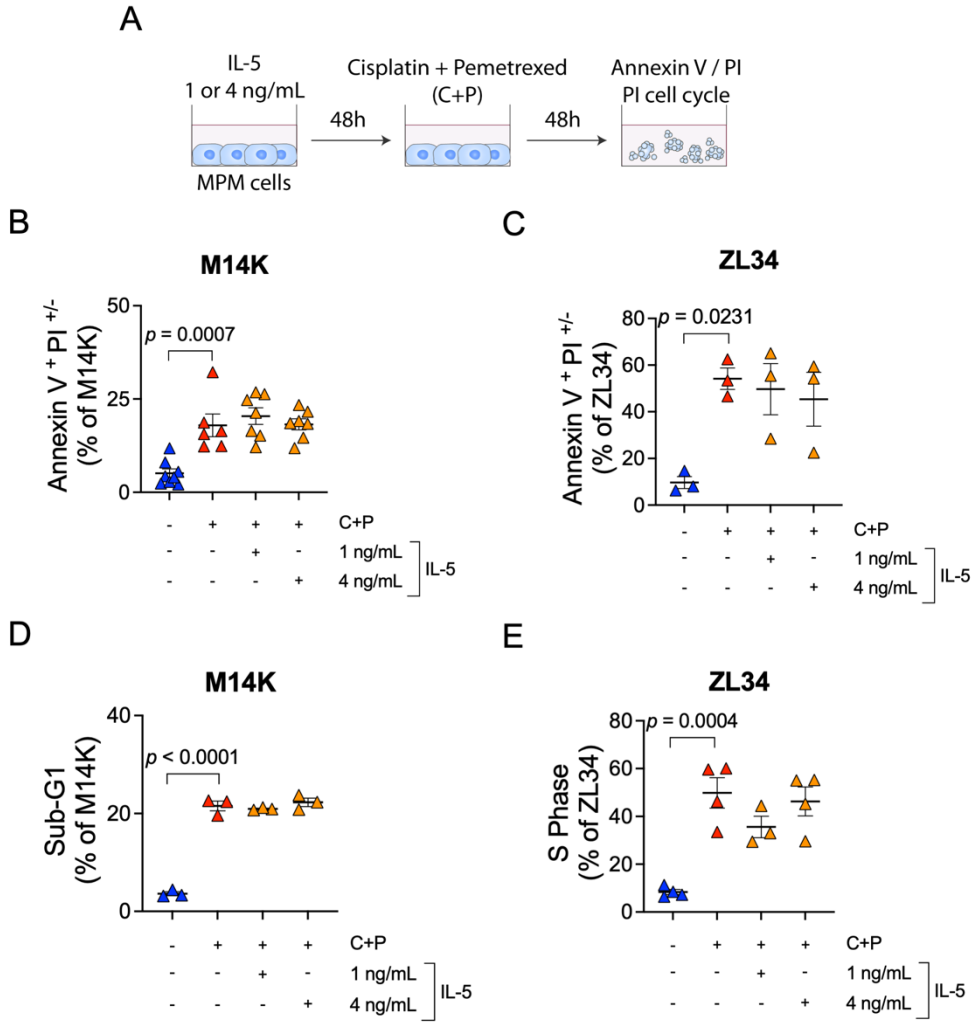

Supplementary Figure 8 – IL-5 does not affect response to C+P. (A) Experimental design. M14K and ZL34 cells were cultured in presence of mock or interleukin-5 (IL-5) at 1 and 4 ng/mL for 48 hours. After treatment with 10 µM C+P for 48 hours, apoptotic rates and cell cycle profiles were analyzed by flow cytometry. Apoptotic rates estimated by Annexin V/PI labeling in M14K **(B)** and ZL34 cells **(C)**. After ethanol permeabilization and PI staining, the proportion of M14K in Sub-G1 **(D)** and ZL34 in S **(E)** were determined by flow cytometry. Data are expressed as means +/- SD, each point representing an independent test. Normality was checked by Shapiro-Wilk and equality of the variances was checked by Brown-Forsythe. The variance of the means was compared by one-way ANOVA followed by Tukey's multiple comparison test.

Chapter 4

Discussion and Conclusion

1. Eosinophils and mesothelioma patients

MPM is a rare and aggressive cancer associated with asbestos exposure. Despite the complete or partial ban of asbestos use since the 1970's in most countries, incidence of MPM is still increasing worldwide [13,14]. This is mainly due to the long latency period of 30 to 60 years between exposure and neoplasm development [13,15]. MPM prognosis remains globally poor and available treatments only extend patients' survival by a few months [60,63]. The mechanisms involved in therapy resistance are still not well understood, but the TME is hypothesized to play a major role.

Eosinophils are granulocytic leukocytes that develop in the bone marrow from pluripotent progenitors under the regulation of transcription factors (GATA-1, PU.1 and c/EBP) and signalling molecules (IL-3, IL-5 and eotaxins) [89,95]. They are composed of granules containing various proteins (MBP, EPX, EPX, EDN and Gal10) and are the source of cytokines (*e.g.*, IL-4, IL-6, IL-13), growth factors (*e.g.*, GM-CSF, VEGF) and enzymes [95]. Eosinophils produce both anti- (*e.g.,* TNF-α, granzyme, cationic proteins, IL-10 and IL-12) and pro-tumorigenic molecules (*e.g.,* TGF-β1, VEGF) [169]. Thereby, the presence of eosinophils either in the blood, tumor or pleural effusion is associated with both good and bad prognosis in different cancers [151]. Regarding MPM, cases associated with PBE and EPE have been reported. Indeed, two independent cases of patients with EPE, with eosinophils representing 47-49% of the cells, who showed no response to treatment and a particularly fast deterioration were reported [188,215]. However, the involvement of eosinophils in MPM prognosis and/or response to treatment has not yet been studied.

In this context, this thesis aims at studying and understanding (1) the link between eosinophils and patients' survival and response to chemotherapy, (2) the mechanisms involved in the inhibition of MPM response to chemotherapy driven by eosinophils.

1.1. Eosinophils can be pro- and antitumorigenic in the tumour microenvironment

Eosinophils pleiotropy and heterogeneity (*see Chapter 12.3.1*) can explain the seemingly conflicting reports on eosinophils' role in different cancer prognosis (**Table 4**). Indeed, a tissue-based classification of eosinophils has been suggested and the distinction between E1 and E2 eosinophils, based on the balance between T_H1 and T_H2 cytokine expression pattern, has emerged [132,216]. Alternatively, the notion that eosinophils might undergo phenotypic changes according to their TME has also been conveyed [178,200]. According to this classification in mice, E1 eosinophils exhibit $CD101^{low}$, CD62L, $Siglec\text{-}F^{med}$ expression whereas E2 eosinophils are characterized by high expression of Siglec-F and CD101, acquisition of CD11c expression and lack of CD62L [132]. This extreme classification is following the M1/M2 and T_H1/T_H2 paradigm. However, transcriptomic analysis of macrophages demonstrated that macrophages polarization is following a continuous spectrum of activation rather than

the dichotomous M1/M2 model [38]. The reality of eosinophils activation and shaping in the TME might be more complex than E1/E2 and is likely dependent on the TME that they infiltrate.

This merits attention as eosinophils' phenotypic and transcriptomic changes in response to the cancer type could help predict their functions in the TME. In fact, gene expression analysis of primary intratumoral eosinophils in colorectal cancer revealed distinct transcriptome signatures [217]. This study supports the premise that eosinophils' role in the TME is tissue- and context-dependent. Bulk and single-cell RNA sequencing, as well as proteomics, should be exploited to identify tumour-infiltrating eosinophils sub-populations. However, this approach might face challenges as the isolation of eosinophil RNA is complex due to the presence of high potent RNAses in their granules. Thereby, at least partly due to this reason, eosinophils are absent from the majority of transcriptome profiling databases (*e.g.*, the cancer Genome Atlas) and from single-cell sequencing studies [169]. Despite these obstacles, eosinophil polarization in different TME should be further investigated.

1.2. Peripheral blood eosinophil count prior therapy correlates with MPM response to therapy and shorter survival in patients

The retrospective analysis of 230 patients' data highlighted that patients with an AEC $\geq$ 220/µL prior to chemotherapy administration have a worse outcome and relapse more rapidly [199]. As this analysis highlighted that in one centre (Liège CHU), there was no correlation, the study should be extended to other centres to assess if the conclusions can be drawn broadly. Furthermore, due to the retrospective nature of this study, information was often lacking and thus patients had to be excluded. A prospective study could be considered to address the limitations of a retrospective study and, more importantly, to confirm our observations.

Of note, in this study, patients that presented asthma, active parasitic infection or allergy, autoimmune disease and ongoing medication were excluded because those are factors that affect eosinophils blood levels. This phenomenon is beyond the scope of this thesis but merits further attention. Indeed, epidemiological studies and meta-analysis have highlighted a link between allergy and oncology [178,218]. For example, in a study, glioma, pancreatic cancer and paediatric cancer were inversely correlated with asthma whereas lung cancer was positively associated [219]. Moreover, a prospective study, based on family history of allergy highlighted an inverse correlation between colorectal cancer and allergic diseases [220]. As eosinophils are prominent features of asthma, allergy, and atopy, they likely play a role in the outcome of this subset of patients as they can exert pro- or antitumoral properties and shape the TME. This question clearly deserves further investigation.

1.3. Eosinophils do not infiltrate MPM tumours and remain in the peripheral blood or pleural fluid

Besides the study of blood eosinophils, we tried to investigate the presence of eosinophils in MPM tumour biopsies. Immunohistological hematoxylin & eosin staining was used to phenotypically identify eosinophils, in parallel of CCR3 labelling. This revealed the presence of eosin and CCR3 positive cells in some biopsies, likely highlighting the presence of eosinophils (**Appendix 1**). However, this was a rare phenomenon as only two biopsies stained positive for both eosin and CCR3. Other tumours were CCR3 positive, but the labelling did not colocalize with eosin. Considering that CCR3 can be expressed by other cells, the combination of CCR3, IL-5Rα and Siglec-8 is commonly used to identify eosinophils with certainty [92,169]. This triple-labelling should be considered for further investigations. However, eosinophils may degranulate in the TME and thus not stain for eosin, CCR3, IL-5Rα and Siglec-8. To accurately identify eosinophils infiltration and activation in the TME, staining of eosinophil-specific granule proteins is recommended. However, no standardized immunohistochemical staining technique is currently available [169]. Therefore, it cannot be determined with certainty whether eosinophil cells or associated factors are present in MPM biopsies.

If the absence of eosinophils within tumour is confirmed, which seems likely in the absence of eosin staining, it would suggest that eosinophils remain predominantly in the bone marrow, the peripheral blood and in the pleural fluid, influencing tumour response through paracrine (microenvironment) and/or exocrine (macroenvironment) mechanisms.

2. Eosinophils associated factors inhibit MPM response to chemotherapy

In addition to patients' data analysis, *in vitro* and mice experiments provided a biological mechanism revealing that eosinophils inhibit MPM response to chemotherapy (**Figure 15** and **Figure 19**). As we could not prove the presence of eosinophils in MPM tumours and considering that eosinophils associated factors have been identified in pleural fluids of asbestos exposed patients [167,185,186], we hypothesized that eosinophils factors mediated MPM sensitivity to chemotherapy.

First, given that IL-5 is a potent cytokine strongly associated with eosinophils, we investigated its role in MPM chemoresistance. We used different concentrations of IL-5 which reflected physiological conditions. However, there was no correlation between any of the tested concentrations and MPM cell apoptosis (**Supplementary Figure 8**). This does not completely exclude a role of IL-5 in MPM chemoresistance but indicates that IL-5 does not directly interacts with MPM cells. In concordance with these observations, Stathopoulos *et al.* showed that IL-5 does not interact with tumour cells but rather acts on the pleural microenvironment [187]. Preliminary data obtained in the lab further support a role of eosinophil factors in shaping the TME, specifically macrophages (Halkin L., *et al*). As macrophages are essential mediators of MPM tumor growth and are the predominant infiltrating cells in the TME [32,36], IL-5 could also play an indirect role through macrophages. Of note, in addition to IL-5, eosinophils also secrete IL-4 and IL-13 that drive macrophage polarization towards the M2 phenotype [26,104,135].

Following the results with IL-5, we then assessed the role of eosinophil proteins in MPM chemoresistance. As CLC-P/Gal10 is an abundant eosinophil protein (7-10% of the total eosinophil protein content) [118,119], we investigated its role. The results are discussed in the next paragraphs.

2.1. Roles of galectins in MPM

Galectins are a family of lectins that all contain conserved carbohydrate-recognition domains (CRDs) [221]. In mammals, 16 galectins have been identified, but only 12 of them have been found in humans. They are classified into three subfamilies according to their structure: the prototypical galectins (including Gal-1, -2, -7, -10, -13, -14 and -16) have a single CRD and form noncovalent homodimers; the tandem-repeat type galectins (including Gal-4, -8, -9 and -12) contain two homologous CRDs that covalently interact through a linker peptide; the chimera-type (Gal-3) contain a single CRD connected to a N-terminal sequence involved in their self-oligomerization [221,222]. Galectins can bind to a number of ligands and thus, exert a plethora of biological functions including cell proliferation, migration, adhesion, regulation of cell death and intracellular signal transduction [223,224].

Besides their functions under homeostatic conditions, galectins have been reported to contribute to many cancers by regulating tumorigenesis, metastasis, cell death resistance, evasion of immune surveillance and angiogenesis by interacting with glycosylated receptors [222–225]. Importantly, galectins exert various functions in tumours and regulate tumours through different mechanisms [226]. For example, Gal1 and Gal3 have been shown to confer drug resistance by enhancing the efflux of cytotoxic drugs [227]. However, most studies have been focused on Gal1 and Gal3 and on more importantly on their intrinsic expression by cancer cells, with recent emergence of studies on Gal7 and Gal9 [225]. Accordingly, a study has demonstrated that human MPM tumours express high levels of Gal9 and that targeting Gal9 increase apoptosis and M2 depletion [228]. Furthermore, two other studies have found that Gal1 and Gal3 are less expressed in MPM pleural fluids compared to other cancers [229,230]. Finally, Mundt *et al.* highlighted that high levels of Gal1 in MPM pleural fluids correlated with lower OS, which was consistent with its documented roles.

Here, we have highlighted a role for a galectin produced by eosinophils: CLC-P/Gal10. Indeed, we showed that extracellular CLC-P/Gal10 inhibited mesothelioma response to cisplatin and pemetrexed chemotherapy (**Figure 17**). In contrast to other galectins, CLC-P/Gal10 and its role in cancer has been less extensively studied.

2.1.1. As a phospholipase, CLC-P/Gal10 can lead to lipid droplets formation

Before its sequencing that showed sequence characteristics of galectins, CLC-P/Gal10 has long been considered as a lysophospholipase (LPLase). Indeed, CLC-P/Gal10 has moderate sequence similarity and near structural identity to members of the galectin family, but no sequence similarities to any known LPLase [125]. Hence, it has been designated galectin-10. However, since then, conflicting reports have emerged on its role as a LPLase [121,125]. Indeed, Ackerman *et al.* have suggested that CLC-P/Gal10 does not have a LPLase activity but rather binds to a LPLase inhibitor. Following their publication, Weller *et al.* have re-evaluated CLC/Gal10 as a LPLase and have highlighted further evidence that CLC-P/Gal10 might, indeed, exert LPLase activities. Independently of the mechanism, LPLase activity is increased in presence of CLC-P/Gal10.

LPLase activity is involved in lipid droplets production. Indeed, CLC/Gal10 hydrolyses the ester link of glycerophospholipids, releasing an esterified fatty acid and a lysophospholipid as Weller *et al.* suggested with the hydrolysation of lysopalmitoyl into palmitate and glycerophosphorylcholine [121]. This could lead to an increase in the extracellular fatty acid pool available for cancer cells. As most cells prefer extracellular lipid for the formation of new structural lipids, this mechanism could lead to the accumulation of lipids in the lens of the bilayer membrane, which in turn would lead to the formation of lipid droplets [231].

Furthermore, CLC-P/Gal10 can also be internalized in MPM cells. Once inside the cell, CLC-P/Gal10 could also act as a LPLase and take part in the Land cycle that regulates lipid droplet size [232]. In the Land cycle, the phospholipase A2 removes the fatty acid from phosphatidylcholine to form lysophosphatidylcholine. This reaction is reversible, and the formation of phosphatidylcholine is mediated by lysophosphatidylcholine acyltransferases [232]. In this context, CLC/GAL10 would have a similar activity to the phospholipase A2 and thus would promote the formation of lysophosphatidylcholine at the expense of phosphatidylcholine. Interestingly, inhibition of phosphatidylcholine production is linked to larger lipid droplets [232,233].

Importantly, lipid droplets accumulation provides lipid content and energy that can regulate cancer cell proliferation, migration, infiltration, stress resistance and apoptosis [231,234]. Besides regulating cancer aggressiveness and apoptosis, lipid droplets are associated with chemoresistance in some cancers. Indeed, in colorectal cancer, lipid droplets accumulation protects cancer cells from oxaloplatine-induced cell death by impairing the caspase cascade activation and inhibiting intrinsic and extrinsic endoplasmic reticulum (ER) stress-mediated apoptosis [235]. The accumulation of lipid droplets by the action of CLC-P/Gal10 might thus protect MPM cells from cisplatin-induced apoptosis.

Besides the reduction of MPM cell apoptosis in presence of CLC-P/Gal10, evidence supporting this hypothesis is the use of N-ethylmaleimide (NEA) to pharmacologically inhibit CLC-P/Gal10 in differentiated EOL1 supernatant (**Figure 17E**). In this experiment, when Dif-EOL1 supernatant was pretreated with NEA, M14K response to cisplatin and pemetrexed was almost completely restored. Given that NEA has been reported to be an inhibitor of the lysophospholipase activity of CLC-P/Gal10 [236], it could inhibit lipid droplet formation in MPM cells and indirectly resistance to chemotherapy. This hypothesis merits further investigation to confirm the implication of CLC-P/Gal10 in lipid droplets formation. To this aim, the status of CLC-P/Gal10 as a LPLase or as an inhibitor of LPLase inhibitor should be confirmed. Then, the lipid droplets formation as well as their size and volume should be quantified in the presence of eosinophil supernatant and/or CLC-P/Gal10.

2.1.2. CLC-P/Gal10 protects MPM cells by inducing senescence

Administration of chemotherapy induces DNA lesions that initiate a signal cascade, the DNA damage response (DDR) [50,73]. The DDR can lead either to a repair of the lesion or to apoptosis or to senescence. Senescence can be induced by DNA damage, oncogenic signalling and oxidative stress [237]. Considering that a hallmark of MPM is oxidative stress, it is not surprising that mesothelioma cultures derived from patients biopsies show basal senescence [238]. Notwithstanding, cisplatin and pemetrexed are able to induce senescence in several tumours, including MPM [238–241]. However, increased expression of senescence markers in MPM patients after chemotherapy administration is linked with lack of response and worse prognosis [239]. Consistently, there is a link between the basal senescence by MPM cells and chemoresistance [238].

In this thesis, we show that cisplatin and pemetrexed induce senescence-associated β-galactosidase (SA-β-gal) activity (**Supplementary Figure 6**). Furthermore, SA-β-gal activity staining revealed that Dif-EOL1 and primary eosinophils supernatant both increase treated MPM cells senescence. Pharmacological inhibition of CLC-P/Gal10 in eosinophil supernatant with NEA reversed this phenotype and reduced SA-β-gal activity. On the other hand, addition of recombinant human Gal10 in MPM culture increases senescence after treatment. This indicates that eosinophils and eosinophil-derived Gal10 may induce MPM cell chemoresistance by promoting senescence instead of apoptosis. Moreover, the GO analysis of biological process (GO:BP) is consistent with those observations as cell-cycle related genes were also affected by Dif-EOL1 supernatant (**Appendix 4** and **Appendix 5**).

Indeed, senescence is a cellular state in which cells undergo cell cycle arrest but remain viable and metabolically active [240,242]. As it stops tumour proliferation and development, this mechanism may appear as a favourable process for patients' outcome. However, tumours characterized by senescence stop growing but do not regress. Furthermore, senescence eventually leads to therapy resistance and/or aggressive relapse [237,242]. Indeed, senescent cancer cell subpopulations have been shown to escape the senescence state and relapse [243,244]. Those cells that exit chemotherapy-induced senescence by bypassing cell cycle arrest can actually boost tumour growth [245]. In addition to this unwanted side effect, a senescence-associated secretory phenotype (SASP) can develop. SASP correlates with an altered secretome composed of autocrine and paracrine growth as well as invasion-inducing signaling molecules [241,242]. This SASP has been shown to promote inflammation, tissue invasion, enhanced metastasis and therapy resistance [242]. Accordingly, SASP markers should be investigated in the context of eosinophil supernatant and CLC-P/Gal10 in MPM chemoresistance. However, SASP is cell type dependent and no truly specific marker has been identified thus far [242]. Indeed, SASP growth factors (*e.g.*, VEGF, TGF-β), matrix metalloproteinases (*e.g.*, MMP3, MMP9), interleukins (*e.g.*, IL-1α, IL-6, IL-8), cytokines and chemokines (*e.g.*, CCL2) [242,246] are also involved in many other pathways. However, other tools to identify SASP are in development. Indeed, Basisty *et al.* have developed the "SASP Atlas" which is a comprehensive proteomic database for soluble SASP-proteins and SASP factors contained in exosomal cargo [247]. This resource highlights the diversity of SASP factors and their specificity according to stressor (*e.g.*, genotoxic stress, oncogene, treatment) and cell type (*e.g.*, fibroblasts *vs* epithelial cells). This offers the possibility of identifying SASP biomarkers specific to cancers and, thus, their involvement in cancer progression and chemoresistance [247].

In addition, as tumour cells bypassing cell cycle arrest have been shown to promote tumour progression [248], this mechanism should also be further investigated. This could be especially important for non-epithelioid MPM cells as we showed that chemotherapeutic treatment of non-epithelioid ZL34 primarily induces cell cycle arrest in S phase (**Supplementary Figure 2**) rather than the DNA fragmentation observed in epithelioid M14K cells (**Figure 15I**). In presence of Dif-EOL1

supernatant, the percentage of cells blocked in S phase is reduced. This might reflect cells that bypassed the cell cycle arrest induced by senescence.

Finally, senescence might not necessarily be a completely distinct mechanism from lipid droplets. Indeed, Flor *et al.* have showed that, in senescent cells, lipid regulatory proteins including proteins related to lipid droplets and phospholipases are upregulated [249].

2.1.3. CLC-P/Gal10 may mediate MPM autophagy

In addition to the increased senescence observed in chemoresistant MPM primary cells, Oehl *et al.* have also observed an increase of the autophagy markers LC3B and p62 in these cells [238]. This observation is not surprising given that autophagy and senescence exert overlapping and complementary functions in cancer progression and response to therapy [250]. Autophagy (or "macroautophagy") is a process by which cells restore their energy balance through the digestion of proteins, organelles and cytoplasmic components [251]. Autophagy regulates tumorigenesis, tumour metastasis, invasion and proliferation, and can modulate drug resistance [226,251]. Indeed, autophagy can be induced in response to chemotherapy and can protect cancer cells by blocking apoptosis through the existing crosstalk between autophagy and apoptosis pathways [250]. Moreover, pharmacological or genetic suppression of autophagy enhances cancer cells chemo-sensitivity [250]. This is the case for mesothelioma.

Indeed, it was demonstrated that the inhibition or silencing of autophagy increases cleaved PARP, caspase-3, -8 and -9 and decreases the autophagy marker LC3 in MPM cells treated with pemetrexed [252]. The role of autophagy in protecting MPM cells from pemetrexed was thus highlighted. In addition to this study, Follo *et al.* showed that in 3D multicellular and *ex vivo* MPM spheroids, the inhibition of autophagy potentiates caspase-3/-7 chemosensitivity [253]. The same team has also identified a protein, ATG13, as an autophagy marker that correlates with the autophagic flux in those spheroids [254]. This protein furthermore positively correlates with patients' outcome in MPM [254].

In addition to this evidence, galectin regulated pathways have been shown to be associated with autophagy [226]. Indeed Gal1 and Gal3 both enhance cancer cell survival by increasing autophagy and decreasing apoptosis [224]. In this light, considering the senescence results obtained and the interplay between senescence and autophagy, the role of CLC-P/Gal10 in autophagy induction should be assessed.

2.2. Galectin-10 may not be the only factor influencing MPM response to chemotherapy

Notwithstanding evidence that CLC-P/Gal10 is involved in MPM chemoresistance, this hypothetic model has some limitations. Indeed, despite the high similarities between human and mouse eosinophils, the latter do not express CLC-P/Gal10 [255]. However, Ym1 crystals, also called pseudo-CLCs, have been identified in mice [124,256]. It is not clear whether Ym1 exert the exact same effects of CLC-P/Gal10. Nonetheless, we showed that peripheral blood eosinophilia in mice also inhibits tumor response to chemotherapy (**Figure 19C**). This indicates that other eosinophilic factors are likely involved in MPM chemoresistance. Moreover, when looking closer at the senescence results, recombinant Gal10 alone was not sufficient to induce the same level of senescence as primary eosinophil supernatant (**Supplementary Figure 6D**). This does not invalidate the conclusion but indicates that other eosinophil factors may be involved in MPM resistance to chemotherapy.

2.2.1. Eosinophils extracellular traps

Considering that CLC-P/Gal10 does not have a secretory sequence, it is not a typical secreted protein [121]. It has been shown, however, that CLC-P is associated with EETosis (*see Chapter 12.2.4*) [124,127]. Dosage of double stranded DNA in Dif-EOL1 supernatant revealed that eosinophil DNA was indeed released in the extracellular milieu (

Appendix 2), indicating possible EETosis. Furthermore, confocal analysis of a co-culture between eosinophils and MPM cells highlighted the formation of EETs towards M14K cells (**Figure 17B**). This evidence seems to indicate that EETs might indeed play a role in mesothelioma. The first hypothesis would be that, as cisplatin is a DNA-binding drug, it would bind to EETs rather than MPM cells DNA thus protecting MPM cells from DNA damage. However, our data indicate that eosinophils factors interact with MPM cells rather than with cisplatin and/or pemetrexed. Indeed, an experiment consisting in adding supernatant and chemotherapy in the culture at the same time revealed that this timing did not protect MPM cells from the drugs (**Supplementary Figure 3**). If cisplatin would bind directly to EETs, the timing would not have influenced the results. Furthermore, RNA-sequencing of MPM cells also revealed many transcriptomic changes in presence of Dif-EOL1 supernatant (**Figure 16**). Of note, unsupervised GO analysis of the non-epithelioid ZL34 MPM cells highlighted the GO terms nucleotide binding (GO:0000166) and DNA binding (GO:0003677), perhaps also highlighting other mechanisms.

Several studies have shown that extracellular DNA levels are elevated in the serum of many cancer patients, especially when they have an invasive metastatic cancer [257]. Furthermore, a study conducted by Leon *et al.* highlighted that the reduction of extracellular DNA levels after radiotherapy could significantly improve patients'

clinical condition [258]. More recently, eosinophils and EETs were detected Hodgkin's lymphoma patients' cancer tissues [259]. This suggests a uncovered role of EETs in cancer. Therefore, the involvement of EETs in cancer deserves further investigation.

Given that neutrophil extracellular traps (NETs) can interact with several TLRs including TLR9 [260], EETs could also interact with it. The recognition of those EETs could, in turn, activate the cGAS-STING pathway. When cGAS recognizes double stranded DNA, it activates a cascade involving several proteins (*i.e.,* STING, TBK1 and IRF3) [261]. Ultimately, this process can induce nuclear factor-κB (NF-κB) dependent autophagy or senescence, further supporting previous evidence as well as the role of CLC-P/GAL10 in both these mechanisms.

2.2.2. Eosinophils granule proteins: opposing roles in different cancers?

Besides CLC-P/Gal10 eosinophils also contain other proteins: MBP, EPX, ECP and EDN. However, these proteins exert potent cytotoxic activities and rather mediate tissue damage [151,167]. Indeed, MBP is cytotoxic to mammalian cells by disrupting the integrity of membranes while EPX promotes oxidative stress via ROS and NOS, leading to cell death [167]. In colorectal cancer, co-culture with eosinophils leads to the release of ECP, EDN, granzyme A and TNF-α that kill cancer cells *in vitro* [262]. This is in accordance with the antitumorigenic role of eosinophils in colorectal cancer. However, co-culture of differentiated EOL1 and MPM cells showed opposite results as differentiated-EOL1 also induced MPM chemoresistance (**Appendix 3**). Considering that peripheral blood eosinophils are correlated with better prognosis in colorectal cancer whereas they are correlated with worse prognosis in MPM, it is not surprising to find different results *in vitro* for MPM compared to colorectal cancer.

In this light, maybe the role of eosinophil cationic proteins should be assessed in the context of MPM.

3. What about immunotherapy?

During this thesis, the focus has been given to chemotherapy as it was the only standard treatment for unresectable MPM at the time. However, in 2021 the FDA approved the combination of the immune checkpoint inhibitors (ICIs) nivolumab (anti-PD1) and ipilimumab (anti-CTLA4) as first-line treatment for unresectable MPM [4]. Even if this combination has been incorporated into guidelines, chemotherapy is still widely used. Indeed, the CheckMate 743 showed that, in the epithelioid subtype, immunotherapy did not significantly improve patients outcome compared to chemotherapy [60]. Furthermore, immune checkpoint immunotherapy induces undesired side effects. In this light, the general practice in France and United States is to still treat MPM patients with epithelioid subtype with cisplatin (or carboplatin) and pemetrexed.

Nonetheless, since the publication of the CheckMate 743, focus has been given to immunotherapy and other combinations are being evaluated for MPM. In addition, the administration of chemotherapy and immunotherapy is also being studied in phase II and phase III trials [263]. Considering my data, I think that the involvement of eosinophils in MPM response to ICIs should be investigated. Of note, two independent studies highlighted that an increase in AEC was associated with better response to ICIs, and that this effect was more significant when the increase occurred during ICIs treatment [264,265]. Regarding MPM, Yamazoe *et al.* reported a case where a patient with sarcomatoid MPM presenting PBE responded to nivolumab [266]. It should be noted that this patient did not only present high AEC but also an elevation of all white blood cell types. The involvement of eosinophils in MPM response to ICI treatment should therefore be assessed before and during ICI treatment.

In our retrospective study, only 4 patients received ICIs in first line. The reason is that the use of nivolumab and ipilimumab in MPM was not yet approved when the study was initiated (2019). Furthermore, information on patients' survival and response was lacking when the study was finalized. More hindsight should become increasingly available. To strengthen the conclusions, a prospective study involving different hospitals should be considered.

Besides eosinophils, the role of CLC-P/Gal10 in ICI response should also be investigated. Indeed, other galectins can shape the TME and the response to immunotherapy [227,267]. Gal-1, -3 and -9 have been shown to regulate the balance of T_H1/T_H2 cells in the TME [267,268]. Gal1 has been shown to promote the T_H2 response or expansion of Tregs [227]. Moreover, Gal1 inhibition is correlated with enhanced antitumor activity [227,269]. Regarding CLC-P/Gal10, Persson *et al.* showed that it promotes T_H2 immunity and T cell suppression [119,124]. By analogy with Gal1, even if the homology is very limited, this would suggest that using monoclonal antibodies targeting CLC-P/Gal10, or more broadly eosinophils, could improve immunotherapy.

4. Targeting eosinophils in MPM therapy

Interestingly, our mice experiment revealed that the resolution of eosinophilia with a monoclonal antibody targeting Siglec-F restored tumour response to cisplatin and pemetrexed (**Figure 19E**). For human, an anti-siglec-8 antibody (lirentelimab) has been developed to treat eosinophil-mediated diseases but not yet in cancer. Other monoclonal antibodies reducing eosinophil levels have been developed for the treatment of asthma (*see Chapter 12.3.5*). Antibodies targeting IL-5 (mepolizumab and reslizumab), IL-5Rα (benralizumab) and IL-4/IL-13 (dupilumab) significantly decrease eosinophil levels and asthma exacerbation [156]. Among those, mepolizumab, reslizumab and benralizumab did not exert any safety risk for the patient and are thus approved [270]. However, benralizumab is only advised for severe eosinophilic conditions [270]. As our study did not reveal a group with acute hypereosinophilia, only mepolizumab and/or reslizumab seem to be adequate for MPM patients.

Alternatively, glucocorticoids have also been assessed to reduce blood eosinophil levels. Indeed, glucocorticoids are immunosuppressors, exert anti-inflammatory effects and increase eosinophils apoptosis [271]. In the CHU cohort in Lille, patients systematically received glucocorticoid (*i.e.*, methylprednisolone) before treatment to prevent pemetrexed-associated rash, emesis and inflammatory side effects, according to recommendations [272–274]. We did not observe any change in myeloid subsets during glucocorticoid administration. This finding is in accordance with the study of Aston *et al.,* who found that, besides neutrophils, the administration of glucocorticoids did not impact the proportions of myeloid subsets neither in the peripheral blood nor in mesothelioma tumors [275]. Glucocorticoids do not seem to be a good alternative to mepolizumab and/or reslizumab for MPM patients. These two monoclonal antibodies should be evaluated in an interventional study to assess whether their administration increases response rates of MPM patients.

My results indicate that clinical management should determine eosinophil counts in the peripheral blood prior to treatment administration. This approach is easy to implement as it only requires a blood draw, which is less invasive and presents lower risks than pleural fluid and tumour biopsies. A prospective study would require a careful data management of blood counts obtained during routine clinical practice. This analysis would thus validate the conclusions that we recently reported in Frontiers in Immunology. If confirmed, an interventional study may investigate the ability of an anti-eosinophilic treatment to improve patient's outcome and/or relapse. Thanks to the clinical practice of asthma, the dosing, timing and side effects of mepolizumab and reslizumab are known. Since the half-life of the mepolizumab and reslizumab are 20-35 and 24 days respectively [276,277], a single dose of 100 mg mepolizumab or 3 mg/kg of reslizumab at one month before chemotherapy is predicted to be the optimal to improve MPM patients' response.

5. Conclusion

In conclusion, this thesis highlighted an adverse effect of peripheral blood eosinophils counts in therapeutic response and patients' survival. The inhibitory mechanism is mediated at least in part by the Charcot-Leyden crystal protein/Galectin-10. Preclinical mouse models validate this conclusion and open new prospects of therapeutic intervention.

Chapter 5

List of Publications and Communications

1. Publications in scientific journals as first (co)-author:

- **First authorship:**

Willems M., *et al*: Excess of blood eosinophils prior to therapy correlates with worse prognosis in mesothelioma (2023) *Front. Immunol.*, **14**: 1148798. doi: 10.3389/fimmu.2023.1148798

Brossel H.*,,Willems M.*, *et al*: Activation of DNA damage tolerance pathways may improve immunotherapy of mesothelioma (2021) *Cancers* **13**: 3211. doi:10.3390/cancers13133211

2. Oral communications and posters

- **Oral presentations:**

'Influence des éosinophiles sur la réponse des cellules de mésothéliome pleural malin à la chimiothérapie' at the International Congress "2èmes journées francophones sur le mésothéliome", Nantes, France (2019).

'Eosinophils inhibit response to chemotherapy: mechanisms and preclinical study in mesothelioma' at GIGA-Cancer seminars, Liège, Belgium (2021).

'Eosinophils inhibit response to chemotherapy: mechanisms and preclinical study in mesothelioma' at GIGA-Cancer seminars, Liège, Belgium (2023).

'Eosinophils inhibit response to chemotherapy: mechanisms and preclinical study in mesothelioma' at International Mesothelioma Interest Group (IMIG), Lille, France (2023).

- **Posters:**

'Influence des éosinophiles sur la réponse des cellules de mésothéliome pleural malin à la chimiothérapie' at the GIGA-Cancer day, Liège, Belgique (2022).

Chapter 6

Bibliography

1. Chen SE, Pace MB. Malignant pleural mesothelioma. *Am J Heal Pharm*. 2012;69(5):377-385. doi:10.2146/ajhp110281
2. Yap TA, Aerts JG, Popat S, Fennell DA. Novel insights into mesothelioma biology and implications for therapy. *Nat Rev*. 2017;17(8):475-488. doi:10.1038/nrc.2017.42
3. Janes SM, Alrifai D, Fennell DA. Perspectives on the Treatment of Malignant Pleural Mesothelioma. Longo DL, ed. *N Engl J Med*. 2021;385(13):1207-1218. doi:10.1056/NEJMra1912719
4. Popat S, Baas P, Faivre-Finn C, et al. Malignant pleural mesothelioma: ESMO Clinical Practice Guidelines for diagnosis, treatment and follow-up. *Ann Oncol*. 2022;33(2):129-142. doi:10.1016/j.annonc.2021.11.005
5. Alì G, Bruno R, Fontanini G. The pathological and molecular diagnosis of malignant pleural mesothelioma: a literature review. *J Thorac Dis*. 2018;10(Suppl 2):S276-S284. doi:10.21037/jtd.2017.10.125
6. Robinson BW, Musk AW, Lake RA. Malignant mesothelioma. *Lancet*. 2005;366(9483):397-408. doi:10.1016/S0140-6736(05)67025-0
7. Verma V, Ahern CA, Berlind CG, et al. Survival by Histologic Subtype of Malignant Pleural Mesothelioma and the Impact of Surgical Resection on Overall Survival. *Clin Lung Cancer*. 2018;19(6):e901-e912. doi:10.1016/j.cllc.2018.08.007
8. Linton A, Vardy J, Clarke S, van Zandwijk N. The ticking time-bomb of asbestos: Its insidious role in the development of malignant mesothelioma. *Crit Rev Oncol Hematol*. 2012;84(2):200-212. doi:10.1016/j.critrevonc.2012.03.001
9. Gaudino G, Xue J, Yang H. How asbestos and other fibers cause mesothelioma. *Transl Lung Cancer Res*. 2020;9(S1):S39-S46. doi:10.21037/tlcr.2020.02.01
10. Røe OD, Stella GM. Malignant pleural mesothelioma: history, controversy and future of a manmade epidemic. *Eur Respir Rev*. 2015;24(135):115-131. doi:10.1183/09059180.00007014
11. Wagner JC, Sleggs CA, Marchand P. Diffuse Pleural Mesothelioma and Asbestos Exposure in the North Western Cape Province. *Occup Environ Med*. 1960;17(4):260-271. doi:10.1136/oem.17.4.260
12. Asciak R, George V, Rahman NM. Update on biology and management of mesothelioma. *Eur Respir Rev*. 2021;30(159):200226. doi:10.1183/16000617.0226-2020
13. Alpert N, Gerwen M van, Taioli E. Epidemiology of mesothelioma in the 21st century in Europe and the United States, 40 years after restricted/banned asbestos use. *Transl Lung Cancer Res*. 2020;9(S1):S28-S38. doi:10.21037/tlcr.2019.11.11
14. Pira E, Godono A, Ciocan C. Novel issues in the epidemiology of asbestos-related diseases. *Curr Opin Epidemiol Public Heal*. 2022;1(1):4-10. doi:10.1097/PXH.0000000000000002

15. Schillebeeckx E, van Meerbeeck JP, Lamote K. Clinical utility of diagnostic biomarkers in malignant pleural mesothelioma: a systematic review and meta-analysis. *Eur Respir Rev*. 2021;30(162):210057. doi:10.1183/16000617.0057-2021
16. Andujar P, Lacourt A, Brochard P, Pairon J-C, Jaurand M-C, Jean D. Five years update on relationships between malignant pleural mesothelioma and exposure to asbestos and other elongated mineral particles. *J Toxicol Environ Heal Part B*. 2016;19(5-6):151-172. doi:10.1080/10937404.2016.1193361
17. Frank AL. Global use of asbestos - legitimate and illegitimate issues. *J Occup Med Toxicol*. 2020;15(1):16. doi:10.1186/s12995-020-00267-y
18. Carbone M, Ly BH, Dodson RF, et al. Malignant mesothelioma: Facts, Myths, and Hypotheses. *J Cell Physiol*. 2012;227(1):44-58. doi:10.1002/jcp.22724
19. Jasani B, Gibbs A. Mesothelioma Not Associated With Asbestos Exposure. *Arch Pathol Lab Med*. 2012;136(3):262-267. doi:10.5858/arpa.2011-0039-RA
20. Carbone M, Emri S, Dogan AU, et al. A mesothelioma epidemic in Cappadocia: Scientific developments and unexpected social outcomes. *Nat Rev Cancer*. 2007;7(2):147-154. doi:10.1038/nrc2068
21. Carbone M, Baris YI, Bertino P, et al. Erionite exposure in North Dakota and Turkish villages with mesothelioma. *Proc Natl Acad Sci*. 2011;108(33):13618-13623. doi:10.1073/pnas.1105887108
22. Orsi M, Al Hatem C, Leinardi R, Huaux F. Carbon Nanotubes under Scrutiny: Their Toxicity and Utility in Mesothelioma Research. *Appl Sci*. 2020;10(13):4513. doi:10.3390/app10134513
23. Visci G, Rizzello E, Zunarelli C, Violante FS, Boffetta P. Relationship between exposure to ionizing radiation and mesothelioma risk: A systematic review of the scientific literature and meta-analysis. *Cancer Med*. 2022;11(3):778-789. doi:10.1002/cam4.4436
24. Toyokuni S. Iron overload as a major targetable pathogenesis of asbestos-induced mesothelial carcinogenesis. *Redox Rep*. 2014;19(1):1-7. doi:10.1179/1351000213Y.0000000075
25. Donaldson K, Murphy FA, Duffin R, Poland CA. Asbestos, carbon nanotubes and the pleural mesothelium: a review of the hypothesis regarding the role of long fibre retention in the parietal pleura, inflammation and mesothelioma. *Part Fibre Toxicol*. 2010;7(1):5. doi:10.1186/1743-8977-7-5
26. Hamaidia M, Staumont B, Duysinx B, Louis R, Willems L. Improvement of malignant pleural mesothelioma immunotherapy by epigenetic modulators. *Curr Top Med Chem*. 2016;16(7):777-787. doi:10.2174/1568026615666150825141152
27. Carbone M, Kratzke RA, Testa JR. The pathogenesis of mesothelioma. *Semin Oncol*. 2002;29(1):2-17. doi:10.1053/sonc.2002.30227
28. Robinson BWS, Lake RA. Advances in Malignant Mesothelioma. *N Engl J Med*. 2005;353(15):1591-1603. doi:10.1056/NEJMra050152

29. Hiriart E, Deepe R, Wessels A. Mesothelium and Malignant Mesothelioma. *J Dev Biol*. 2019;7(2):1-7. doi:10.3390/jdb7020007
30. Attanoos RL, Gibbs AR. Pathology of malignant mesothelioma. *Histopathology*. 1997;30(5):403-418. doi:10.1046/j.1365-2559.1997.5460776.x
31. Sanchez VC, Pietruska JR, Miselis NR, Hurt RH, Kane AB. Biopersistence and potential adverse health impacts of fibrous nanomaterials: what have we learned from asbestos? *Wiley Interdiscip Rev Nanomedicine Nanobiotechnology*. 2009;1(5):511-529. doi:10.1002/wnan.41
32. Minnema-Luiting J, Vroman H, Aerts J, Cornelissen R. Heterogeneity in Immune Cell Content in Malignant Pleural Mesothelioma. *Int J Mol Sci*. 2018;19(4):1041. doi:10.3390/ijms19041041
33. Chu GJ, van Zandwijk N, Rasko JEJ. The Immune Microenvironment in Mesothelioma: Mechanisms of Resistance to Immunotherapy. *Front Oncol*. 2019;9:1366. doi:10.3389/fonc.2019.01366
34. Cersosimo F, Barbarino M, Lonardi S, et al. Mesothelioma Malignancy and the Microenvironment: Molecular Mechanisms. *Cancers (Basel)*. 2021;13(22):5664. doi:10.3390/cancers13225664
35. Mossman BT, Shukla A, Heintz NH, Verschraegen CF, Thomas A, Hassan R. New Insights into Understanding the Mechanisms, Pathogenesis, and Management of Malignant Mesotheliomas. *Am J Pathol*. 2013;182(4):1065-1077. doi:10.1016/j.ajpath.2012.12.028
36. Hiltbrunner S, Mannarino L, Kirschner MB, et al. Tumor Immune Microenvironment and Genetic Alterations in Mesothelioma. *Front Oncol*. 2021;11:660039. doi:10.3389/fonc.2021.660039
37. Tedesco J, Jaradeh M, Vigneswaran WT. Malignant Pleural Mesothelioma: Current Understanding of the Immune Microenvironment and Treatments of a Rare Disease. *Cancers (Basel)*. 2022;14(18):4415. doi:10.3390/cancers14184415
38. Hamaidia M, Gazon H, Hoyos C, et al. Inhibition of EZH2 methyltransferase decreases immunoediting of mesothelioma cells by autologous macrophages through a PD-1–dependent mechanism. *JCI Insight*. 2019;4(18):e128474. doi:10.1172/jci.insight.128474
39. Murray PJ, Allen JE, Biswas SK, et al. Macrophage Activation and Polarization: Nomenclature and Experimental Guidelines. *Immunity*. 2014;41(1):14-20. doi:10.1016/j.immuni.2014.06.008
40. Salaroglio IC, Kopecka J, Napoli F, et al. Potential Diagnostic and Prognostic Role of Microenvironment in Malignant Pleural Mesothelioma. *J Thorac Oncol*. 2019;14(8):1458-1471. doi:10.1016/j.jtho.2019.03.029
41. Chéné A-L, D'Almeida S, Blondy T, et al. Pleural Effusions from Patients with Mesothelioma Induce Recruitment of Monocytes and Their Differentiation into M2 Macrophages. *J Thorac Oncol*. 2016;11(10):1765-1773. doi:10.1016/j.jtho.2016.06.022

42. Cornelissen R, Lievense LA, Maat AP, et al. Ratio of Intratumoral Macrophage Phenotypes Is a Prognostic Factor in Epithelioid Malignant Pleural Mesothelioma. Gangopadhyay N, ed. *PLoS One*. 2014;9(9):e106742. doi:10.1371/journal.pone.0106742
43. Lapidot M, Saladi SV, Salgia R, Sattler M. Novel Therapeutic Targets and Immune Dysfunction in Malignant Pleural Mesothelioma. *Front Pharmacol*. 2021;12(13):806570. doi:10.3389/fphar.2021.806570
44. Delves PJ, Martin SJ, Burton DR, Roitt IM. Specific Acquired Immunity. In: *Roitt's Essential Immunology*. 13th ed. Chichester: John Wiley & Sons, Inc.; 2017.
45. Wherry EJ. T cell exhaustion. *Nat Immunol*. 2011;12(6):492-499. doi:10.1038/ni.2035
46. Klampatsa A, O'Brien SM, Thompson JC, et al. Phenotypic and functional analysis of malignant mesothelioma tumor-infiltrating lymphocytes. *Oncoimmunology*. 2019;8(9):1-12. doi:10.1080/2162402X.2019.1638211
47. Marcq E, Waele J De, Audenaerde J Van, et al. Abundant expression of TIM-3, LAG-3, PD-1 and PD-L1 as immunotherapy checkpoint targets in effusions of mesothelioma patients. *Oncotarget*. 2017;8(52):89722-89735. doi:10.18632/oncotarget.21113
48. Harber J, Kamata T, Pritchard C, Fennell D. Matter of TIME: the tumor-immune microenvironment of mesothelioma and implications for checkpoint blockade efficacy. *J Immunother cancer*. 2021;9(9):e003032. doi:10.1136/jitc-2021-003032
49. Pardoll DM. The blockade of immune checkpoints in cancer immunotherapy. *Nat Rev Cancer*. 2012;12(4):252-264. doi:10.1038/nrc3239
50. Brossel H, Fontaine A, Hoyos C, et al. Activation of DNA Damage Tolerance Pathways May Improve Immunotherapy of Mesothelioma. *Cancers (Basel)*. 2021;13(13):3211. doi:10.3390/cancers13133211
51. Scherpereel A, Wallyn F, Albelda SM, Munck C. Novel therapies for malignant pleural mesothelioma. *Lancet Oncol*. 2018;19(3):e161-e172. doi:10.1016/S1470-2045(18)30100-1
52. Scherpereel A, Opitz I, Berghmans T, et al. ERS/ESTS/EACTS/ESTRO guidelines for the management of malignant pleural mesothelioma. *Eur Respir J*. 2020;55(6):1900953. doi:10.1183/13993003.00953-2019
53. Zhang WW, Wu X, Wu L, Zhang WW, Zhao X. Advances in the diagnosis, treatment and prognosis of malignant pleural mesothelioma. *Ann Transl Med*. 2015;3(13):182. doi:10.3978/j.issn.2305-5839.2015.07.03
54. Husain AN, Colby T, Ordonez N, et al. Guidelines for Pathologic Diagnosis of Malignant Mesothelioma: 2012 Update of the Consensus Statement from the International Mesothelioma Interest Group. *Arch Pathol Lab Med*. 2013;137(5):647-667. doi:10.5858/arpa.2012-0214-OA

55. Ordóñez NG. The diagnostic utility of immunohistochemistry in distinguishing between epithelioid mesotheliomas and squamous carcinomas of the lung: a comparative study. *Mod Pathol*. 2006;19(3):417-428. doi:10.1038/modpathol.3800544
56. Berzenji L, Van Schil PE, Carp L. The eighth TNM classification for malignant pleural mesothelioma. *Transl Lung Cancer Res*. 2018;7(5):543-549. doi:10.21037/tlcr.2018.07.05
57. Milano MT, Zhang H. Malignant Pleural Mesothelioma: A Population-Based Study of Survival. *J Thorac Oncol*. 2010;5(11):1841-1848. doi:10.1097/JTO.0b013e3181f1cf2b
58. Van Gerwen M, Alpert N, Wolf A, et al. Prognostic factors of survival in patients with malignant pleural mesothelioma: an analysis of the National Cancer Database. *Carcinogenesis*. 2019;40(4):529-536. doi:10.1093/carcin/bgz004
59. Brcic L, Kern I. Clinical significance of histologic subtyping of malignant pleural mesothelioma. *Transl Lung Cancer Res*. 2020;9(3):924-933. doi:10.21037/tlcr.2020.03.38
60. Baas P, Scherpereel A, Nowak AK, et al. First-line nivolumab plus ipilimumab in unresectable malignant pleural mesothelioma (CheckMate 743): a multicentre, randomised, open-label, phase 3 trial. *Lancet*. 2021;397(10272):375-386. doi:10.1016/S0140-6736(20)32714-8
61. Zalcman G, Mazieres J, Margery J, et al. Bevacizumab for newly diagnosed pleural mesothelioma in the Mesothelioma Avastin Cisplatin Pemetrexed Study (MAPS): a randomised, controlled, open-label, phase 3 trial. *Lancet*. 2016;387(10026):1405-1414. doi:10.1016/S0140-6736(15)01238-6
62. Davis A, Ke H, Kao S, Pavlakis N. An Update on Emerging Therapeutic Options for Malignant Pleural Mesothelioma. *Lung Cancer Targets Ther*. 2022;13:1-12. doi:10.2147/LCTT.S288535
63. Vogelzang NJ, Rusthoven JJ, Symanowski J, et al. Phase III Study of Pemetrexed in Combination With Cisplatin Versus Cisplatin Alone in Patients With Malignant Pleural Mesothelioma. *J Clin Oncol*. 2003;21(14):2636-2644. doi:10.1200/JCO.2003.11.136
64. Liang J, Lu T, Chen Z, Zhan C, Wang Q. Mechanisms of resistance to pemetrexed in non-small cell lung cancer. *Transl Lung Cancer Res*. 2019;8(6):1107-1118. doi:10.21037/tlcr.2019.10.14
65. Zucali PA, De Vincenzo F, Simonelli M, Lorenzi E, Perrino M, Santoro A. The Role of Pemetrexed in the Pharmacotherapy of Malignant Pleural Mesothelioma. *Clin Med Insights Ther*. 2010;2:CMT.S1166. doi:10.4137/CMT.S1166
66. Cinausero M, Rihawi K, Sperandi F, Melotti B, Ardizzoni A. Chemotherapy treatment in malignant pleural mesothelioma: a difficult history. *J Thorac Dis*. 2018;10(S2):S304-S310. doi:10.21037/jtd.2017.10.19

67. Cantini L, Hassan R, Sterman DH, Aerts JGJ V. Emerging Treatments for Malignant Pleural Mesothelioma: Where Are We Heading? *Front Oncol*. 2020;10:343. doi:10.3389/fonc.2020.00343
68. Siddik ZH. Cisplatin: mode of cytotoxic action and molecular basis of resistance. *Oncogene*. 2003;22(47):7265-7279. doi:10.1038/sj.onc.1206933
69. Rollins KD, Lindley C. Pemetrexed: A multitargeted antifolate. *Clin Ther*. 2005;27(9):1343-1382. doi:10.1016/j.clinthera.2005.09.010
70. Dasari S, Bernard Tchounwou P. Cisplatin in cancer therapy: Molecular mechanisms of action. *Eur J Pharmacol*. 2014;740:364-378. doi:10.1016/j.ejphar.2014.07.025
71. Ghosh S. Cisplatin: The first metal based anticancer drug. *Bioorg Chem*. 2019;88:102925. doi:10.1016/j.bioorg.2019.102925
72. Browning RJ, Reardon PJT, Parhizkar M, et al. Drug Delivery Strategies for Platinum-Based Chemotherapy. *ACS Nano*. 2017;11(9):8560-8578. doi:10.1021/acsnano.7b04092
73. Aldossary SA. Review on Pharmacology of Cisplatin: Clinical Use, Toxicity and Mechanism of Resistance of Cisplatin. *Biomed Pharmacol J*. 2019;12(1):07-15. doi:10.13005/bpj/1608
74. Amable L. Cisplatin resistance and opportunities for precision medicine. *Pharmacol Res*. 2016;106:27-36. doi:10.1016/j.phrs.2016.01.001
75. Ishida S, McCormick F, Smith-McCune K, Hanahan D. Enhancing Tumor-Specific Uptake of the Anticancer Drug Cisplatin with a Copper Chelator. *Cancer Cell*. 2010;17(6):574-583. doi:10.1016/j.ccr.2010.04.011
76. Chen S-J, Kuo C-C, Pan H-Y, Tsou T-C, Yeh S-C, Chang J-Y. Mechanistic basis of a combination d-penicillamine and platinum drugs synergistically inhibits tumor growth in oxaliplatin-resistant human cervical cancer cells in vitro and in vivo. *Biochem Pharmacol*. 2015;95(1):28-37. doi:10.1016/j.bcp.2015.03.006
77. Chen S, Kuo C, Pan H, Tsou T, Yeh S-C, Chang J. Desferal regulates hCtr1 and transferrin receptor expression through Sp1 and exhibits synergistic cytotoxicity with platinum drugs in oxaliplatin-resistant human cervical cancer cells in vitro and in vivo. *Oncotarget*. 2016;7(31):49310-49321. doi:10.18632/oncotarget.10336
78. Yang T, Chen M, Chen T, Thakur A. Expression of the copper transporters hCtr1, ATP7A and ATP7B is associated with the response to chemotherapy and survival time in patients with resected non-small cell lung cancer. *Oncol Lett*. 2015;10(4):2584-2590. doi:10.3892/ol.2015.3531
79. Galluzzi L, Senovilla L, Vitale I, et al. Molecular mechanisms of cisplatin resistance. *Oncogene*. 2012;31(15):1869-1883. doi:10.1038/onc.2011.384
80. Chen S-H, Chang J-Y. New Insights into Mechanisms of Cisplatin Resistance: From Tumor Cell to Microenvironment. *Int J Mol Sci*. 2019;20(17):4136. doi:10.3390/ijms20174136

81. Berquist BR, Wilson DM. Pathways for repairing and tolerating the spectrum of oxidative DNA lesions. *Cancer Lett*. 2012;327(1-2):61-72. doi:10.1016/j.canlet.2012.02.001
82. Duan M, Ulibarri J, Liu KJ, Mao P. Role of Nucleotide Excision Repair in Cisplatin Resistance. *Int J Mol Sci*. 2020;21(23):9248. doi:10.3390/ijms21239248
83. Giovannetti E, Zucali PA, Assaraf YG, et al. Role of proton-coupled folate transporter in pemetrexed resistance of mesothelioma: clinical evidence and new pharmacological tools. *Ann Oncol*. 2017;28(11):2725-2732. doi:10.1093/annonc/mdx499
84. Sato Y, Tomita M, Soga T, Ochiai A, Makinoshima H. Upregulation of Thymidylate Synthase Induces Pemetrexed Resistance in Malignant Pleural Mesothelioma. *Front Pharmacol*. 2021;12:718675. doi:10.3389/fphar.2021.718675
85. Hanahan D, Weinberg RA. Hallmarks of Cancer: The Next Generation. *Cell*. 2011;144(5):646-674. doi:10.1016/j.cell.2011.02.013
86. Šmahel M. PD-1/PD-L1 Blockade Therapy for Tumors with Downregulated MHC Class I Expression. *Int J Mol Sci*. 2017;18(6):1331. doi:10.3390/ijms18061331
87. Hotta K, Fujimoto N. Current evidence and future perspectives of immune-checkpoint inhibitors in unresectable malignant pleural mesothelioma. *J Immunother Cancer*. 2020;8(1):e000461. doi:10.1136/jitc-2019-000461
88. Kay ABB. The early history of the eosinophil. *Clin Exp Allergy*. 2015;45(3):575-582. doi:10.1111/cea.12480
89. Rothenberg ME, Hogan SP. The Eosinophil. *Annu Rev Immunol*. 2006;24(1):147-174. doi:10.1146/annurev.immunol.24.021605.090720
90. Klion AD, Ackerman SJ, Bochner BS. Contributions of Eosinophils to Human Health and Disease. *Annu Rev Pathol Mech Dis*. 2020;15(1):179-209. doi:10.1146/annurev-pathmechdis-012419-032756
91. Klion A. Recent advances in understanding eosinophil biology. *F1000Research*. 2017;6(0):1084. doi:10.12688/f1000research.11133.1
92. Weller PF, Spencer LA. Functions of tissue-resident eosinophils. *Nat Rev Immunol*. 2017;17(12):746-760. doi:10.1038/nri.2017.95
93. Jacobsen EA, Jackson DJ, Heffler E, et al. Eosinophil Knockout Humans: Uncovering the Role of Eosinophils Through Eosinophil-Directed Biological Therapies. *Annu Rev Immunol*. 2021;39(1):719-757. doi:10.1146/annurev-immunol-093019-125918
94. Rosenberg HF, Dyer KD, Foster PS. Eosinophils: changing perspectives in health and disease. *Nat Rev Immunol*. 2013;13(1):9-22. doi:10.1038/nri3341
95. Kovalszki A, Weller PF. Eosinophils and Eosinophilia. In: Rich RR, Fleisher TA, Shearer WT, Schroeder HW, Frew A, Weyand CM, eds. *Clinical Immunology*. Elsevier; 2019:349-361.e1. doi:10.1016/B978-0-7020-6896-6.00024-7

96. Drissen R, Buza-Vidas N, Woll P, et al. Distinct myeloid progenitor–differentiation pathways identified through single-cell RNA sequencing. *Nat Immunol*. 2016;17(6):666-676. doi:10.1038/ni.3412
97. Jacobsen SEW, Nerlov C. Haematopoiesis in the era of advanced single-cell technologies. *Nat Cell Biol*. 2019;21(1):2-8. doi:10.1038/s41556-018-0227-8
98. Bouffi C, Kartashov A V., Schollaert KL, et al. Transcription Factor Repertoire of Homeostatic Eosinophilopoiesis. *J Immunol*. 2015;195(6):2683-2695. doi:10.4049/jimmunol.1500510
99. Du J, Stankiewicz MJ, Liu Y, et al. Novel Combinatorial Interactions of GATA-1, PU.1, and C/EBPε Isoforms Regulate Transcription of the Gene Encoding Eosinophil Granule Major Basic Protein. *J Biol Chem*. 2002;277(45):43481-43494. doi:10.1074/jbc.M204777200
100. Nishinakamura R, Nakayama N, Hirabayashi Y, et al. Mice deficient for the IL-3/GM-CSF/IL-5 βc receptor exhibit lung pathology and impaired immune response, while βIL3 receptor-deficient mice are normal. *Immunity*. 1995;2(3):211-222. doi:10.1016/1074-7613(95)90046-2
101. Nishinakamura R, Miyajima A, Mee PJ, Tybulewicz VLJ, Murray R. Hematopoiesis in mice lacking the entire granulocyte-macrophage colony-stimulating factor/interleukin-3/interleukin-5 functions. *Blood*. 1996;88(7):2458-2464. doi:10.1182/blood.v88.7.2458.bloodjournal8872458
102. Mishra A, Hogan SP, Lee JJ, Foster PS, Rothenberg ME. Fundamental signals that regulate eosinophil homing to the gastrointestinal tract. *J Clin Invest*. 1999;103(12):1719-1727. doi:10.1172/JCI6560
103. Mesnil C, Raulier S, Paulissen G, et al. Lung-resident eosinophils represent a distinct regulatory eosinophil subset. *J Clin Invest*. 2016;126(9):3279-3295. doi:10.1172/JCI85664
104. Marichal T, Mesnil C, Bureau F. Homeostatic Eosinophils: Characteristics and Functions. *Front Med*. 2017;4:101. doi:10.3389/fmed.2017.00101
105. Molofsky AB, Nussbaum JC, Liang HE, et al. Innate lymphoid type 2 cells sustain visceral adipose tissue eosinophils and alternatively activated macrophages. *J Exp Med*. 2013;210(3):535-549. doi:10.1084/jem.20121964
106. Matthews AN, Friend DS, Zimmermann N, et al. Eotaxin is required for the baseline level of tissue eosinophils. *Proc Natl Acad Sci*. 1998;95(11):6273-6278. doi:10.1073/pnas.95.11.6273
107. Menzies-Gow A, Robinson DS. Eosinophil chemokines and chemokine receptors: Their role in eosinophil accumulation and activation in asthma and potential as therapeutic targets. *J Asthma*. 2001;38(8):605-613. doi:10.1081/JAS-100107538

108. Menzies-Gow A, Ying S, Sabroe I, et al. Eotaxin (CCL11) and Eotaxin-2 (CCL24) Induce Recruitment of Eosinophils, Basophils, Neutrophils, and Macrophages As Well As Features of Early- and Late-Phase Allergic Reactions Following Cutaneous Injection in Human Atopic and Nonatopic Volunteers. *J Immunol*. 2002;169(5):2712-2718. doi:10.4049/jimmunol.169.5.2712
109. Nussbaum JC, Van Dyken SJ, von Moltke J, et al. Type 2 innate lymphoid cells control eosinophil homeostasis. *Nature*. 2013;502(7470):245-248. doi:10.1038/nature12526
110. Bochner BS. Siglec-8 on human eosinophils and mast cells, and Siglec-F on murine eosinophils, are functionally related inhibitory receptors. *Clin Exp Allergy*. 2009;39(3):317-324. doi:10.1111/j.1365-2222.2008.03173.x
111. Kvarnhammar AM, Cardell LO. Pattern-recognition receptors in human eosinophils. *Immunology*. 2012;136(1):11-20. doi:10.1111/j.1365-2567.2012.03556.x
112. Shamri R, Xenakis JJ, Spencer LA. Eosinophils in innate immunity: an evolving story. *Cell Tissue Res*. 2011;343(1):57-83. doi:10.1007/s00441-010-1049-6
113. Fettrelet T, Gigon L, Karaulov A, Yousefi S, Simon H-U. The Enigma of Eosinophil Degranulation. *Int J Mol Sci*. 2021;22(13):7091. doi:10.3390/ijms22137091
114. Kita H, Bochner BS. Biology of Eosinophils. In: Adkinson FN, Bochner BS, Burks WA, et al., eds. *Middleton's Allergy: Principles and Practice*. 8th ed. Philadelphia: Elsevier Saunders; 2009:265-279.
115. HOGAN SP, ROSENBERG HF, MOQBEL R, et al. Eosinophils: Biological Properties and Role in Health and Disease. *Clin Exp Allergy*. 2008;38(5):709-750. doi:10.1111/j.1365-2222.2008.02958.x
116. Blanchard C, Rothenberg ME. Biology of the Eosinophil. *Adv Immunol*. 2009;101:81-121. doi:10.1016/S0065-2776(08)01003-1
117. Gelfand EW, Venge P, Simon D, et al. Eosinophils in Human Disease. In: Lee JJ, Rosenberg HF, eds. *Eosinophils in Health and Disease*. 1st ed. Oxford: Elsevier; 2013:431-536. doi:10.1016/B978-0-12-394385-9.00013-4
118. Acharya KR, Ackerman SJ. Eosinophil Granule Proteins: Form and Function. *J Biol Chem*. 2014;289(25):17406-17415. doi:10.1074/jbc.R113.546218
119. Lingblom C, Andersson J, Andersson K, Wennerås C. Regulatory Eosinophils Suppress T Cells Partly through Galectin-10. *J Immunol*. 2017;198(12):4672-4681. doi:10.4049/jimmunol.1601005
120. Melo RCN, Wang H, Silva TP, et al. Galectin-10, the protein that forms Charcot-Leyden crystals, is not stored in granules but resides in the peripheral cytoplasm of human eosinophils. *J Leukoc Biol*. 2020;108(1):139-149. doi:10.1002/JLB.3AB0220-311R

121. Weller PF, Wang H, Melo RCN. The Charcot–Leyden crystal protein revisited—A lysopalmitoylphospholipase and more. *J Leukoc Biol*. 2020;108(1):105-112. doi:10.1002/JLB.3MR0320-319RR
122. Grozdanovic MM, Doyle CB, Liu L, et al. Charcot-Leyden crystal protein/galectin-10 interacts with cationic ribonucleases and is required for eosinophil granulogenesis. *J Allergy Clin Immunol*. 2020;146(2):377-389.e10. doi:10.1016/j.jaci.2020.01.013
123. Porter LM, Cowburn AS, Farahi N, et al. Hypoxia causes IL-8 secretion, Charcot Leyden crystal formation, and suppression of corticosteroid-induced apoptosis in human eosinophils. *Clin Exp Allergy*. 2017;47(6):770-784. doi:10.1111/cea.12877
124. Persson EK, Verstraete K, Heyndrickx I, et al. Protein crystallization promotes type 2 immunity and is reversible by antibody treatment. *Science (80-)*. 2019;364(6442):eaaw4295. doi:10.1126/science.aaw4295
125. Ackerman SJ, Liu L, Kwatia MA, et al. Charcot-Leyden Crystal Protein (Galectin-10) Is Not a Dual Function Galectin with Lysophospholipase Activity but Binds a Lysophospholipase Inhibitor in a Novel Structural Fashion. *J Biol Chem*. 2002;277(17):14859-14868. doi:10.1074/jbc.M200221200
126. Melo RCN, Weller PF. Contemporary understanding of the secretory granules in human eosinophils. *J Leukoc Biol*. 2018;104(1):85-93. doi:10.1002/JLB.3MR1217-476R
127. Fukuchi M, Kamide Y, Ueki S, et al. Eosinophil ETosis–Mediated Release of Galectin-10 in Eosinophilic Granulomatosis With Polyangiitis. *Arthritis Rheumatol*. 2021;73(9):1683-1693. doi:10.1002/art.41727
128. Lombardi C, Berti A, Cottini M. The emerging roles of eosinophils: Implications for the targeted treatment of eosinophilic-associated inflammatory conditions. *Curr Res Immunol*. 2022;3:42-53. doi:10.1016/j.crimmu.2022.03.002
129. Lee JJ, Jacobsen EA, McGarry MP, Schleimer RP, Lee NA. Eosinophils in health and disease: the LIAR hypothesis. *Clin Exp Allergy*. 2010;40(4):563-575. doi:10.1111/j.1365-2222.2010.03484.x
130. Kita H. Eosinophils: multifaceted biological properties and roles in health and disease. *Immunol Rev*. 2011;242(1):161-177. doi:10.1111/j.1600-065X.2011.01026.x
131. Kanda A, Yun Y, Bui D Van, et al. The multiple functions and subpopulations of eosinophils in tissues under steady-state and pathological conditions. *Allergol Int*. 2021;70(1):9-18. doi:10.1016/j.alit.2020.11.001
132. Abdala-Valencia H, Coden ME, Chiarella SE, et al. Shaping eosinophil identity in the tissue contexts of development, homeostasis, and disease. *J Leukoc Biol*. 2018;104(1):95-108. doi:10.1002/JLB.1MR1117-442RR

133. Chu VT, Fröhlich A, Steinhauser G, et al. Eosinophils are required for the maintenance of plasma cells in the bone marrow. *Nat Immunol*. 2011;12(2):151-159. doi:10.1038/ni.1981
134. Berek C. Eosinophils: important players in humoral immunity. *Clin Exp Immunol*. 2015;183(1):57-64. doi:10.1111/cei.12695
135. Wu D, Molofsky AB, Liang H-E, et al. *Eosinophils Sustain Adipose Alternatively Activated Macrophages Associated with Glucose Homeostasis*. Vol 332.; 2011. doi:10.1126/science.1201475
136. Shah K, Ignacio A, McCoy KD, Harris NL. The emerging roles of eosinophils in mucosal homeostasis. *Mucosal Immunol*. 2020;13(4):574-583. doi:10.1038/s41385-020-0281-y
137. Cosway EJ, White AJ, Parnell SM, et al. Eosinophils are an essential element of a type 2 immune axis that controls thymus regeneration. *Sci Immunol*. 2022;7(69):eabn3286. doi:10.1126/sciimmunol.abn3286
138. Rodrigo-Muñoz JM, Gil-Martínez M, Sastre B, del Pozo V. Emerging Evidence for Pleiotropism of Eosinophils. *Int J Mol Sci*. 2021;22(13):7075. doi:10.3390/ijms22137075
139. Fabre V, Beiting DP, Bliss SK, et al. Eosinophil Deficiency Compromises Parasite Survival in Chronic Nematode Infection. *J Immunol*. 2009;182(3):1577-1583. doi:10.4049/jimmunol.182.3.1577
140. Simon H-U, Yousefi S, Germic N, et al. The Cellular Functions of Eosinophils: Collegium Internationale Allergologicum (CIA) Update 2020. *Int Arch Allergy Immunol*. 2020;181(1):11-23. doi:10.1159/000504847
141. Linch SN, Kelly AM, Danielson ET, Pero R, Lee JJ, Gold JA. Mouse Eosinophils Possess Potent Antibacterial Properties In Vivo. *Infect Immun*. 2009;77(11):4976-4982. doi:10.1128/IAI.00306-09
142. Torrent M, Navarro S, Moussaoui M, Nogués MV, Boix E. Eosinophil Cationic Protein High-Affinity Binding to Bacteria-Wall Lipopolysaccharides and Peptidoglycans. *Biochemistry*. 2008;47(11):3544-3555. doi:10.1021/bi702065b
143. Rugeles MT, Trubey CM, Bedoya VI, et al. Ribonuclease is partly responsible for the HIV-1 inhibitory effect activated by HLA alloantigen recognition. *AIDS*. 2003;17(4):481-486. doi:10.1097/00002030-200303070-00002
144. Sabogal Piñeros YS, Bal SM, Dijkhuis A, et al. Eosinophils capture viruses, a capacity that is defective in asthma. *Allergy*. 2019;74(10):1898-1909. doi:10.1111/all.13802
145. Ferastraoaru D, Hudes G, Jerschow E, et al. Eosinophilia in Asthma Patients Is Protective Against Severe COVID-19 Illness. *J Allergy Clin Immunol Pract*. 2021;9(3):1152-1162.e3. doi:10.1016/j.jaip.2020.12.045
146. Mateos González M, Sierra Gonzalo E, Casado Lopez I, et al. The Prognostic Value of Eosinophil Recovery in COVID-19: A Multicentre, Retrospective Cohort Study on Patients Hospitalised in Spanish Hospitals. *J Clin Med*. 2021;10(2):305. doi:10.3390/jcm10020305

147. Liu F, Xu A, Zhang Y, et al. Patients of COVID-19 may benefit from sustained Lopinavir-combined regimen and the increase of Eosinophil may predict the outcome of COVID-19 progression. *Int J Infect Dis*. 2020;95:183-191. doi:10.1016/j.ijid.2020.03.013
148. Nair AP, Soliman A, Al Masalamani MA, et al. Clinical Outcome of Eosinophilia in Patients with COVID-19: A Controlled Study. *Acta Biomed*. 2020;91(4):e2020165. doi:10.23750/abm.v91i4.10564
149. Ravin KA, Loy M. The Eosinophil in Infection. *Clin Rev Allergy Immunol*. 2016;50(2):214-227. doi:10.1007/s12016-015-8525-4
150. Wen T, Rothenberg ME. The Regulatory Function of Eosinophils. Gordon S, ed. *Microbiol Spectr*. 2016;4(5):257-269. doi:10.1128/microbiolspec.MCHD-0020-2015
151. Simon SCS, Utikal J, Umansky V. Opposing roles of eosinophils in cancer. *Cancer Immunol Immunother*. 2019;68(5):823-833. doi:10.1007/s00262-018-2255-4
152. Akuthota P, Wang HB, Spencer LA, Weller PF. Immunoregulatory roles of eosinophils: a new look at a familiar cell. *Clin Exp Allergy*. 2008;38(8):1254-1263. doi:10.1111/j.1365-2222.2008.03037.x
153. Lotfi R, Lotze MT. Eosinophils induce DC maturation, regulating immunity. *J Leukoc Biol*. 2008;83(3):456-460. doi:10.1189/jlb.0607366
154. Yang D, Chen Q, Rosenberg HF, et al. Human Ribonuclease A Superfamily Members, Eosinophil-Derived Neurotoxin and Pancreatic Ribonuclease, Induce Dendritic Cell Maturation and Activation. *J Immunol*. 2004;173(10):6134-6142. doi:10.4049/jimmunol.173.10.6134
155. Yang D, Chen Q, Su SB, et al. Eosinophil-derived neurotoxin acts as an alarmin to activate the TLR2–MyD88 signal pathway in dendritic cells and enhances Th2 immune responses. *J Exp Med*. 2008;205(1):79-90. doi:10.1084/jem.20062027
156. Cusack RP, Whetstone CE, Xie Y, Ranjbar M, Gauvreau GM. Regulation of Eosinophilia in Asthma—New Therapeutic Approaches for Asthma Treatment. *Cells*. 2021;10(4):817. doi:10.3390/cells10040817
157. Kay AB, Phipps S, Robinson DS. A role for eosinophils in airway remodelling in asthma. *Trends Immunol*. 2004;25(9):477-482. doi:10.1016/j.it.2004.07.006
158. Choi Y, Sim S, Park H-S. Distinct functions of eosinophils in severe asthma with type 2 phenotype: clinical implications. *Korean J Intern Med*. 2020;35(4):823-833. doi:10.3904/kjim.2020.022
159. Nakagome K, Nagata M. Involvement and Possible Role of Eosinophils in Asthma Exacerbation. *Front Immunol*. 2018;9:2220. doi:10.3389/fimmu.2018.02220
160. Jacobsen EA, Ochkur SI, Lee NA, Lee JJ. Eosinophils and asthma. *Curr Allergy Asthma Rep*. 2007;7(1):18-26. doi:10.1007/s11882-007-0026-y

161. Tzankov A, Reichard KK, Hasserjian RP, Arber DA, Orazi A, Wang SA. Updates on eosinophilic disorders. *Virchows Arch*. 2023;482(1):85-97. doi:10.1007/s00428-022-03402-8
162. Kovalszki A, Weller PF. Eosinophilia. *Prim Care Clin Off Pract*. 2016;43(4):607-617. doi:10.1016/j.pop.2016.07.010
163. Shomali W, Gotlib J. World Health Organization-defined eosinophilic disorders: 2022 update on diagnosis, risk stratification, and management. *Am J Hematol*. 2022;97(1):129-148. doi:10.1002/ajh.26352
164. Falchi L, Verstovsek S. Eosinophilia in Hematologic Disorders. *Immunol Allergy Clin North Am*. 2015;35(3):439-452. doi:10.1016/j.iac.2015.04.004
165. Montgomery ND, Dunphy CH, Mooberry M, et al. Diagnostic Complexities of Eosinophilia. *Arch Pathol Lab Med*. 2013;137(2):259-269. doi:10.5858/arpa.2011-0597-RA
166. Tefferi A, Patnaik MM, Pardanani A. Eosinophilia: secondary, clonal and idiopathic. *Br J Haematol*. 2006;133(5):468-492. doi:10.1111/j.1365-2141.2006.06038.x
167. Reichman H, Karo-Atar D, Munitz A. Emerging Roles for Eosinophils in the Tumor Microenvironment. *Trends in Cancer*. 2016;2(11):664-675. doi:10.1016/j.trecan.2016.10.002
168. Davis BP, Rothenberg ME. Eosinophils and Cancer. *Cancer Immunol Res*. 2014;2(1):1-8. doi:10.1158/2326-6066.CIR-13-0196
169. Grisaru-Tal S, Itan M, Klion AD, Munitz A. A new dawn for eosinophils in the tumour microenvironment. *Nat Rev Cancer*. 2020;20(10):594-607. doi:10.1038/s41568-020-0283-9
170. Lowe D, Jorizzo J, Hutt MSR. Tumour-associated eosinophilia: a review. *J Clin Pathol*. 1981;34(12):1343-1348. doi:10.1136/jcp.34.12.1343
171. Stefanini M, Claustro JC, Motos RA, Bendigo LL. Blood and bone marrow eosinophilia in malignant tumors. Role and nature of blood and tissue eosinophil colony-stimulating factor(s) in two patients. *Cancer*. 1991;68(3):543-548. doi:10.1002/1097-0142(19910801)68:3<543::aid-cncr2820680317>3.0.co;2-3
172. Todenhöfer T, Wirths S, von Weyhern CH, et al. Severe paraneoplastic hypereosinophilia in metastatic renal cell carcinoma. *BMC Urol*. 2012;12(1):7. doi:10.1186/1471-2490-12-7
173. Anagnostopoulos GK, Sakorafas GH, Kostopoulos P, et al. Disseminated colon cancer with severe peripheral blood eosinophilia and elevated serum levels of interleukine-2, interleukine-3, interleukine-5, and GM-CSF. *J Surg Oncol*. 2005;89(4):273-275. doi:10.1002/jso.20173
174. Takeuchi E, Okano Y, Machida H, et al. Eosinophilic pleural effusion due to lung cancer has a better prognosis than non-eosinophilic malignant pleural effusion. *Cancer Immunol Immunother*. 2022;71(2):365-372. doi:10.1007/s00262-021-02994-5

175. Jacquelot N, Seillet C, Wang M, et al. Blockade of the co-inhibitory molecule PD-1 unleashes ILC2-dependent antitumor immunity in melanoma. *Nat Immunol*. 2021;22(7):851-864. doi:10.1038/s41590-021-00943-z
176. Grisaru-Tal S, Rothenberg ME, Munitz A. Eosinophil–lymphocyte interactions in the tumor microenvironment and cancer immunotherapy. *Nat Immunol*. 2022;23(9):1309-1316. doi:10.1038/s41590-022-01291-2
177. Curran CS, Evans MD, Bertics PJ. GM-CSF Production by Glioblastoma Cells Has a Functional Role in Eosinophil Survival, Activation, and Growth Factor Production for Enhanced Tumor Cell Proliferation. *J Immunol*. 2011;187(3):1254-1263. doi:10.4049/jimmunol.1001965
178. Varricchi G, Galdiero MR, Loffredo S, et al. Eosinophils: The unsung heroes in cancer? *Oncoimmunology*. 2018;7(2):e1393134. doi:10.1080/2162402X.2017.1393134
179. Cho H, Lim S-J, Won KY, et al. Eosinophils in Colorectal Neoplasms Associated with Expression of CCL11 and CCL24. *J Pathol Transl Med*. 2016;50(1):45-51. doi:10.4132/jptm.2015.10.16
180. Lorena S, Oliveira D, Dorta R, Landman G, Kowalski L. Eotaxin expression in oral squamous cell carcinomas with and without tumour associated tissue eosinophilia. *Oral Dis*. 2003;9(6):279-283. doi:10.1034/j.1601-0825.2003.00958.x
181. Erreni M, Bianchi P, Laghi L, et al. Chapter 5 Expression of Chemokines and Chemokine Receptors in Human Colon Cancer. In: *Methods in Enzymology*. Vol 460. 1st ed. Elsevier Inc.; 2009:105-121. doi:10.1016/S0076-6879(09)05205-7
182. Lotfi R, Lee JJ, Lotze MT. Eosinophilic Granulocytes and Damage-associated Molecular Pattern Molecules (DAMPs). *J Immunother*. 2007;30(1):16-28. doi:10.1097/01.cji.0000211324.53396.f6
183. Carretero R, Sektioglu IM, Garbi N, Salgado OC, Beckhove P, Hämmerling GJ. Eosinophils orchestrate cancer rejection by normalizing tumor vessels and enhancing infiltration of CD8(+) T cells. *Nat Immunol*. 2015;16(6):609-617. doi:10.1038/ni.3159
184. Puxeddu I, Berkman N, Nissim Ben Efraim AH, et al. The role of eosinophil major basic protein in angiogenesis. *Allergy*. 2009;64(3):368-374. doi:10.1111/j.1398-9995.2008.01822.x
185. Georas SN, Beck LA, Stellato C. What Is Eotaxin Doing in the Pleura? *Am J Respir Cell Mol Biol*. 2002;26(4):384-387. doi:10.1165/ajrcmb.26.4.f235
186. Comar M, Zanotta N, Zanconati F, et al. Chemokines involved in the early inflammatory response and in pro-tumoral activity in asbestos-exposed workers from an Italian coastal area with territorial clusters of pleural malignant mesothelioma. *Lung Cancer*. 2016;94:61-67. doi:10.1016/j.lungcan.2016.01.020

187. Stathopoulos GT, Sherrill TP, Karabela SP, et al. Host-derived interleukin-5 promotes adenocarcinoma-induced malignant pleural effusion. *Am J Respir Crit Care Med*. 2010;182(10):1273-1281. doi:10.1164/rccm.201001-0001OC
188. Takeuchi E, Takahashi N, Morizumi S, et al. Interleukin-5-producing malignant pleural mesothelioma with eosinophilic pleural effusion. *Thorac cancer*. 2020;11(10):3043-3046. doi:10.1111/1759-7714.13652
189. Oehl K, Vrugt B, Opitz I, Meerang M. Heterogeneity in Malignant Pleural Mesothelioma. *Int J Mol Sci*. 2018;19(6):1603. doi:10.3390/ijms19061603
190. Mola S, Pinton G, Erreni M, et al. Inhibition of the Histone Methyltransferase EZH2 Enhances Protumor Monocyte Recruitment in Human Mesothelioma Spheroids. *Int J Mol Sci*. 2021;22(9):4391. doi:10.3390/ijms22094391
191. Lievense LA, Cornelissen R, Bezemer K, Kaijen-Lambers MEH, Hegmans JPJJ, Aerts JGJ V. Pleural Effusion of Patients with Malignant Mesothelioma Induces Macrophage-Mediated T Cell Suppression. *J Thorac Oncol*. 2016;11(10):1755-1764. doi:10.1016/j.jtho.2016.06.021
192. Hamaidia M, Gazon H, Hoyos C, et al. Inhibition of EZH2 methyltransferase decreases immunoediting of mesothelioma cells by autologous macrophages through a PD-1-dependent mechanism. *JCI Insight*. 2019;4(18):1-17. doi:10.1172/jci.insight.128474
193. Gauttier V, Pengam S, Durand J, et al. Selective SIRPα blockade reverses tumor T cell exclusion and overcomes cancer immunotherapy resistance. *J Clin Invest*. 2020;130(11):6109-6123. doi:10.1172/JCI135528
194. Hoyos C, Fontaine A, Jacques J-R, et al. HDAC Inhibition with Valproate Improves Direct Cytotoxicity of Monocytes against Mesothelioma Tumor Cells. *Cancers (Basel)*. 2022;14(9):2164. doi:10.3390/cancers14092164
195. Wu L, Kohno M, Murakami J, et al. Defining and targeting tumor-associated macrophages in malignant mesothelioma. *Proc Natl Acad Sci*. 2023;120(9):e2210836120. doi:10.1073/pnas.2210836120
196. Cimen F, Agackiran Y, Düzgün S, Aloglu M, Senturk A, Atikcan S. Factors affecting the life expectancy in malignant pleural mesothelioma: Our 10 years of studies and experience. *Medicine (Baltimore)*. 2022;101(39):e30711. doi:10.1097/MD.0000000000030711
197. Fournel L, Charrier T, Huriet M, et al. Prognostic impact of inflammation in malignant pleural mesothelioma: A large-scale analysis of consecutive patients. *Lung Cancer*. 2022;166:221-227. doi:10.1016/j.lungcan.2022.03.014
198. Okita R, Okada M, Inokawa H, Murakami T, Ikeda E. Prognostic values of preoperative C-reactive protein, albumin, and neutrophil ratios in patients with malignant pleural mesothelioma who underwent extrapleural pneumonectomy. *Surg Oncol*. 2022;43:101813. doi:10.1016/j.suronc.2022.101813
199. Willems M, Scherpereel A, Wasielewski E, et al. Excess of blood eosinophils prior to therapy correlates with worse prognosis in mesothelioma. *Front Immunol*. 2023;14:1148798. doi:10.3389/fimmu.2023.1148798

200. Sibille A, Corhay J-L, Louis R, Ninane V, Jerusalem G, Duysinx B. Eosinophils and Lung Cancer: From Bench to Bedside. *Int J Mol Sci*. 2022;23(9):5066. doi:10.3390/ijms23095066
201. Adamko DJ, Wu Y, Gleich GJ, Lacy P, Moqbel R. The induction of eosinophil peroxidase release: improved methods of measurement and stimulation. *J Immunol Methods*. 2004;291(1-2):101-108. doi:10.1016/j.jim.2004.05.003
202. Friedrich J, Seidel C, Ebner R, Kunz-Schughart LA. Spheroid-based drug screen: considerations and practical approach. *Nat Protoc*. 2009;4(3):309-324. doi:10.1038/nprot.2008.226
203. Tomizawa H, Yamada Y, Arima M, et al. Galectin-10 as a Potential Biomarker for Eosinophilic Diseases. *Biomolecules*. 2022;12(10):1385. doi:10.3390/biom12101385
204. Cordier Kellerman L, Valeyrie L, Fernandez N, et al. Regression of AK7 malignant mesothelioma established in immunocompetent mice following intratumoral gene transfer of interferon gamma. *Cancer Gene Ther*. 2003;10(6):481-490. doi:10.1038/sj.cgt.7700594
205. Johnston LK, Bryce PJ. Understanding Interleukin 33 and Its Roles in Eosinophil Development. *Front Med*. 2017;4:51. doi:10.3389/fmed.2017.00051
206. De Fonseka D, Arnold DT, Morley AJ, et al. Lymphocyte predominance in blood, pleural fluid, and tumour stroma; a prognostic marker in pleural mesothelioma. *BMC Pulm Med*. 2022;22(1):173. doi:10.1186/s12890-022-01968-2
207. Tsolaki V, Zarogiannis S, Zygoulis P, et al. Malignant mesothelioma cells secrete natriuretic peptides: Data and diagnostic clinical implications. *Respirology*. 2020;25(10):1060-1065. doi:10.1111/resp.13788
208. Schmitter D, Lauber B, Fagg B, Stahel RA. Hematopoietic Growth Factors Secreted By Seven Human Pleural Mesothelioma Cell Lines: Interleukin-6 Production as a Common Feature. *Int J Against Cancer*. 1992;51:296-301.
209. Blum W, Schwaller B. Calretinin is essential for mesothelioma cell growth/survival in vitro: A potential new target for malignant mesothelioma therapy? *Int J Cancer*. 2013;133(9):2077-2088. doi:10.1002/ijc.28218
210. Frei C, Opitz I, Soltermann A, et al. Pleural mesothelioma side populations have a precursor phenotype. *Carcinogenesis*. 2011;32(9):1324-1332. doi:10.1093/carcin/bgr127
211. Keller M, Reis K, Hjerpe A, Dobra K, Aspenström P. Cytoskeletal organization correlates to motility and invasiveness of malignant mesothelioma cells. *Cancers (Basel)*. 2021;13(4):1-23. doi:10.3390/cancers13040685
212. Guillon J, Petit C, Toutain B, Guette C, Lelièvre E, Coqueret O. Chemotherapy-induced senescence, an adaptive mechanism driving resistance and tumor heterogeneity. *Cell Cycle*. 2019;18(19):2385-2397. doi:10.1080/15384101.2019.1652047

213. Wang L, Lankhorst L, Bernards R. Exploiting senescence for the treatment of cancer. *Nat Rev Cancer*. 2022;22(6):340-355. doi:10.1038/s41568-022-00450-9
214. Dellon ES, Peterson KA, Murray JA, et al. Anti–Siglec-8 Antibody for Eosinophilic Gastritis and Duodenitis. *N Engl J Med*. 2020;383(17):1624-1634. doi:10.1056/NEJMoa2012047
215. Yamazaki M, Ohwada A, Miyaji A, et al. Pulmonary Paragonimiasis with Coincidental Malignant Mesothelioma. *Intern Med*. 2008;47(11):1027-1031. doi:10.2169/internalmedicine.47.0852
216. Wechsler ME, Munitz A, Ackerman SJ, et al. Eosinophils in Health and Disease: A State-of-the-Art Review. *Mayo Clin Proc*. 2021;96(10):2694-2707. doi:10.1016/j.mayocp.2021.04.025
217. Reichman H, Itan M, Rozenberg P, et al. Activated Eosinophils Exert Antitumorigenic Activities in Colorectal Cancer. *Cancer Immunol Res*. 2019;7(3):388-400. doi:10.1158/2326-6066.CIR-18-0494
218. Rigoni A, Colombo MP, Pucillo C. Mast cells, basophils and eosinophils: From allergy to cancer. *Semin Immunol*. 2018;35:29-34. doi:10.1016/j.smim.2018.02.001
219. Turner MC, Chen Y, Krewski D, Ghadirian P. An overview of the association between allergy and cancer. *Int J Cancer*. 2006;118(12):3124-3132. doi:10.1002/ijc.21752
220. Jacobs EJ, Gapstur SM, Newton CC, Turner MC, Campbell PT. Hay Fever and Asthma as Markers of Atopic Immune Response and Risk of Colorectal Cancer in Three Large Cohort Studies. *Cancer Epidemiol Biomarkers Prev*. 2013;22(4):661-669. doi:10.1158/1055-9965.EPI-12-1229
221. Yang R-Y, Rabinovich GA, Liu F-T. Galectins: structure, function and therapeutic potential. *Expert Rev Mol Med*. 2008;10(17):e17. doi:10.1017/S1462399408000719
222. Li C-H, Chang Y-C, Chan M-H, Yang Y-F, Liang S-M, Hsiao M. Galectins in Cancer and the Microenvironment: Functional Roles, Therapeutic Developments, and Perspectives. *Biomedicines*. 2021;9(9):1159. doi:10.3390/biomedicines9091159
223. Porębska N, Poźniak M, Matynia A, et al. Galectins as modulators of receptor tyrosine kinases signaling in health and disease. *Cytokine Growth Factor Rev*. 2021;60:89-106. doi:10.1016/j.cytogfr.2021.03.004
224. Navarro P, Martínez-Bosch N, Blidner AG, Rabinovich GA. Impact of Galectins in Resistance to Anticancer Therapies. *Clin Cancer Res*. 2020;26(23):6086-6101. doi:10.1158/1078-0432.CCR-18-3870
225. Fuselier C, Dumoulin A, Paré A, et al. Placental Galectins in Cancer: Why We Should Pay More Attention. *Cells*. 2023;12(3):437. doi:10.3390/cells12030437

226. Liu D, Zhu H, Li C. Galectins and galectin-mediated autophagy regulation: new insights into targeted cancer therapy. *Biomark Res*. 2023;11(1):22. doi:10.1186/s40364-023-00466-9
227. Chou F-C, Chen H-Y, Kuo C-C, Sytwu H-K. Role of Galectins in Tumors and in Clinical Immunotherapy. *Int J Mol Sci*. 2018;19(2):430. doi:10.3390/ijms19020430
228. Bertino P, Premeaux TA, Fujita T, et al. Targeting the C-terminus of galectin-9 induces mesothelioma apoptosis and M2 macrophage depletion. *Oncoimmunology*. 2019;8(8):e1601482. doi:10.1080/2162402X.2019.1601482
229. Mundt F, Johansson HJ, Forshed J, et al. Proteome Screening of Pleural Effusions Identifies Galectin 1 as a Diagnostic Biomarker and Highlights Several Prognostic Biomarkers for Malignant Mesothelioma. *Mol Cell Proteomics*. 2014;13(3):701-715. doi:10.1074/mcp.M113.030775
230. Blanquart C, Gueugnon F, Nguyen J-M, et al. CCL2, Galectin-3, and SMRP Combination Improves the Diagnosis of Mesothelioma in Pleural Effusions. *J Thorac Oncol*. 2012;7(5):883-889. doi:10.1097/JTO.0b013e31824c9272
231. Petan T, Jarc E, Jusović M. Lipid Droplets in Cancer: Guardians of Fat in a Stressful World. *Molecules*. 2018;23(8):1941. doi:10.3390/molecules23081941
232. Moessinger C, Klizaite K, Steinhagen A, et al. Two different pathways of phosphatidylcholine synthesis, the Kennedy Pathway and the Lands Cycle, differentially regulate cellular triacylglycerol storage. *BMC Cell Biol*. 2014;15(1):43. doi:10.1186/s12860-014-0043-3
233. Penno A, Hackenbroich G, Thiele C. Phospholipids and lipid droplets. *Biochim Biophys Acta - Mol Cell Biol Lipids*. 2013;1831(3):589-594. doi:10.1016/j.bbalip.2012.12.001
234. Olzmann JA, Carvalho P. Dynamics and functions of lipid droplets. *Nat Rev Mol Cell Biol*. 2019;20(3):137-155. doi:10.1038/s41580-018-0085-z
235. Cotte AK, Aires V, Fredon M, et al. Lysophosphatidylcholine acyltransferase 2-mediated lipid droplet production supports colorectal cancer chemoresistance. *Nat Commun*. 2018;9(1):322. doi:10.1038/s41467-017-02732-5
236. Weller PF, Bach DS, Austen KF. Biochemical characterization of human eosinophil Charcot-Leyden crystal protein (lysophospholipase). *J Biol Chem*. 1984;259(24):15100-15105. doi:10.1016/s0021-9258(17)42520-8
237. Erenpreisa J, Cragg MS. Three steps to the immortality of cancer cells: senescence, polyploidy and self-renewal. *Cancer Cell Int*. 2013;13(1):92. doi:10.1186/1475-2867-13-92
238. Oehl K, Kresoja-Rakic J, Opitz I, et al. Live-Cell Mesothelioma Biobank to Explore Mechanisms of Tumor Progression. *Front Oncol*. 2018;8:40. doi:10.3389/fonc.2018.00040

239. Sidi R, Pasello G, Opitz I, et al. Induction of senescence markers after neo-adjuvant chemotherapy of malignant pleural mesothelioma and association with clinical outcome: An exploratory analysis. *Eur J Cancer*. 2011;47(2):326-332. doi:10.1016/j.ejca.2010.09.044
240. Ewald JA, Desotelle JA, Wilding G, Jarrard DF. Therapy-Induced Senescence in Cancer. *JNCI J Natl Cancer Inst*. 2010;102(20):1536-1546. doi:10.1093/jnci/djq364
241. Canino C, Mori F, Cambria A, et al. SASP mediates chemoresistance and tumor-initiating-activity of mesothelioma cells. *Oncogene*. 2012;31(26):3148-3163. doi:10.1038/onc.2011.485
242. Chambers CR, Ritchie S, Pereira BA, Timpson P. Overcoming the senescence-associated secretory phenotype (SASP): a complex mechanism of resistance in the treatment of cancer. *Mol Oncol*. 2021;15(12):3242-3255. doi:10.1002/1878-0261.13042
243. Elmore LW, Di X, Dumur C, Holt SE, Gewirtz DA. Evasion of a single-step, chemotherapy-induced senescence in breast cancer cells: implications for treatment response. *Clin Cancer Res*. 2005;11(7):2637-2643. doi:10.1158/1078-0432.CCR-04-1462
244. Roberson RS, Kussick SJ, Vallieres E, Chen S-YJ, Wu DY. Escape from therapy-induced accelerated cellular senescence in p53-null lung cancer cells and in human lung cancers. *Cancer Res*. 2005;65(7):2795-2803. doi:10.1158/0008-5472.CAN-04-1270
245. Medema JP. Escape from senescence boosts tumour growth. *Nature*. 2018;553(7686):37-38. doi:10.1038/d41586-017-08652-0
246. Kuilman T, Peeper DS. Senescence-messaging secretome: SMS-ing cellular stress. *Nat Rev Cancer*. 2009;9(2):81-94. doi:10.1038/nrc2560
247. Basisty N, Kale A, Jeon OH, et al. A proteomic atlas of senescence-associated secretomes for aging biomarker development. Serrano M, ed. *PLOS Biol*. 2020;18(1):e3000599. doi:10.1371/journal.pbio.3000599
248. Milanovic M, Fan DNY, Belenki D, et al. Senescence-associated reprogramming promotes cancer stemness. *Nature*. 2018;553(7686):96-100. doi:10.1038/nature25167
249. Flor AC, Wolfgeher D, Wu D, Kron SJ. A signature of enhanced lipid metabolism, lipid peroxidation and aldehyde stress in therapy-induced senescence. *Cell Death Discov*. 2017;3(1):17075. doi:10.1038/cddiscovery.2017.75
250. Gewirtz DA. Autophagy and senescence in cancer therapy. *J Cell Physiol*. 2013;229(1):6-9. doi:10.1002/jcp.24420
251. Li X, Zhou Y, Li Y, et al. Autophagy: A novel mechanism of chemoresistance in cancers. *Biomed Pharmacother*. 2019;119:109415. doi:10.1016/j.biopha.2019.109415

252. Hwang K-E, Kim Y-S, Jung J-W, et al. Inhibition of autophagy potentiates pemetrexed and simvastatin-induced apoptotic cell death in malignant mesothelioma and non-small cell lung cancer cells. *Oncotarget*. 2015;6(30):29482-29496. doi:10.18632/oncotarget.5022
253. Follo C, Cheng Y, Richards WG, Bueno R, Broaddus VC. Inhibition of autophagy initiation potentiates chemosensitivity in mesothelioma. *Mol Carcinog*. 2018;57(3):319-332. doi:10.1002/mc.22757
254. Barbone D, Follo C, Echeverry N, et al. Autophagy Correlates with the Therapeutic Responsiveness of Malignant Pleural Mesothelioma in 3D Models. Wang Y-J, ed. *PLoS One*. 2015;10(8):e0134825. doi:10.1371/journal.pone.0134825
255. Lee JJ, Jacobsen EA, Ochkur SI, et al. Human versus mouse eosinophils: "That which we call an eosinophil, by any other name would stain as red." *J Allergy Clin Immunol*. 2012;130(3):572-584. doi:10.1016/j.jaci.2012.07.025
256. Guo L, Johnson RS, Schuh JCL. Biochemical Characterization of Endogenously Formed Eosinophilic Crystals in the Lungs of Mice. *J Biol Chem*. 2000;275(11):8032-8037. doi:10.1074/jbc.275.11.8032
257. Mamtimin M, Pinarci A, Han C, et al. Extracellular DNA Traps: Origin, Function and Implications for Anti-Cancer Therapies. *Front Oncol*. 2022;12:869706. doi:10.3389/fonc.2022.869706
258. Leon SA, Shapiro B, Sklaroff DM, Yaros MJ. Free DNA in the serum of cancer patients and the effect of therapy. *Cancer Res*. 1977;37(3):646-650. http://www.ncbi.nlm.nih.gov/pubmed/837366.
259. Francischetti IMB, Alejo JC, Sivanandham R, et al. Neutrophil and Eosinophil Extracellular Traps in Hodgkin Lymphoma. *HemaSphere*. 2021;5(9):e633. doi:10.1097/HS9.0000000000000633
260. Fernández-Domínguez IJ, Manzo-Merino J, Taja-Chayeb L, Dueñas-González A, Pérez-Cárdenas E, Trejo-Becerril C. The role of extracellular DNA (exDNA) in cellular processes. *Cancer Biol Ther*. 2021;22(4):267-278. doi:10.1080/15384047.2021.1890319
261. Zheng J, Mo J, Zhu T, et al. Comprehensive elaboration of the cGAS-STING signaling axis in cancer development and immunotherapy. *Mol Cancer*. 2020;19(1):133. doi:10.1186/s12943-020-01250-1
262. Legrand F, Driss V, Delbeke M, et al. Human Eosinophils Exert TNF-α and Granzyme A-Mediated Tumoricidal Activity toward Colon Carcinoma Cells. *J Immunol*. 2010;185(12):7443-7451. doi:10.4049/jimmunol.1000446
263. Messori A, Trippoli S. Current treatments for inoperable mesothelioma: indirect comparisons based on individual patient data reconstructed retrospectively from 4 trials. *J Chemother*. 2023;35(2):158-162. doi:10.1080/1120009X.2022.2061183

264. Okauchi S, Shiozawa T, Miyazaki K, et al. Association between peripheral eosinophils and clinical outcomes in patients with non-small cell lung cancer treated with immune checkpoint inhibitors. *Polish Arch Intern Med*. 2021;131(2):152-160. doi:10.20452/pamw.15776
265. Alves A, Dias M, Campainha S, Barroso A. Peripheral blood eosinophilia may be a prognostic biomarker in non-small cell lung cancer patients treated with immunotherapy. *J Thorac Dis*. 2021;13(5):2716-2727. doi:10.21037/jtd-20-3525
266. Yamazoe M, Ozasa H, Kim YH. Effectiveness of Nivolumab on Sarcomatoid Malignant Pleural Mesothelioma With Eosinophilia and Eosinophilic Pleural Effusion. *J Thorac Oncol*. 2019;14(11):e251-e253. doi:10.1016/j.jtho.2019.06.007
267. Rabinovich GA, Conejo-García JR. Shaping the Immune Landscape in Cancer by Galectin-Driven Regulatory Pathways. *J Mol Biol*. 2016;428(16):3266-3281. doi:10.1016/j.jmb.2016.03.021
268. Jin Q-Y, Li Y-S, Qiao X-H, Yang J-W, Guo X-L. Targeting galectins in T cell-based immunotherapy within tumor microenvironment. *Life Sci*. 2021;277(44):119426. doi:10.1016/j.lfs.2021.119426
269. Nambiar DK, Aguilera T, Cao H, et al. Galectin-1-driven T cell exclusion in the tumor endothelium promotes immunotherapy resistance. *J Clin Invest*. 2019;129(12):5553-5567. doi:10.1172/JCI129025
270. Jackson DJ, Korn S, Mathur SK, et al. Safety of Eosinophil-Depleting Therapy for Severe, Eosinophilic Asthma: Focus on Benralizumab. *Drug Saf*. 2020;43(5):409-425. doi:10.1007/s40264-020-00926-3
271. Cook AM, McDonnell AM, Lake RA, Nowak AK. Dexamethasone co-medication in cancer patients undergoing chemotherapy causes substantial immunomodulatory effects with implications for chemo-immunotherapy strategies. *Oncoimmunology*. 2016;5(3):1-11. doi:10.1080/2162402X.2015.1066062
272. Hazarika M, White RM, Booth BP, et al. Pemetrexed in malignant pleural mesothelioma. *Clin Cancer Res*. 2005;11(3):982-992. http://www.ncbi.nlm.nih.gov/pubmed/15709163.
273. Sakurada T, Kakiuchi S, Tajima S, et al. Pemetrexed-Induced Rash May Be Prevented by Supplementary Corticosteroids. *Biol Pharm Bull*. 2015;38(11):1752-1756. doi:10.1248/bpb.b15-00435
274. Sakurada T, Nokihara H, Koga T, et al. Prevention of Pemetrexed-Induced Rash Using Low-Dose Corticosteroids: A Phase II Study. *Oncologist*. 2022;27(7):e554-e560. doi:10.1093/oncolo/oyab077
275. Aston WJ, Hope DE, Cook AM, et al. Dexamethasone differentially depletes tumour and peripheral blood lymphocytes and can impact the efficacy of chemotherapy/checkpoint blockade combination treatment. *Oncoimmunology*. 2019;8(11):e1641390. doi:10.1080/2162402X.2019.1641390

276. Hom S, Pisano M. Reslizumab (Cinqair): An Interleukin-5 Antagonist for Severe Asthma of the Eosinophilic Phenotype. *Pharm Ther*. 2017;42(9):564-568. http://www.ncbi.nlm.nih.gov/pubmed/28890642.
277. Tsukamoto N, Takahashi N, Itoh H, Pouliquen I. Pharmacokinetics and pharmacodynamics of mepolizumab, an anti–interleukin 5 monoclonal antibody, in healthy Japanese male subjects. *Clin Pharmacol Drug Dev*. 2016;5(2):102-108. doi:10.1002/cpdd.205

Chapter 7

Appendices

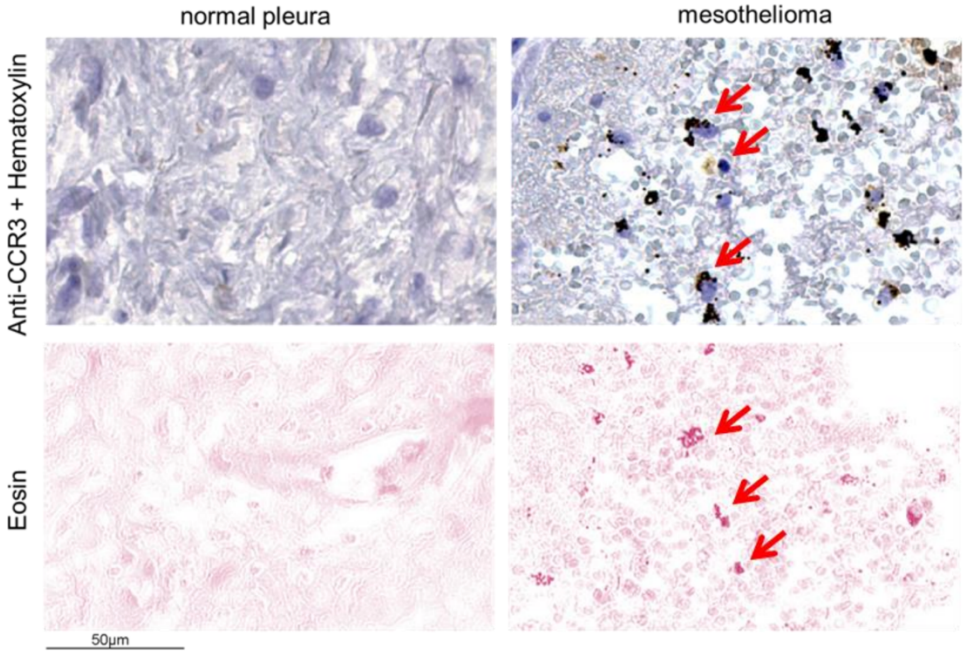

Appendix 1 – Staining of normal pleura and mesothelioma biopsies. Biopsies were stained for Hematoxylin and CCR3 as well as for eosin. Red arrows highlight cells staining for CCR3 and eosin.

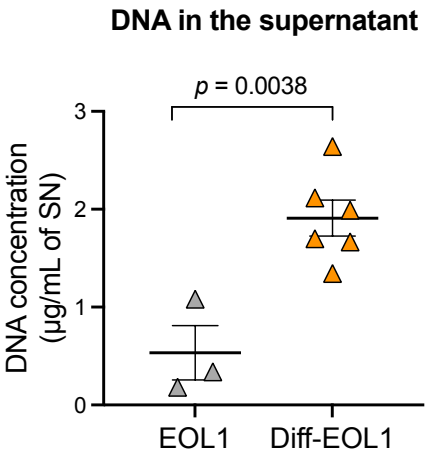

Appendix 2 – DNA quantification in EOL1 and Diff-EOL1 supernatant. Supernatant from EOL1 progenitor and Dif-EOL1 were collected and stored at -20°C. Double strand DNA was quantified using Quant-IT Picogreen® dsDNA Reagent and kits (Invitrogen).

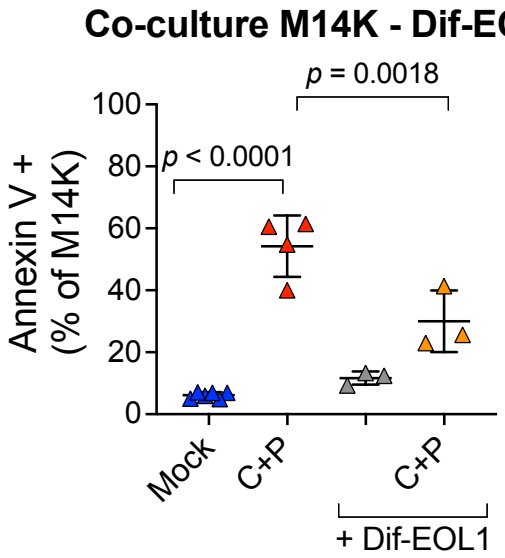

Appendix 3 – M14K co-cultivated with Dif-EOL1 present lower apoptotic rates. M14K cells were co-cultivated in a 1:1 ratio with 1:1 CFSE-labelled Dif-EOL1. Cells were then labeled for Annexin V and apoptotic rates of M14K were measured.

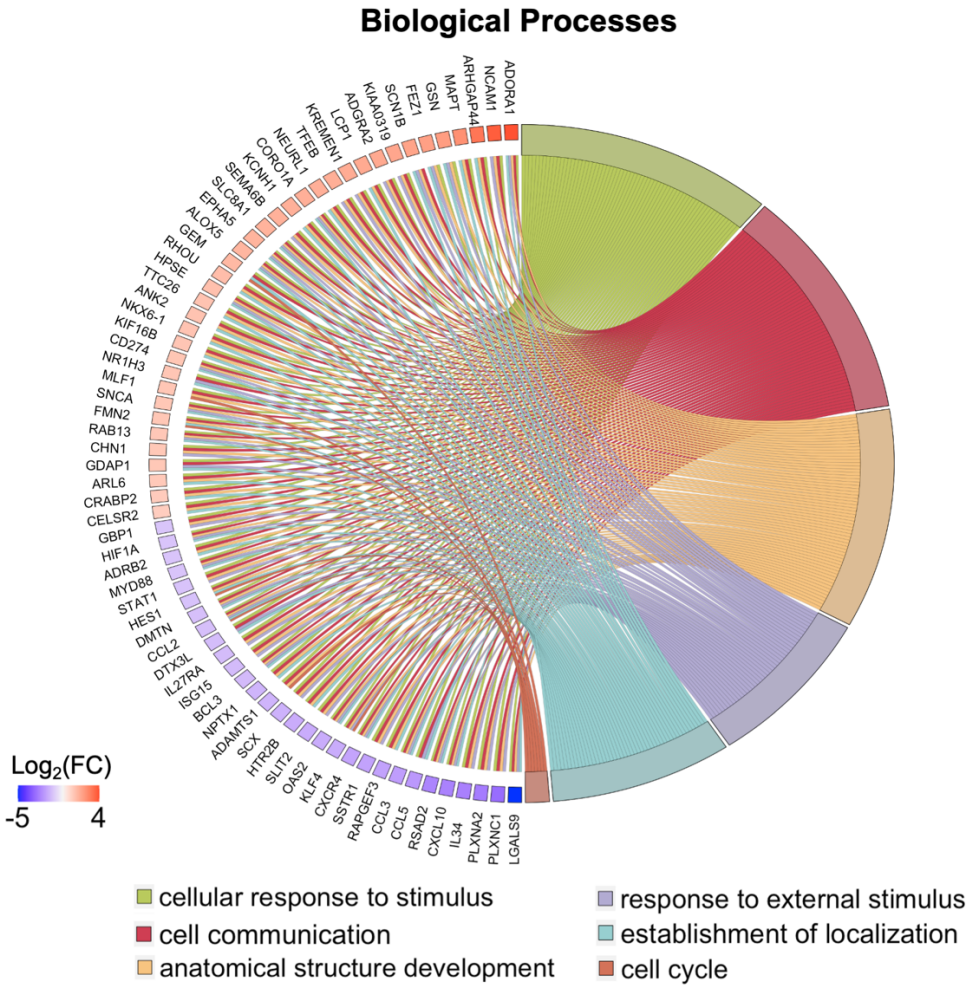

Appendix 4 – GO analysis of M14K treated in presence or not of Dif-EOL1.
Representative chord diagram for the 6 most significative pathways from GO: Biological Process (GO:BP) between the condition M14K C+P + SN Dif-EOL1 and M14K C+P. The chords show a relationship between Log2(FoldChange) of DEGs (left semi-circle) and their enriched GO:BP or GO:KEGG pathways (right semi-circle). C+P: cisplatin + pemetrexed; DEGs: differentially expressed genes; GO: Gene ontology.

Appendix 5 – GO terms associated with cell cycle in the top 50 GO:BP. The list of the top 50 GO:BP in the analysis of M14K treated in presence or not of Dif-EOL1 was extracted. Among the top 50 GO, those associated with cell cycle are listed with their adj_pvalue and associated genes. GO: Gene ontology, BP: Biological Process.

	ID	term	adj_pvalue	genes
31	GO:0007049	cell cycle	1,09E-68	CASP3, MYBL2, SAPCD2, LIG1, KIF2C, RRM2, TP53, SPAG5, MCM2, CDT1, CCNB2, KIF20A, FOXM1, PLK1, AURKB, RRM1, BTG2, BIRC5, NCAPD2, TACC3, TOP2A, POLE, ATP2B4, NDC80, BOP1, E2F1, CDC20, GEM, PIDD1, ANLN, MCM4, TRIP13, KIF4A, RAD54L, KIFC1, CENPA, UBE2C, HJURP, EXOC6B, DLGAP5, MAPRE3, KIF11, PKMYT1, C11orf80, PDGFRB, DTL, CENPV, CDCA5, RAD51AP1, BRCA1, CCNA2, CDCA3, EXO1, CENPH, BUB1, CDC25C, TENT5B, CDCA8, CDC45, FANCI, SKA3, CHAF1A, CHAF1B, FANCD2, XRCC3, KNL1, TDRKH, SUV39H1, BUB1B, FANCA, ATRIP, RAD51, CDCA2, KIFC2, NCAPG, NEK2, WDHD1, CDK1, SPC25, CABLES1, BRSK1, CCNE2, NES, CIT, DDIAS, DONSON, CENPK, NUPR1, NR4A1, CHTF18, PIMREG, STXBP4, ESCO2, KIF18A, ID3, CCDC57, FOXO4, DSCC1, CDC25A, NUF2, BRIP1, CDC7, CEP126, CDKN1C, TUBGCP5, ANK3, HAUS8, CDK18, PCLAF, CYP1A1, DNA2, MEI1, WNT4, OIP5, KIF14, PBX1, RGS2, MKI67, WDR76, EDN1, NEK11, PTGS2, BARD1, TGFB2, FAM110A, MAPK13, PBK, KLF4, SOX15, IL1B, TPD52L1, GPNMB, SMARCD3, FAM107A, CDK11A, CDC14A, TNF, SLC26A8, KIF18B, INSC, TUBAL3, ZCWPW1, TGM1, PER2, RGS14, RMI1
34	GO:0022402	cell cycle process	3,24E-64	MYBL2, SAPCD2, LIG1, KIF2C, RRM2, TP53, SPAG5, MCM2, CDT1, CCNB2, KIF20A, FOXM1, PLK1, AURKB, RRM1, BIRC5, NCAPD2, TACC3, TOP2A, POLE, ATP2B4, NDC80, E2F1, CDC20, GEM, PIDD1, ANLN, MCM4, TRIP13, KIF4A, RAD54L, KIFC1, CENPA, UBE2C, HJURP, EXOC6B, DLGAP5, MAPRE3, KIF11, PKMYT1, C11orf80, PDGFRB, DTL, CENPV, CDCA5, RAD51AP1, BRCA1, CCNA2, CENPH, BUB1, CDC25C, CDCA8, CDC45, SKA3, FANCD2, XRCC3, KNL1, TDRKH, BUB1B, FANCA, ATRIP, RAD51, CDCA2, KIFC2, NCAPG, NEK2, CDK1, SPC25, BRSK1, CCNE2, NES, CIT, DONSON, CENPK, STXBP4, ESCO2, KIF18A, CCDC57, FOXO4, DSCC1, CDC25A, NUF2, BRIP1, CDC7, CEP126, CDKN1C, TUBGCP5, ANK3, HAUS8, CDK18, PCLAF, CYP1A1, DNA2, MEI1, WNT4, OIP5, KIF14, PBX1, MKI67, WDR76, EDN1
44	GO:1903047	mitotic cell cycle process	1,96E-58	MYBL2, SAPCD2, LIG1, KIF2C, RRM2, TP53, SPAG5, MCM2, CDT1, CCNB2, KIF20A, FOXM1, PLK1, AURKB, RRM1, BIRC5, NCAPD2, TACC3, POLE, NDC80, E2F1, CDC20, PIDD1, ANLN, MCM4, TRIP13, KIF4A, KIFC1, CENPA, UBE2C, EXOC6B, DLGAP5, KIF11, PKMYT1, PDGFRB, DTL, CDCA5, BRCA1, CCNA2, CENPH, BUB1, CDC25C, CDCA8, CDC45, FANCD2, XRCC3, BUB1B, RAD51, CDCA2, KIFC2, NCAPG, NEK2, CDK1, SPC25, BRSK1, CCNE2, NES, CIT, DONSON, CENPK, ESCO2, KIF18A, CCDC57, FOXO4, DSCC1, CDC25A, NUF2, CDC7, CEP126, CDKN1C, ANK3, CDK18, CYP1A1, DNA2, KIF14, PBX1, MKI67, EDN1, NEK11, BARD1, FAM110A, PBK, KLF4, IL1B, TPD52L1, GPNMB, SMARCD3, FAM107A, CDC14A, TNF, KIF18B, INSC
45	GO:0000278	mitotic cell cycle	2, 81E-58	MYBL2, SAPCD2, LIG1, KIF2C, RRM2, TP53, SPAG5, MCM2, CDT1, CCNB2, KIF20A, FOXM1, PLK1, AURKB, RRM1, BTG2, BIRC5, NCAPD2, TACC3, POLE, NDC80, E2F1, CDC20, GEM, PIDD1, ANLN, MCM4, TRIP13, KIF4A, KIFC1, CENPA, UBE2C, EXOC6B, DLGAP5, KIF11, PKMYT1, PDGFRB, DTL, CDCA5, BRCA1, CCNA2, CENPH, BUB1, CDC25C, CDCA8, CDC45, SKA3, FANCD2, XRCC3, BUB1B, RAD51, CDCA2, KIFC2, NCAPG, NEK2, WDHD1, CDK1, SPC25, BRSK1, CCNE2, NES, CIT, DONSON, CENPK, ESCO2, KIF18A, CCDC57, FOXO4, DSCC1, CDC25A, NUF2, CDC7, CEP126, CDKN1C, TUBGCP5, ANK3, CDK18, CYP1A1, DNA2, KIF14, PBX1, MKI67, EDN1, NEK11, BARD1, FAM110A, PBK, KLF4, IL1B, TPD52L1, GPNMB, SMARCD3, FAM107A, CDK11A, CDC14A, TNF, KIF18B, INSC, TUBAL3, RGS14